HYDROLOGICAL MODELLING OF AN AGRICULTURAL WATERSHED USING HEC-HMS, REMOTE SENSING AND GIS

A THESIS SUBMITTED TO
THE ANAND AGRICULTURAL UNIVERSITY
IN PARTIAL FULFILMENT OF THE REQUIREMENT FOR THE AWARD OF DEGREE

OF

Master of Technology

IN

AGRICULTURAL ENGINEERING

BY
PAMPANIYA NIRAVKUMAR K.
B. Tech. (Agricultural Engineering)
(Reg. No: 04-2266-2013)

COLLEGE OF AGRICULTURAL ENGINEERING AND TECHNOLOGY
ANAND AGRICULTURAL UNIVERSITY
GODHRA-389 001

JUNE - 2015

Hydrological Modeling of an Agricultural Watershed using HEC-HMS, Remote Sensing and GIS

ABSTRACT

Runoff estimation is very important for water resources planning and management. Hydrological modeling is inevitable for accurate and precise estimation of runoff from a watershed. A major problem in the hydrological modeling is the inadequate field measured data to describe the hydrologic processes.With unavailability or limited availability of data, the quantitative understanding and prediction of the runoff generation processes and its transmission to the watershed outlet remains one of the most challenging area of hydrology. The use of remote sensing and GIS, in combination with semi distributed hydrological model provides new possibilities for deriving spatially distributed time series of input variables, as well as new means for calibration and validation of the hydrological model. In the present study, the HEC-HMS model is applied to the Hadaf river watershed, which is predominant with agricultural land and falls under semi-arid zone, where water resources planning and management is necessary for irrigation scheduling, water harvesting, flood control, drought mitigation and design of various engineering structures. In this study four different events of meteorological & discharge data, DEM, LISS-III and LISS-IV remote sensing imagery, soil maps are applied as inputs for HEC-HMS models. The effect of different resolution of DEMs, effect of land use change, effect of different resolution of land use imagery are also evaluated to assess their effectiveness in watershed delineation & drainage network, runoff generation, prediction accuracy, respectively. Two of the important transformation methods namely SCS UH and Clark UH are evaluated for performance comparison. Two of the important optimization methods (i.e. Univariate Gradient method and Nelder Mead method) are also evaluated to assess their effectiveness for rainfall runoff modeling. Initially, geo-morphological analysis of the watershed is carried out using the capabilities of remote sensing and GIS to prioritize the watershed for soil and water conservation measures. Then, conceptual hydrological HEC-HMS model is applied to transform rainfall into runoff for two of the selected event, and thereafter, the parameters related to initial loss, unit hydrographs, reservoir and channel routing, were calibrated and validated using the another two events in the watershed. It is found in this study that instead of low resolution (i.e. 90 m) SRTM DEM found to be better than ASTER DEM. Significant change in land use is observed from year 2008 to 2012 in this study. The finer resolution remote sensing image LISS-IV produced better classification and resulted in improved accuracy of HEC-HMS modeling. It is found that the Clark method produces better results than SCS-UH transformation method in rainfall-runoff simulation in terms of both the runoff peak and runoff volume. In parameter optimization, the overall performance of Nelder Mead method is found better than Univariate Gradient method. Better performance of all these models for the new event of rainfall-runoff transformation approves the applicability of HEC-HMS model in the study area. The findings in the present study are very useful for water resources engineers, researchers and will play an important role in water resources planning and management.

KEYWORDS: *Watershed, Runoff, Remote Sensing, GIS, HEC-HMS.*

COLLEGE OF AGRICULTURAL ENGINEERING AND TECHNOLOGY
ANAND AGRICULTURAL UNIVERSITY,
GODHRA – 389 001

Dr. M. K. Tiwari **Tel. No. (02672) 265128**
Assistant Professor **Email: tiwari.iitkgp@gmail.com**

CERTIFICATE

This is to certify that the thesis entitled **"HYDROLOGICAL MODELING OF AN AGRICULTURAL WATERSHED USING HEC-HMS, REMOTE SENSING AND GIS"** submitted by Mr. **NIRAVKUMAR KARASHANBHAI PAMPANIYA (Reg. No. 04-2266-2013)** in partial fulfillment of the requirement for the award of the degree of **Master of Technology** in **Agricultural Engineering** to the Anand Agricultural University is a record of bonafide research work carried out by him under my guidance and supervision.

Place : Anand **(Dr. M. K. Tiwari)**

Date : / /2015 **Major Advisor**

fACKNOWLEDGEMENT

I thought the time to write this section never would have arrived. Now I've reached the end and it is time to express my deep hearted gratitude to all the people who have encouraged me to finish this work.

It is indeed a pleasure to convey my gratitude to my guide, ***Dr. M. K. Tiwari, Assistant Professor, College of Agricultural Engineering and Technology, Anand Agricultural University, Godhra*** *for his guidance, understanding, patience and most importantly his friendship during my post graduate studies and research work. His mentorship was paramount in providing a well-rounded experience consistent my long term career goals. He encouraged me to not only grow as a researcher but also as an instructor and an independent thinker, I am indebted to him more than he knows.*

I am obliged to the members of my advisory committee, ***Dr. M. L. Gaur****, Professor and Head (SWE), College of Agricultural Engineering and Technology, Godhra,* ***Dr. Pankaj Gupta,*** *Associate Professor (FMPE), College of Agricultural Engineering and Technology, Godhra,* ***Dr. M. M. Trivedi,*** *Associate Professor, Polytechnic in Agricultural Engineering, Dahod, and* ***Dr. P. K. Singh,*** *Assistant Professor, Polytechnic in Agricultural Engineering, Dahod for their valuable and timely guidance & keenly reviewing the manuscript of the thesis.*

I am truly indebted and gratified to Dr. S. K. Raul, Er. D. K. Vyas, Dr. Niraj Seth, Dr. Navneetkumar and all the staff members of the College of Agricultural Engineering and Technology, Anand Agricultural University, Godhra for their support and ever willing co-operation during the period of my study to move this work from idea to reality.

I also very grateful to Dr. T. P. Singh, Director, and Mr. Vijay Singh, Project Scientist, Bhaskaracharya Institute for Space Application and Geo-Informatics (BISAG), Gandhinagar, Gujarat for their help for providing a necessary remote sensing data .

I am very thankful to State Water Data Center, Gandhinagar and Umariya Irrigation Project, Umariya, Dahod. Panam Circle office, Godhra for providing required data of the study area.

We specially thank to my friends Suryaprakash Suryavanshi, Jigar Patel, Jaydev Kanzariya, Kripa Shukla, Jasmin Bhimani, Happin Bhanderi, Prateek Kumar and Vipin Sule for their moral support and helping hands at the critical junctures during the thesis work.

Diction is not enough to express my unboundfil gratitude and regards from my inner core of the heart to my parents Shri Karashanbhai and Smt. Sajanben, younger brother Abhaybhai, elder sister Minaben and my fiancée Riya Barad for their unending encouragement, patience, sacrifice and everlasting love which made this endeavour possible.

Last but not the least, a million thanks to "Lord", the almighty that made me for my life through all tests in the past years. You have made my life more bountiful. May your name be exalted, honored, and glorified.

Place: Godhra

Date: / /2015 *(Nirav Pampaniya)*

CONTENTS

LIST OF TABLES

`

LIST OF FIGURES

`

`

`

`

ABBREVIATIONS AND SYMBOLS

Particular		Description
%	:	Percentage
<	:	Less than
>	:	Greater than
°C	:	Degree centigrade
ASTER	:	Advance Space Borne Thermal Emission And Reflection
BISAG	:	Bhaskaracharya Institute for Space Application and Geo-informatics
CBERS	:	China–Brazil Earth Resources Satellite
DEM	:	Digital Elevation Model
ERDAS	:	Earth Resources Data Analysis System
ESRI	:	Environmental Systems Research Institute
et al.	:	And other
ETM+	:	Enhanced Thematic Mapper Plus
GIS	:	Geographic Information System
GPS	:	Global Positioning System
GSMaP	:	Global Satellite Mapping of Precipitation
GSSHA	:	Gridded Surface Subsurface Hydrologic Analysis
ha	:	Hectare
HEC-HMS	:	Hydrologic Engineering Center-Hydrologic Modelling System
HEC-RAS	:	Hydrologic Engineering Centers River Analysis System
HSG	:	Hydrological Soil Group
i.e.	:	That is
IHACRES	:	Identification of unit Hydrographs and Component flows from Rainfall, Evaporation and Stream flow data
IRS	:	Indian Remote Sensing
K	:	Travel time through reach
km	:	Kilometer
km / km^2	:	Kilometer per square kilometer
km^{-1}	:	Per kilometer
km^2	:	Square kilometer
LISS	:	Linear Imaging Self-Scanning Sensor

LULC	:	land use and land cove
m	:	Meter
m^3	:	Cubic meter
m^3/s	:	Cubic meter per second
MAPE	:	Mean Absolute Percentage Error
mm	:	Millimeter
MSE	:	Mean Square Error
MVK	:	Moving Vector with Kalman filter
MW	:	Megawatt
NIH	:	National Institute of Hydrology
NRCS-CN	:	Natural Resources Conservation Services Curve Number
NRSC	:	National Remote Sensing Centre
NSE	:	Nash suttcliffe efficiency
PAN	:	Panchromatic
PRMSE	:	Peak-weighted Root Mean Square Error
r	:	Correlation coefficients
R^2	:	Coefficient of determination
RESOURSAT	:	Resourcesat
RMSE	:	Root Mean Square Error
RS	:	Remote Sensing
S	:	Potential maximum retention
SAGA	:	System for Automated Geoscientific Analyses
SCS	:	Soil Conservation Service
SCS-CN	:	Soil Conservation Service-Curve Number
SDSM	:	Statistical Down Scaling Model
SI	:	International System
SMA	:	Soil Moisture Accounting algorithm
SOI	:	Survey of India
SRTM	:	Shuttle Radar Topographic Mission
SUFI	:	Sequential Uncertainty Fitting
SWAT	:	Soil and Water Assessment Tool
TM	:	Thematic Mapper
TN	:	Total Nitrogen

TP	:	Total Phosphorus
UH	:	Unit hydrograph
USA	:	United States of America
USACE	:	United States Army Corps of Engineers
USDA	:	United States Department of Agriculture
WBNM	:	Watershed Bounded Network Model
WEPP	:	Water Erosion Prediction Project
X	:	Weighting Coefficient

CHAPTER I

INTRODUCTION

Human population of the Indian subcontinent is ever increasing there by increasing the demand for water for domestic, agricultural and industrial use. India supports about 16 % of the world population on 2.4 % of world's land and 4 % of world's water resource (Mane *et al*., 2013). This rapid increase in population necessitates an adequate management of land and water resources. As the major portion of the country's population depends on agriculture, it is difficult to utilize the resource without proper management of land and water. Hence, wise utilization and sound management of these resources shall be everybody's responsibility. Agriculture could be effective only when it gets sufficient water at the right time. Therefore, to ensure sustainable agricultural development, there should be reliable supply of land and water as well as land and water management systems. If people engaged in agriculture get sufficient water throughout the year, it is possible to harvest higher yields from a smaller size of land and keep labour busy on production throughout the year.

It is estimated that out of the 4×10^8 m^3 average annual precipitation that falls over India, the utilizable surface and groundwater resources are merely $0.69\times10^8 m^3$ and $0.432\times10^8 m^3$, respectively (Sharda and Juyal, 2006). In the coming decades, ever increasing population, global warming, climate change, surface and ground water pollution will certainly decline the fresh water supply. Keeping all these factors in mind, the quantification and measurement of surface water resources is essential for sustainable resource utilization. For this purpose the estimation of surface runoff is essential. For the assessment of water yield potential, planning of water conservation measures, recharging the ground water zones and reducing the sedimentation and flooding hazards downstream the correct runoff estimation is an inevitable. The availability of accurate information on runoff in India is however, scarce and therefore, there is an urgent need to generate information on runoff to promote watershed development and management programmes. Runoff from a watershed system is usually measured with the help of the gauging stations generally installed at the watershed outlets. This requires substantial investment of time and money and usually is not a practical option. In India, most of the agricultural watersheds are ungauged, having no past record for the study of rainfall-runoff processes (Sarangi *et*

al., 2005). Therefore, understanding the rainfall-runoff relationship for estimation of runoff is of paramount importance. This accurate estimation of runoff is effectively and efficiently done by hydrological modelling.

In this regard, the main purpose of modelling is to know the natural system and to provide the information and knowledge to increase human welfare, protect the environment and sustainable management of water resources in a temporal and economic manner. Modelling is nothing but a process to make a replica of ground happenings. Hydrological and hydraulic modelling can produce the demo of incidents configured out from basin, hydrologic and hydraulic elements and parameters for event and its update. More ground detail and expertise can serve more acceptable model result. The use of hydrological modelling systems for water resources planning and management is becoming increasingly popular. Since these hydrological models mostly deal with land phase of hydrological cycle, data related to topography and physical parameters of watershed are a necessary pre-requisite for these models. Computer based geographic information system furnish this requirement efficiently. These systems link land cover data to topographic data and to other information related to geographic locations. When applied to hydrologic systems, non-topographic information can include description of soils, land use, ground cover, ground water conditions, as well as man-made systems and their characteristics on or below the land surface.

Since the middle of the 19th century, different methods have been demonstrated by hydrologists to assess the impact of rainfall on runoff (Clarke, 1973; Beven, 1985; Wheater *et al.*, 1993; Refsgaard, 1996; Beven, 2001; Kumar *et al.*, 2005; Wheater *et al.*, 2008). These rainfall runoff models are broadly classified into three categories: empirical or black box, conceptual and physically based models. Black box models normally contain no physically based input and output transfer functions and therefore, are considered to be purely empirical models. Conceptual rainfall-runoff models usually incorporate interconnected physical elements with simplified forms, and each element is used to represent a significant or dominant constituent hydrologic process of the rainfall-runoff transformation. Physically based model are distributed models consists a large number of parameters as input to the model.

Accurate surface runoff estimation plays a significant role for different water resources planning and management. Runoff is the among the most important

hydrologic variables and its reliable predictions in terms of quantity and rate of runoff from the land surface into streams and rivers are very important especially for ungauged watersheds (Nayak and Jaiswal, 2003). A rainfall-runoff model is a mathematical model describing the rainfall-runoff relations of a catchment area, drainage basin or watershed. More precisely, it produces the surface runoff hydrograph as a response to a rainfall hydrograph as input. In other words, the model calculates the conversion of rainfall into runoff. A rainfall runoff model can be really helpful in the case of calculating discharge from a basin. The transformation of rainfall into runoff over a catchment is known to be very complex hydrological phenomenon, as this process is highly nonlinear, time-varying and spatially distributed.

Hydrological model is a simplified representation of natural system. The rainfall runoff transformation is one of the most frequently used phenomena in hydrology. It determines the runoff generation from the watershed. Numerous methods have been developed by different researchers to simulate the rainfall runoff transformation processes. Although a variety of rainfall runoff models are available, selection of a suitable rainfall runoff model for a given watershed is essential to ensure efficient planning and management of watersheds. In this study to understand the rainfall runoff processes the attempt has been taken to define this rainfall runoff modelling processes from knowledge driven modelling techniques. This way of rainfall-runoff modelling is based on detailed descriptions of the system and the processes involved in producing runoff. The best examples of knowledge-driven modelling are called as conceptual and physically-based model approaches. This approach generally use a mathematical framework based on mass, momentum and energy conservation equations in a spatially distributed model sphere, and parameter values that are directly related to catchments' characteristics.

One of the recent thrusts in hydrologic modeling is the assessment of the effects of land use and land cover changes on water resources and floods (Yang *et al.*, 2012), which are essential for planning and operation of civil water resource projects, and for early flood warning. The influence of urbanization as one of the important land use and land cover changes on runoff and floods within watersheds is one of the main research topics in the past decades. It is widely recognized that urbanization changes hydrological processes within watersheds by altering surface infiltration characteristics. The expected results of urbanization include reducing infiltration,

baseflow, lag times, increasing storm flow volumes, peak discharge, frequency of floods, and surface runoff (Hollis, 1975; Arnold and Gibbons, 1996; Smith *et al.*, 2005; Dougherty *et al.*, 2006; Ogden *et al.*, 2011).

A major problem in the hydrology is the inadequate field measured data to describe the hydrologic processes. With unavailability or limited availability of data, the quantitative understanding and prediction of the runoff generation processes and its transmission to the watershed outlet remains one of the most challenging areas of hydrology. Traditional techniques for design flood estimation include the rational method, empirical methods, flood frequency method, unit hydrograph techniques, and watershed models. The unit hydrograph techniques and watershed models can be used to estimate the design flood hydrograph in addition to the magnitude of the design flood peak (Kalita, 2008). Remote sensing (RS) technique has been identified as a tool to produce information in spatial and temporal domain very efficiently in digital form with high resolution, instead of point measurement that is cumbersome, hectic and time exhaustive. The use of RS technology involves large amount of spatial data management and requires an efficient system to handle such data. Geographic Information System (GIS) can store, analyses, retrieve and display spatial data for solving complex planning and management problems has been used to provide compatible spatial and temporal input data for hydrological models and are extremely relevant as a means of estimating a number of key variables specifically in situation where distributed hydrological models are used. The use of RS data and GIS, in combination with semi distributed hydrological model, provides new possibilities for deriving spatially distributed time series of input variables, as well as new means for calibration and validation of the hydrological model. Remote Sensing and GIS, the upcoming advanced computer based tool and techniques which give one step more help in these types of scientific works related to different states of water directly and indirectly. Thus, in this study the capabilities of RS and GIS is applied to generate input data in form of thematic maps such as digital elevation model, land use/land cover and soil map for a physically based semi distributed hydrological model.

The integration of geographic information systems, remote sensing and HEC-HMS hydrologic modelling systems for water resources planning and management is becoming increasingly popular. Since HEC-HMS model mostly deals with land phase of hydrological cycle, data related to topography and physical parameters of the catchments is a necessary pre-requisite for this model. Therefore, the integration of

HEC-HMS with GIS and remote sensing technique ensures the quality of the output, demand less labour and human resource, ends timely and becomes economical. Hence, the result from such integrated models is important for sound decision making and benefits the community at large.

The semi distributed HEC-HMS hydrologic model is applied in the study. The HEC-HMS model is designed to simulate rainfall runoff processes of networked watershed systems which include sub-basins, reaches, junctions, reservoirs, diversions, sources, and sinks. In the lumped modelling approach the average rainfall of the catchment to develop the rainfall runoff model is considered. The catchment has been divided in to the number of sub catchments to consider variation in the geomorphological parameters.

The Hydrologic Engineering Center-Hydrologic Modelling System (HEC-HMS) was originally developed to simulate the rainfall-runoff processes of dendrite watershed systems. Later, it was improved to solve significant hydrological problems including large river basin water supply, flood hydrology, and small urban or natural watershed runoff. In the HEC-HMS model, watershed physical descriptions are accomplished through the basin component. Furthermore, basin component includes loss, transform, and base flow calculations through different approaches to determine catchment runoffs. In this study, SCS-CN loss method, SCS unit hydrograph, and Muskingum approaches are selected as loss, transform, and routing methods, respectively. Meteorological data analysis is performed through the meteorology component of the model. The HEC-HMS model is applied to the Hadaf river watershed, situated in the semi-arid middle region of Gujarat. Calibration-validation process is conducted by using observed discharge data at the outlet of the basin.

In this study an agricultural dominated watershed upstream of the Hadaf dam is selected. The area is predominant with agricultural land and falls under semi-arid zone, where water resources planning and management is necessary for irrigation scheduling, water harvesting, flood control, drought mitigation and design of various engineering structures. Considering the importance of water especially in semi-arid region, it is required to understand the rainfall-runoff relationship precisely. For this purpose HEC-HMS model is explored for precise runoff simulation in the watershed. To address the above issues, after comprehensive review of literature the following objectives are formulated in this study for the selected agricultural watershed in middle region of Gujarat.

Objectives:-

1. To study the geomorphological parameters of the study area using Remote Sensing and GIS.
2. To calibrate and validate HEC-HMS model to simulate runoff in the watershed.
3. To optimize and evaluate performance of different unit hydrograph for runoff simulation.
4. To evaluate effect of land use change on runoff in the watershed using HEC-HMS model.

CHAPTER II
REVIEW OF LITERATURE

This chapter presents comprehensive reviews related to the rainfall runoff simulation using hydrologic models coupled with Remote Sensing (RS) and Geographic Information System (GIS). This chapter presents wide applications of these modelling techniques in different watersheds in India and across the globe situated in different hydro-climatic zones. The reviews are categorized in the following sections:

2.1 Morphological Characteristics Analysis Using Remote Sensing and GIS

Pandey *et al.* (2004) indicated that morphometric analysis of a watershed coupled with landuse/cover information can play an important role in predicting the hydrological behaviour of a Karson watershed. Various morphological parameters viz., area, perimeter, elevation, stream length, stream order were determined using ArcInfo. GIS integration of landuse/cover information with morphometric parameters has been used to delineate the areas suitable for adopting soil and water conservation measures.

Chopra *et al.* (2005) carried out morphometric analysis of two sub-watersheds using RS and GIS techniques. Detailed drainage map prepared from aerial photographs and SOI toposheets was updated using latest IRS-1D PAN sharpened LISS-III analog data. Updated drainage maps were used for the morphometric analysis of the two sub-watersheds both the sub-watersheds show dendritic to sub-dendritic drainage pattern with moderate drainage texture. High bifurcation ratio indicated a strong structural control on the drainage. In spite of mountainous relief, low drainage density value indicates that the area is underlain by impermeable sub-surface material. Circulatory and elongation ratios show that both the sub-watersheds have elongated shape.

Galgale and Shinde (2006) described morphological characteristics like stream order, drainage density, aerial extent, watershed length and width, channel length, channel slope and relief aspects of watershed are important in understanding

the hydrology of watershed. Runoff response of the watershed is different for different slopes, shapes, length widths and area of watershed. Response is also affected by the factor like drainage density, length of over land flow, stream frequency, relative relief and relief ratio. Computation of watershed morphological characteristics is pre-requisite to further detailed hydrological analysis and modelling of the watershed. Hydrologists have attempted to relate the hydrologic response of watersheds to watershed morphological characteristics. These characteristics are first determined manually from the topographic and stream network map of the watershed. Manual computation in order to generate these characteristics is not only tedious and error prone, but also time consuming. Computers can be used to compute these characteristics. Afterward, GIS being used for the generation of morphologic characteristics.

Sharma *et al.* (2007) carried out morphometric analysis using GIS technique in Uttala nala watershed, a tributary of Son River. The study area extends over a total area of about 4763 ha. The methodology adopted for this study involved digitazation of watershed boundary, sub-watersheds boundaries and drainage network to derive morphometric parameters in GIS environment. The study area has eight sub-watersheds. Analysis of drainage network shows that Uttala nala watershed is of 5^{th} order type. Elevation ranges from 460 to 800 m. above Mean Sea level. Drainage density varies from 1.53 to 3.30 km/km^2.

Pankaj and Kumar (2009) evaluated morphological parameter using GIS for the five sub-watershed of song river (tributary of the Ganga river). GIS analysis techniques to evaluate and compare linear, relief and aerial morphometry of the five sub-watersheds of Song River (tributary of the Ganga river) with special reference to landslide incidences, for future development and planning of the watershed. The drainage pattern of the song river basin is mainly structurally controlled and the area is characterized by high to moderate relief. The asymmetric factor indicates that the tectonic rotation of the four sub-watersheds is upward on the right side of the drainage basin and only one sub-watershed is downward. It is found in the study that the numbers of the landslide incidences are also more in the upward side, than the down ward side of the song river basin.

Saptarshi and Raghavendra (2009) discussed that the automated watershed delineation technique using the spline interpolated filled Digital Elevation Model (DEM) is effective in converging slopes of the area in which the stream patterns match with the manually digitized stream patterns of the topographical map. The various vector spatial layers like the slope/aspect, landuse/cover, runoff potential, soil erosion potential and the associated attribute information governing the criteria for different conservation structures can act as input layers in integrated spatial analysis module in GIS environment to evolve derived layers indicating the locations of conservation sites meeting the requisite criteria. The reliability of suitable conservation sites suggested out of integrated spatial GIS analysis could be ascertained using the multi criteria analysis incorporating the various factors controlling soil erosion process in the micro-watershed groups.

Eze and Efiong (2010) examined the morphometric parameters of the Calabar River Basin with emphasis on its implication for hydrologic processes. Data for this study were obtained from topographic map which were subject to field confirmation. The result revealed that the basin area was 1514 km^2. There were 223 streams with a total stream length of 516.34 km. The textural dissection was considered to be low as drainage density, stream frequency and drainage intensity values were 0.34 km^{-1}, 0.15 km^{-1} and 0.05 respectively. The basin was found to be strongly elongated with circularity ratio of 0.34 and elongation ratio of 0.64. The average bifurcation ratio was 2.83. The very low value of drainage intensity implies that drainage density and stream frequency have very little effect on the extent to which the surface has been lowered by agents of denudation. These low values of drainage density, stream frequency and drainage intensity also imply that surface runoff is not quickly removed from the basin, making it susceptible to flooding, gully erosion and landslides, particularly in the lower part of the basin.

Nageswara *et al.* (2010) proved that the RS, GIS and global positioning system (GPS) has to be an efficient tool in delineation of drainage pattern and water resources management and its planning. GIS and image processing techniques have been adopted for the identification of morphological features and analyzing their properties of the Lower Gostani River Basin area in Andhra Pradesh state, India. The basin morphometric parameters such as linear and aerial aspects of the river basin

were determined and computed. It is 7th order drainage basin and drainage pattern mainly in sub-dendritic to dendritic type. It is observed that the drainage density value is low which indicates the basin is highly permeable subsoil and thick vegetative cover. The circularity ratio value reveals that the basin is strongly elongated and highly permeable homogenous geologic materials. The study was recommended to help the local people to utilize the resources for sustainable development of the basin area.

Pareta and Pareta (2011) used Resourcesat-1 LISS-IV Mx satellite imagery for detailed geomorphological and hydrogeological study of Karawan watershed. For morphometric analysis, ASTER data was used for preparing DEM and GIS was used in evaluation of linear, areal and relief aspects of morphometric parameters. Watershed boundary, flow accumulation, flow direction, stream ordering; and contour, slope-aspect, hillshade have been prepared using ArcHydro Tool; Surface Tool in ArcGIS 10.0 software. Different thematic maps i.e. geological, geomorphological, lineament density, groundwater favourable zone, and drainage density have been prepared by using ArcGIS 10.0 software. Authors have computed more than 85 morphometric parameter of all aspects. Based on all morphometric parameters analysis; that the erosional development of the area by the streams has progressed well beyond maturity and that lithology has had an influence in the drainage development. The hydromorphogeological units such as structural landforms, structural hills (vindhyan sediments), denudational hills (volcanic), deccan plateau, and fluvial landforms were identified and appropriate field confirmations were made. The geomorphic units such as lineaments, faults, factures, and pediplains were identified under structural landforms. The deeply and moderately weathered buried pediplains are the potential zones for groundwater targeting.

Akbari *et al.* (2012) focused on geomorphological studies of a small catchment Nima-Wira catchment situated in the Krishna river basin, Andhra Pradesh, India. In this study, geomorphological characteristics of Nima-Wira catchment in the Krishna River Basin were determined using GIS and in order to determine the geomorphological parameters required Shuttle Radar Topographic Mission (SRTM) and Cartosat image were procured for year 2001 and 2009 respectively, both the images used for finding out watershed boundary using SWAT in ArcGIS 9.3

software. Results after eight years gap geomorphological analysis were done. Geomorphological parameters were calculated for year 2001 and 2009. The results showed that the basin relief, relief ratio, ruggedness number, constant of channel maintenance, number of streams, stream frequency values decreased over past eight years. The results of the study were found to be useful for further hydrological investigations and were the major inputs to various hydrological models.

Paul and Inayathulla (2012) carried out morphometric analysis and prioritization of nine sub-watersheds of Hebbal valley, located in Bangalore district of Karnataka state, India using RS and GIS techniques. The morphometric parameters considered for analysis were stream order, stream length, bifurcation ratio, drainage density, stream frequency, texture ratio, form factor, circulatory ratio, elongation ratio, relief ratio, length of overland flow and basin shape. The watershed has a dendritic drainage pattern. The bifurcation ratio varies from 1.89 to 3.03 and all sub-watersheds fall under normal basin category. The circularity ratio ranges from 0.42 to 0.78 indicating that all the sub-watersheds except sub-watershed 9 are more or less circular. Elongation ration of all the watersheds except sub-watersheds 3 and 9 are above 0.7 indicating that all the sub-watersheds except sub-watersheds 3 and 9 are more or less circular. The compound parameter values were calculated and prioritization rating of nine sub-watersheds in Hebbal valley was carried out. The sub-watershed with lowest compound parameter value was given the highest priority. The sub-watershed 3 was likely to be subjected to maximum soil erosion and hence was recommended to be provided with immediate soil conservation measures.

Ahmad and Khan (2013) carried out detailed morphometric parameters of the Banas river basin. Detailed drainage map was prepared from Survey of India (SOI) toposheets (45h/5 and 45h/9) and was updated using IRS-P6, LISS-III (Precision geocoded) data of 7th May, 2010 using ArcGIS software. For detailed study, SRTM was used for delineating watershed boundary using SAGA GIS software. GIS analysis techniques were used to evaluate linear and areal morphometric parameters of the basin. Drainage patterns were found to be mainly dendritic to sub-dendritic with fifth order drainage. It was found that the Banas river basin possess high drainage density which is indicative of less permeable material, sparse vegetative cover and moderate to high relief.

Erol (2013) examined morphometric parameters with an emphasis on an analysis of the hydrologic processes of the Aksu watershed. The morphometric parameter data for the study was obtained from field studies and topographic maps, combined using GIS. The results showed that the watershed area is 49.29 km^2. There were 121 sub-streams with a total stream length of 939.51 km. The soil texture of the Aksu watershed was clay loam described as moderately permeable. This textural status was considered to be high as stream frequency and drainage density values were 2.45 and 19 km^{-1}, respectively. The watershed was strongly elongated with a circularity ratio of 0.22 km^{-1} and an elongation ratio of 0.62 which generally represent mountainous and sloping topographic conditions. Shape parameters such as circularity ratio (0.22), compactness coefficient (2.11), and elongation ratio (0.62) demonstrate that the shape of the Aksu watershed was a longitudinal shape with a heterogeneous geological structure. Despite the textural dissection, these results and high values of stream frequency and drainage density verify that the watershed was a mountainous area with low amount of vegetation, weak and not very permeable subsoil, thereby having a great proportion of surface runoff. These results also imply that surface runoff was quickly removed from the watershed. In the watershed, human induced soil degradation was likely to have a negative impact on water quality and quantity due to the negative effects on the stream network. It was therefore advised that human activities should be included in the management plan to enhance the watershed health and sustainability.

Babu *et al.* (2014) used SRTM (Shuttle Radar Topographic Mission) data for preparing DEM (Digital Elevation Model), Aspect Map and Slope Map for the Chalakudi River Basin. Geographical Information System (GIS) was used for the evaluation of linear, areal and relief aspects of morphometric parameters. The drainage density of the basin was estimated 2.54 and the lower-order streams mostly dominate the basin. The high basin relief indicated high runoff and sediment transport. The elongation ratio of the Chalakudi Basin was estimated 0.48 and indicated that the shape of the basin was elongated. The development of stream segments in the basin area was more or less effected by rainfall. Relief ratio indicated that the discharge capability of watershed was very high and the groundwater potential was meagre. The low value of drainage density in spite of mountainous

relief indicated that the area was covered by dense vegetation and resistant rocks permeated by fracture and joints. The results of study were helpful in watershed development planning and wise utilization of natural resources.

Patel *et al.* (2015) focused on the identification of suitable sites for locating water harvesting structures using morphometric analysis and multi-criteria based decision support system. The Hathmati watershed of river Hathmati at Idar taluka, Sabarkantha district, Gujarat was experiencing excessive runoff and soil erosion due to high intensity rainfall. Earth observation dataset such as Digital Elevation Model and Geographic Information System were used in this study to determine the quantitative description of the basin geometry. Several morphometric parameters such as stream length, elongation ratio, bifurcation ratio, drainage density, stream frequency, texture ratio, form factor, circularity ratio, and compactness coefficient were taken into account for prioritization of Hathmati watershed. The overall analysis revealed that Hathmati comprised of 13 mini-watersheds out of which, the watershed number 2 was of utmost priority because it had the highest degradation possibilities. The final results were used to locate the sites suitable for water harvesting structures using geo-visualization technique. After all the analyses, the best possibilities of check dams in the mini-watersheds that can be used for soil and water conservation in the watershed ware presented.

2.2 Application of HEC-HMS Model in Hydrological Modelling

Islam (2004) used SCS CN, SCS Lag, Recession methods in HEC-HMS to simulate the rainfall-runoff model in three small basins. This research found that simulated hydrograph and observed hydrograph were much approached, and simulated out-flow and observed out-flow in the reservoir were also closed.

Yusop *et al.* (2007) examined rainfall-runoff processes in a small oil palm catchment (8.2 ha) in Johor, Malaysia. Storm hydrographs show rapid responses to rainfall with a short time to peak. The estimated initial hydrologic loss for the oil palm catchment was found as 5mm. Despite the low initial loss, the catchment exhibits a high proportion of baseflow, approximately 54 % of the total runoff. On an event basis, the storm flow response factor and runoff coefficient ranges from 0.003 to 0.21, and 0.02 to 0.44, respectively. Peakflow and stormflow volume were moderately

correlated with rainfall. The hydrographs were satisfactorily modelled using the Hydrologic Engineering Centre–Hydrologic Modelling System (HEC-HMS). The efficiency indexes of the calibration and validation exercises were found as 0.81 and 0.82, respectively. Based on these preliminary findings, it was suggested that an oil palm plantation would be able to serve reasonably well in regulating basic hydrological functions.

Bakir and Xingnan (2008) made an attempt was to critically look at the application of HEC-GeoHMS which was an extension of ArcView in HEC-HMS; an HEC package which was a new generation of software developed for rainfall-runoff simulation. The main role of HEC-GeoHMS was to formulate a watershed data structure under the platform of GIS that can be imported directly to HEC-HMS. With the topographic information supplied by HEC-GeoHMS, HEC-HMS works more readily and exactly. The performance of HEC-HMS was compared with that of the Xinanjiang conceptual model using historical flood data from the Wanjiabu catchment in China. The results obtained in the course of this study indicated that HEC-HMS was more convenient for flood stimulation especially in optimizing parameters but not quite accurate as compared with Xinanjiang model. The plausible reason for this could be due to the fact that the Xinanjiang model had more parameters thereby making it flexible to fit a flood event. Based on the results obtained as stated, it was thus suggested that with improvement in data conditions, runoff yield could be calculated on grid format and results for both models appropriately enhanced.

Verma *et al.* (2009) carried out rainfall-runoff modelling using HEC-HMS and WEPP hydrologic models, and remote sensing and GIS (geographical information system) techniques in the Upper Baitarani River basin of Eastern India. The percent deviation of total runoff volume simulated by HEC-HMS ranges between −2.55 and 31 %, while it varies from −13.96 to 13.05 % for the WEPP model which suggests that the WEPP model simulates annual flow volumes more accurately than the HEC-HMS model for most years. However, the lower values of root mean square error (RMSE) and RMSE-observation standard deviation ratio coupled with the higher values of Nash–Sutcliffe efficiency, percent deviation and coefficient of determination for HEC-HMS during calibration and validation periods indicated that the stream flow simulated by HEC-HMS is more reliable than that simulated by

WEPP. Overall, it was concluded that the HEC-HMS model is superior to the WEPP model for simulating daily stream flow.

Kaushik (2010) carried out rainfall-runoff modelling using the HEC-RAS (v 3.1.3 -May 2005) and HEC-HMS (v 2.2.2 - May 2003) software developed by United States Army Corps of Engineers (USACE) for the River Sabarmati at Ahmedabad. The flows were simulated for the three historical most severe storms designated as design storms by the CWC using the HEC-HMS and HEC-RAS software. Peak flows and river stages in River Sabarmati were computed taking into account, the reservoir storage at the time of storm event based on the rule curves developed by NIH-Roorkee. Based on the analysis carried out in the study, the peak flows and water surface elevations were estimated at various sections in the 9 km stretch of River Sabarmati in Ahmedabad city.

Scharffenberg *et al.* (2010) conceived the Hydrologic Modeling System (HEC-HMS) as a software-based tool for simulating the hydrologic cycle in the context of engineering problem solving. Water movements in the cycle relevant to common problems in water resources engineering were included: precipitation, infiltration, surface runoff, baseflow, and open channel flow. The first generation of the software focused on simulating individual storm events. The second generation of the software added new components for infiltration modeling to permit continuous simulation. Snowmelt and potential evapotranspiration components, along with an advanced reservoir component, were added for the third generation. The software was very adaptable because it includes a variety of model choices for each segment of the hydrologic cycle. It had been used in many studies for achieving goals in flood damage reduction, reservoir and system operation, floodplain regulation, environmental restoration, water supply planning, among others.

Ali *et al.* (2011) studied an empirical land use change model and an event scale, rainfall-runoff model to quantify the impacts of potential land use change on the storm-runoff generation in the Lai Nullah Basin. The HEC-HMS rainfall-runoff model was calibrated and validated for 5 storm events in the study area, and the results showed good consistency between the simulated and measured hydrographs at the outlet (Katarian Bridge) of the basin with Nash–Sutcliffe efficiency ranging from 76 to 98 %. The future land use scenario was forecasted based on Islamabad Master Plan and growth pattern. The calibrated HEC-HMS model was applied for these

future land use scenarios to assess the potential land use impacts on the storm-runoff generation. The results indicated that the future land use as envisaged in the master plan was projected to increase the total runoff between 51.6 and 100.0 % as well as the peak discharge between 45.4 and 83.3 %, and that the magnitude of peak discharge increment relates to the expansion rate of built-up area. The results provided useful information for land use planning and management and the methods applied can serve as a useful tool for future land use impact studies.

Dastorani *et al.* (2011) used HEC-HMS model for prediction of flood and modelling of rainfall-runoff process in Toroq watershed. After calibration of the model, the hyetograph and related hydrographs of 6 rainfall events were used and the observed and estimated hydrographs were compared from different points of view. It was observed that Curve Number (CN) and initial loss are the main parameters affecting the results. Another evaluation was the comparison of the lag time produced by Snyder and SCS methods, showing more accuracy of the lag time predicted by SCS approach. In this study the common hypothesis "initial loss is about 0.2 of S" was also evaluated and observed that in Toroq watershed, the value of 0.22S was found as more reliable for the initial loss. About the comparison of the estimated run off produced by SCS and Snyder approaches, it was seen that the results of SCS approach is more close to the measured values.

Nasri *et al.* (2011) used HEC-HMS hydrological model in the basin of Sheikh Bahaei Dam in Isfahan province to prioritize areas influencing the flood peak discharge to specify areas with highest flood potential. The results showed that areas near the output point of the basin play the highest role in flood development and should be placed in the first priority of watershed management. It was suggested that the results would remarkably contribute to the monitoring system of the area.

Kumar and Bhattacharjya (2011) developed a distributed approach to simulate the rainfall runoff process of a catchment. The catchment area has been divided in to the numbers of divisions equal to the numbers of rain gauge station. The rainfall in a particular rain gauge was considered as uniformly distributed over the entire sub catchments. Spatially distributed catchment characteristics had been obtained from the 90 m resolution SRTM digital elevation data. A lump model was also developed using average rainfall of the catchment. In case of lump model, average rainfall was calculated using thessian polygon method. In order to estimate

runoff from rainfall events, loss rate or infiltration parameters for the basin had to be calculated, which is a basic input for further rainfall runoff modelling. The infiltration capacity of the basin depends on the land use and soil property. Horton's and Green-Ampt equations are most commonly used equations for estimation infiltration of a basin. Curve Number (CN) method is also a widely used method for estimating infiltration characteristics of the watershed, based on the land use property and soil property. Therefore the estimation of infiltration parameters or curve number of the basin was made initially. An inverse model was formulated and solved for estimating the curve numbers for the lump and distributed models.

Paudel et al. (2011) made attempt to differentiate the ability of lumped and distributed models to analyze a common watershed development issue such as land use change. For this, they employed two common US Army Corps of Engineers (USACE) models, well established in the literature and application, using the Hydrologic Engineering Center – Hydrologic Modeling System (HEC-HMS) model in a fully lumped mode and the fully distributed model Gridded Surface Subsurface Hydrologic Analysis (GSSHA). A synthetic watershed was used to establish that a distributed model like GSSHA more intuitively simulates land use change scenarios by distinguishing the spatial location of the change and its effects on the watershed response. An actual watershed at Tifton, Georgia was used to validate the observations made from the synthetic watershed.

Abood *et al.* (2012) attempted to evaluate the performance of HEC-HMS (Hydrological modeling) in simulating the rainfall-runoff using two different rainfall infiltration methods. The rainfall-runoff process for the study area which consist of two catchments namely Kenyir catchment and Berang catchment, Terengganu, Malaysia was simulated using HEC-HMS program. Two methods for estimating infiltration (rainfall abstraction losses) were built in the program. These methods were SCS Curve Number method and Green and Ampt method. The impact of selected method on the accuracy of rainfall-runoff simulation was studied. Statistical analysis include the computation of the coefficient of determination (R^2), the mean square error (MSE) and the Mean Absolute Percentage Error (MAPE) were used to check the accuracy of HEC-HMS simulations using the two infiltration methods. The result showed that the errors in the simulation output using the SCS Curve Number method were 6.5 % for Berang catchment and 8.2 % for Kenyir catchment, while the errors in

the simulation output using Green and Ampt method were 9.13% for Berang catchment and 11.11 % for Kenyir catchment. As a conclusion, it was found that the output of HEC-HMS program was in agreement with the historical recorded data and it was recommended to use the SCS Curve Number infiltration method for the tropical catchment due to its low error in simulation output.

Du *et al.* (2012) used the Hydrologic Engineering Center's Hydrologic Modeling System (HEC-HMS) to calculate runoff and the integrated Markov Chain and Cellular Automata model (CA-Markov model) to develop future land use maps. The model was calibrated and validated using observed daily streamflow data collected at the two outlets of watershed. Landsat Thematic Mapper (TM) images from 1988, 1994, 2006, Enhanced Thematic Mapper Plus (ETM+) images from 2001, 2003 and a China–Brazil Earth Resources Satellite (CBERS) image from 2009 were used to obtain historical land use maps. The simulation results of HEC-HMS model for the various urbanization scenarios indicated that annual runoff, daily peak flow, and flood volume have increased to different degrees due to urban expansion during the study period (1988–2009), and will continue to increase as urban areas increase in the future. These results suggested that integrating distributed land use change model and distributed hydrological model could be a good approach to evaluate the hydrologic impacts of urbanization, which are essential for watershed management, water resources planning, and flood management for sustainable development.

Fasahat *et al.* (2012) used Muskingum model was commonly used hydrological model in this type of studies, which its accuracy depends on the way the coefficients of the corresponding equation (K, X) were obtained. In this research, using statistical data for the 903 km^2 area Jooneghan-Farsan watershed at Chaharmahal & Bakhtiyari province, HEC-HMS model and the recorded flood hydrographs at the local hydrometric station, the effectiveness of the Muskingum model in the flood routing had been investigated. The results on the studied floods show little change in the amount of K and X, found to be 1.9 hour and 0.05 for the watershed.

Meenu *et al.* (2012) evaluated the impacts of possible future climate change scenarios on the hydrology of the catchment area of the Tunga–Bhadra River, upstream of the Tungabhadra dam. The Hydrologic Engineering Center's Hydrologic

Modeling System version 3.4 (HEC-HMS 3.4) was used for the hydrological modelling of the study area. Linear regression- based Statistical DownScaling Model version 4.2 (SDSM 4.2) is used to downscale the daily maximum and minimum temperature, and daily precipitation in the four sub-basins of the study area. The large-scale climate variables for the A2 and B2 scenarios obtained from the Hadley Centre Coupled Model version 3 were used. After model calibration and testing of the downscaling procedure, the hydrological model was run for the three future periods: 2011–2040, 2041–2070, and 2071–2099. The impacts of climate change on the basin hydrology are assessed by comparing the present and future stream flow and the evapotranspiration estimates. Results of the water balance study suggest increasing precipitation and runoff and decreasing actual evapotranspiration losses over the sub-basins in the study area.

Motevalli *et al.* (2012) studied the hydrologic components variation of land use change of the years 1988 and 2009 in Kan watershed. Used the Landsat satellite images, the land use data in those two years was acquired, and through supervised classification were classified into four types of urban use, Complex lands (city, garden and parks), Agricultural-Garden, and Arid lands. According to this classification, the urban use of the watershed was 5.63 and 10.5 per cent of the total watershed area, respectively for study years. Afterwards, used SCS and HEC-HMS model, the watershed runoff and variation of the hydrologic balance components was computed. To run the SCS model via IDW, the total annual precipitation of 27 meteorological stations in Tehran province were used to produce the precipitation layer. In this model through zonal analysis, the relationship between runoff rate and land use change was determined. To simulate the rainfall-runoff for the years 1988 and 2009 using HEC-HMS model, the precipitation data, discharge, daily temperature and also monthly evaporation of the Sooleghan station were used. In the watershed model, the SCS Curve Number method and SCS Unit Hydrograph were selected for precipitation and flow transfer losses, respectively, and Specified Hyetograph in meteorological model was used. The models results showed that the runoff coefficient was increased from 71.79 to 87.25 per cent for SCS model, and from 56.49 to 64.10 per cent for HEC-HMS model.

Mousavi (2012) presented the application of an uncertainty based technique for automatic calibration of the well-known Hydrologic Engineering Center

Hydrologic Modelling System (HEC-HMS) model. Sequential uncertainty fitting (SUFI2) approach had been used in calibration of the HEC-HMS model built for Tamar basin located in north of Iran. The basin was divided into seven subbasins and three routing reaches with 24 parameters to be estimated. From the four events, three were used for calibration and one for verification. Each event was initially calibrated separately. As there was no unique parameter set identified, all events were then calibrated jointly. Based on the scenarios of separately and jointly calibrated events, different candidate parameter sets were inputted to the model verification stage where recalibration of initial abstraction parameters commenced. Some of the candidate parameter sets with no physically meaningful parameter values were withdrawn after recalibration. Then new ranges of parameters were identified based on minimum and maximum values of the remaining parameter sets. The new parameter ranges were used in an uncertainty analysis using SUFI2 technique resulting in much narrower parameter intervals that can simulate both verification and calibration events satisfactorily in a probabilistic sense. Results show that the SUFI2 technique linked to HEC-HMS as a simulation– optimization model can provide a basis for performing uncertainty based automatic calibration of event based hydrologic models.

Pilpayeh and Shahbazi (2012) used HEC-HMS model for evaluation of the impact of change of land cover on peak discharge and flood volume of Bilesavar located in northwestern of Iran. Hydrological model was selected because it is considering the condition of soil, vegetation, land use and land characteristics. In this study, maps of soil hydrological model against with the rainfall-runoff data was calibrated and validated by HEC-HMS model. The results showed that due to changes in land use and degradation of pastures, the flood peak was increased in 100, 50, 25, 10, 5 and 2 different return periods in years. The effect on each peak flood and river flow was also simulated and investigated under the three scenarios, the present, pessimistic and optimistic conditions.

Sardoii *et al.* (2012) compared different methods results of runoff loss evaluation (Initial and constant, Green & Ampt, SCS curve number with regard to various purpose functions (percent error in peak, peak-weighted root mean square) in HEC-HMS model and classifying them. Based on each objective function, the method that approximately in 70% events, had the least peak flow changes take place in first preference as the best method for runoff simulation and other methods placed in next

preferences. Finally, result showed that for two objective functions, Green & Ampt, SCS and Initial and constant method placed in first to three preferences, respectively. So, Green & Ampt method suggested for using in similar area and conditions.

Andrzej (2013) assessed the applicability of HEC-HMS programme to simulate a precipitation flood event in an ungauged basin. The programme had been developed by the Department of the Army Corps of Engineers and enables conducting hydrological calculations for basins with different characteristics and including a number of meteorological factors. The application of this model in Polish conditions was verified in the basin of the Stobnica River – a right tributary of the Wisłok River. The calculations were carried out for the flood event caused by a continuous rain, which occurred in April 1998. Four hydrological models were compared: geomorpho-climatic instantaneous unit hydrograph by Nash – GcIUH Nash, Snyder's synthetic unit hydrograph with the determination of parameters by regression models – Snyder reg and standard method – Snyder stand and Clark's instantaneous unit hydrograph – IUH Clark, where the model parameters were optimized in the programme. The calculations revealed that the best simulation results were obtained with the Snyder stand and Snyder reg models. Further research should be directed to verifying the applicability of HEC-HMS programme for hydrological analyses of much more extensive hydrometric material and basins with different characteristics.

Chinh *et al.* (2013) used HEC-HMS model which uses geographic information system (GIS) database for rainfall runoff and pollutant load simulation. The model was applied in order to simulate the runoff discharge and the pollutant load of total nitrogen (TN) and total phosphorus (TP) in the Chikugo River basin of Kyushu Island, Japan. First, a hydrologic modeling system (HEC-HMS) and GIS software extension tool were used for simulations of elevation, drainage line definition, watershed delineation, drainage feature characterization, and geometric network generation. Then, the spatial distributions of land cover, soil classes, rainfall, and evaporation were analysed in order to simulate the daily runoff discharge at the Chikugo Barrage from April 2005 to December 2007. It was found, that the observed and simulated results for the runoff discharges and pollutant loads were in good agreement and totally consistent, indicated the suitability of the HEC-HMS model to simulate rainfall runoff and pollutant load in the Chikugo River basin.

Eyad and Broder (2013) applied The HEC-HMS and IHACRES rainfall runoff models to simulate a single stream flow event in Wadi Dhuliel arid catchment. Stream flow estimation was performed on the basis of an hourly scale. The aim of this study was to develop a new framework of rainfall-runoff model applications in arid catchments by integrating a re-adjusted satellite-derived rainfall dataset (GSMaP_MVK+) to determine the location of the rainfall storm. The HEC-HMS model input data include soil type, land use/land cover, and slope. By contrast, the lumped model IHACRES was also applied based on hourly rainfall and temperature data. Both models were calibrated and validated using the observed stream flow data set collected at Al- Za'atari discharge station. The performance of IHACRES showed some weaknesses, while the flow comparison between the calibrated stream flow results fits well with the observed stream flow data in HEC-HMS. The Nash-Sutcliffe efficiency (NSE) for the two models was 0.51 and 0.88 respectively.

Golrang *et al.* (2013) reported the indicator watershed of Kushk-Abad Basin as the study area in Khorasan province of Iran divided to 6 sub-basins which was processed geometrically using GIS and HEC-HMS extension. With using HEC-HMS model and emission of individual repetition of the sub-basins, the homogenous flood hydrographs had gained in relation to the recorded precipitation calculated for different sub-basins. For this purpose, first by considering observed events, HEC-HMS model was optimized and calibrated. Then, for evaluating the effects of check dams on time of concentration, it was optimized and calibrated. Then, for evaluating the effects of check dams on time of concentration, it was calculated before and after of check dam's construction by use of field observations and vegetation cover improvement was also estimated after the project. These parameters were imported to HEC-HMS to find out the effects of watershed practices and then flooding condition was simulated. For assessment purposes, peak discharge and flood volume were calculated for before and after construction conditions. Results showed that check dams as mechanical measures had low effect on time of concentration while biological practices lead to decease in curve number with an average value of 4.5. This result in decrease of peak flow and flood volume meanly 19 % and 14 %, respectively.

Halwatura and Najim (2013) employed three different approaches to calibrate and validate the HEC-HMS 3.4 model to Attanagalu Oya (River) catchment

and generate long term flow data for the Oya and the tributaries. Twenty year daily rainfall data from five rain gauging stations scattered within the Attanagalu Oya catchment and monthly evaporation data for the same years for the agro meteorological station Henarathgoda together with daily flow data at Dunamale from 2005 to 2010 were used in the study. GIS layers that were needed as input data for the flow simulation were prepared using Arc GIS 9.2 and used in the HEC-HMS 3.4 calibration of the Dunamale sub catchment using daily flow data from 2005 to 2007. The model was calibrated adjusting three different methods. The model parameters were changed and the model calibration was performed separately for the three selected methods, the Soil Conservation Service Curve Number loss method, the deficit constant loss method (the Snyder unit hydrograph method and the Clark unit hydrograph method) in order to determine the most suitable simulation method to the study catchment. The calibrated model was validated with a new set of rainfall and flow data (2008-2010). The flows simulated from each methods were tested statistically employing the coefficient of performance, the relative error and the residual method. The Snyder unit hydrograph method simulates flows more reliably than the Clark unit hydrograph method. As the loss method, the SCS Curve Number method does not perform well.

Nag *et al.* (2013) used Hydrological Modeling System (HEC-HMS) in engineering practice to determine the drainage characteristics of both rural and urban watersheds. The RESOURSAT data provided useful analysis for the land use and land cover for the image. Thiessen polygons were created using 35 rain gauge stations. It was assigned to different rain gauges stations and areal precipitation of the catchments was calculated. The time series data including rainfall and discharge were processed in MS-excel. Automatic delineation of watershed was done using SWAT Tool in ARC-GIS. In addition other initial setup files i.e basin model, land-use, were created in ArcGIS and ERDAS and imported to HEC –HMS. Model and then was run for a calibration period of January 2000 to January 2010 (10 years). The calibrated parameters were validated for next 10 years. The estimated runoff values were matching with the observed runoff.

Rajasekhar *et al.* (2013) used the natural resources conservation services curve number (NRCS-CN) method is one of the most widely used methods for quick and accurate estimation of surface runoff from un-gauged watersheds, the traditional

NRCS-CN method for calculating the composite curve number is very tedious and consumes a major portion of the hydrologic modeling time. Therefore, geographic information systems (GIS) were being used in combination with the NRCS-CN method. In most of cases, HSG and LULC maps were generated by graphical analyzing software such as ArcGIS, Imagine, and Civil 3D. Shomali sub basin cover an area of near 1800 Km^2. For even more facilitating future analysis and studies the above-mentioned sub basins was divided into five sections (Northern, Southern, Central, Eastern and Western) parts. Values of Curve Number for each of above-mentioned sections were calculated by using NRCS-CN equations. The Curve Number value for Shomali sub basins was about 70.5. Remote Sensing provided a powerful tool for estimating Curve Number values in Shomali sub basin.

Reshma *et al.* (2013) studied Hydrologic Engineering Center – Hydrologic Modelling System (HEC-HMS) hydrological model to simulate runoff process in Walnut Gulch watershed located in Arizona, USA. To compute infiltration, rainfall excess conversion to runoff and flow routing, methods like Green-Ampt, Clark's Unit hydrograph and Kinematic wave routing were chosen. The model was calibrated and validated for the seven rainfall events. From the results, it was observed that HEC-HMS model performs satisfactorily for the simulation runoff for the different rainfall events.

Roy *et al.* (2013) used Hydrologic Modeling System, developed by the Hydrologic Engineering Center, USA (HEC-HMS) (with soil moisture accounting algorithm - SMA) for calibration and validated for Subarnarekha river basin in Eastern India for hydrologic response prediction. The analysis showed that the soil storage, tension zone storage and groundwater 1 storage coefficient as the sensitive parameters for the simulated stream flow. The Nash - Sutcliffe model efficiency criterion, percentage error in volume, the percentage error in peak, and net difference of observed and simulated time to peak, which were used for performance evaluation, have been found to range from (0.72 to 0.84), (4.39 to 19.47 %), (1.9 to 19 %) and (0 to 1 day) respectively, indicating a good performance of the model for simulation of stream flow and thereby quantification of available water. The study also demonstrated that the use of semi-annual parameter sets that account for changing hydrologic conditions improves model performance. It was suggested in the study that

the model might be applied to other watersheds in the Subarnarekha river basin and other hydro -meteorologically similar river basins.

Vassova D. (2013) evaluated peak discharge assessment using various methods applying 24-h storm rainfalls reduced to short duration. Rainfall-runoff models HEC-HMS based on standard Natural Resources Conservation Service hydrologic methods and KINFIL, which combines the Morel-Seytoux infiltration and kinematic wave direct runoff transformation, were used to compute runoff hydrographs. The approach of technical standard and Froehlich's method determined the peak discharges only. The results demonstrated that the peak discharges computed by Froehlich's method are mostly closest to the data provided by CHMI. For the 100-year flood, HEC-HMS based on the Curve Number (CN) method showed the best agreement.

Basarudin *et al.* (2014) intended to quantify the influence of rainfall during extreme rainfall events on the hydrological model in the Kelantan River catchment. Therefore, two dynamic inputs were used in the study: rainfall and river discharge. The extreme flood events in 2008 and 2004 were compared based on rainfall data for both years. The events were modeled via a semi-distributed HEC-HMS hydrological model. Land use change was not incorporated in the study because the study only tries to quantify rainfall changes during these two events to simulate the discharge and runoff value. Therefore, the land use data representing the year 2004 were used as inputs in the 2008 runoff model. The study managed to demonstrate that rainfall change has a significant impact to determine the peak discharge and runoff depth for the study area.

Chatterjee *et al.* (2014) used HEC-HMS model (Hydrologic Modeling System), developed by the Hydrologic Engineering Center, USA (HEC) to evaluate its applicability for the Damodar river basin in eastern India. Sensitivity analysis of the model was carried out for the input parameters. The study revealed that both the peak discharge and runoff volumes to be sensitive to rate of infiltration and percentage of impervious area. The Nash-Sutcliffe model efficiency criterion, percentage error in volume, the percentage error in peak and net difference of observed and simulated time to peak, were used for performance evaluation. The model demonstrated good performance, with aforementioned performance indices

values ranging from 75-81 %, -10.5-19.4 %, -18.0-29.6 % and 0-1 day for simulation of stream flow.

Choudhari *et al.* (2014) used HEC-HMS model to simulate rainfall-runoff process in BalijoreNala Watershed of Odisha, India. To compute runoff volume, peak runoff rate, base flow and flow routing methods SCS curve number, SCS unit hydrograph, Exponential recession and Muskingum routing methods were chosen, respectively. Rainfall-runoff simulation is conducted using 24 random rainstorm events covering four year (2010 – 2013) data. Out of these, 12 events were selected for model calibration and the remaining 12 events for model validation. For calibration of model the statistical tests of error functions like mean absolute relative error (MARE) and root mean square error (RMSE) between the observed and simulated data were conducted. The results indicated values of MARE of 0.20 and 0.25 for runoff depth and peak discharge, respectively. Similarly the values of RMSE between the observed and simulated data were obtained as 2.30 mm and 0.28 m^3/s for runoff depth and peak discharge, respectively. However after parameter optimization the above mentioned error functions reduced to 0.10, 0.12, 0.75 mm and 0.09 m^3/s in sequence. The calibrated model with optimized parameter was used for model validation. The model validation was found to be satisfactory with low values of statistical error functions.

Das (2014) developed a hydrological model by partitioning a river basin into many subbasins by stream-network approach. Soil Conservation Service's (SCS) Curve Number (CN) method in combination with Muskingum routing technique was applied to route the surface runoff from different sub-basins. Hydrologic Modeling System (HEC-HMS) simulation tool was successfully applied for processing the input rainfall data recorded over four rainfall stations namely, Simulia, Rangagora, Kharidwar and Tusama. The performance of the developed model was checked for two severe storms occurred over the catchment. Results indicated that, the predicted runoff volumes obtained from developed model were in good agreement with observed runoff value for both the cases.

Ebrahimiyan and Ghaderi (2014) presented rainfall- runoff process of Mahabad dam basin was simulated by the HEC-HMS conceptual model. The simulating process was done by using the SCS curve number and Initial and Constant Loss methods for calculating the loss rate, and Clark unit hydrograph and Snyder unit

hydrograph for calculating the runoff rate, and their performance was evaluated using statistical criteria, Peak-weighted Root Mean Square Error (PRMSE) and correlation coefficient (R^2). Reviewed the Simulation results indicate a better adaptation of the SCS Curve Number method in compare to initial and Constant Loss method.

Farokhsha and Farokhsha (2014) highlighted the digital map, a digital layer of physical, hydrological basins monastery, is derived by extension from Hec-GeoHMS. In order to identify areas contributing runoff, the basin is divided into several sub-basins. They concluded that precipitation occurred at the beginning of the year 89 to May 1390 is composed of only two sub-basin runoff. In the study, seven rainfall events between April 1386 and May of 1390 were examined. Among them randomly selected 4 events and were simulated in the HEC-HMS program. Model Basin, precipitation losses SCS from curve number method and the conversion of rainfall to runoff and base flow SCS unit hydrograph method with a fixed monthly amount and the meteorological models, precipitation data using the entering data into the model and simulated rainfall - runoff has been done. After calibrating the model using the objective function of the error percentage in peak flow, determining the calculated optimal values of the fitted curve number, initial mortality was estimated precipitation and latency. In order to validate the model, two other rainfall events were used to calculate the optimum accuracy that was confirmed by simulated flood hydrograph in the two events. The results of this research can be important for the effective area of the basin runoff, considering the amount of moisture condition CN, high sensitivity to changes in catchment rainfall amounts of casualties among the best values in the calibration, high accuracy compared to the simulated peak flow runoff production can be mentioned.

Iliasse and Alaoui (2014) applied various techniques and models for catchment delineation, and developing methods to calculate a Curve Number values for the Kalaya river basin located in Northern Morocco, by implementing GIS software (ArcGIS, HEC-GeoHMS), Erdas Imagine and hydrologic modeling (HEC-HMS), in which the estimation of the direct runoff under the scenario with precipitation of 80 mm during the storm event that had occurred between 23 and 24 December 2009. In particular, SCS-CN (Soil Conservation Curve Number) was a model through which the estimation of the direct runoff can be achieved. This method

includes several important properties of the watershed such as Hydrological Soil Groups and land use, which will be input for the HEC-HMS model.

Patel *et al.* (2014) reviewed the hydrological models are primarily used for hydrologic prediction and for understanding hydrologic processes. Watershed hydrological modelling and associated calibration and validation processes require a large set of spatial and temporal data. In practice, the availability and quality of these data are often an issue to cope with. Sometimes one has to compromise the overall modelling quality because of insufficient high-resolution data for developing, calibrating and validating the model. The current paper describes the study of various literatures on development such a strategy by combining fine-scale event and coarse-scale continuous hydrological modelling with Hydrologic Engineering Center Hydrologic Modelling System (HEC-HMS).

Sanyal *et al.* (2014) evaluated how varying degrees of land use/cover (LULC) changes across sub-catchments affects the flood peak at the catchment outlet. The Kona catchment, a part of the upper Damodar Basin in eastern India, was the study site. A HEC-HMS model was set up to simulate rainfall-runoff processes for two LULC scenarios three decades apart. Because of sparse data at the study site, they used the Natural Resource Conservation Service (NRCS) Curve Number (CN) approach to account for the effect of LULC and soil on the hydrologic response. Although a weak ($r = 0.53$) but statistically significant positive linear correlation was found between sub-catchment wise LULC changes and the magnitude of flood peak at the catchment outlet, a number of sub-catchments showed marked deviations from this relationship. The varying timing of flow convergence at different stream orders due to the localised LULC changes makes it difficult to upscale the conventional land use and runoff relationship, evident at the plot scale, to a large basin. However, a simple modelling framework was provided based on easily accessible input data and a freely available and widely used hydrological model (HEC-HMS) to check the possible effect of LULC changes at a particular sub-catchment on the hydrograph at the basin outlet.

Silva *et al.* (2014) carried out study of event and continuous hydrologic modeling in the Kelani River basin in Sri Lanka using the Hydrologic Engineering Center—Hydrologic Modeling System (HEC–HMS). The calibrated, direct runoff and base flow parameters were then used in the continuous hydrologic model. The Green

and Ampt infiltration loss method was used to account for infiltration loss in event-based modeling and a five-layer soil moisture accounting loss method was employed in continuous modeling. The Clark unit hydrograph method and the recession base flow method were used to simulate direct runoff and base flow, respectively. The results in the study depicted the capability of HEC–HMS to reproduce stream flows in the basin to a high accuracy with averaged computed Nash–Sutcliffe efficiencies of 0.91 for event–based simulations and 0.88 for continuous simulations. Simulated river flows affirmed that the event-based hydrologic modeling supported by intensive field data is useful to derive calibrated parameters for continuous hydrologic modeling. The study demonstrated potential of HEC–HMS application in disaster mitigation, flood control, and water management in medium-size river basins in tropical countries.

Laouacheria and Mansouri (2015) compared two hydrological models, namely WBNM and HEC-HMS, and a GIS procedure was used to predict runoff hydrographs of a small urban catchment located in Azzaba city. The aim was to test the effect of catchment size and time steps on runoff hydrograph shape, and to evaluate the catchment reaction to a given rainfall event obtained from the established IDF Curves. Furthermore a sensitivity analysis of the parameters of the models was carried out. In addition the results of the models are compared with the observed runoff data, measured during a storm event that occurred in 11th of Mars, 2014. This calibration was performed by applying different situations of catchment size and time steps. Then, characteristics of calculated hydrographs were compared with the same characteristics of the same observed hydrographs and analyzed statistically. The results were indicated that HEC-HMS provide acceptable simulations in the flood events, which WBNM fail to simulate. Finally, hydrographs simulated by the HEC-HMS model had the best fit with the real situation. It was necessary to generalize this study and build up the data base for the further application of rainfall runoff model in Algeria.

Narasayya (2015) focused on the stream flow estimation of Gumani watershed using a GIS based hydrological model. To reflect the spatial information effectively to the stream flow estimation this study was conducted using Geo spatial Hydrologic modelling extension of HEC-GeoHMS and a Hydrologic Modelling System HEC-HMS. An attempt has been made for estimation of stream flow and comparison with different channel Routing and Loss approaches. Typical software

was used for statistical analysis of rainfall as input for meteorological model to be used in HEC-HMS. The simulation results from HEC-HMS reveals that stream flow gives more from Muskingum routing with Soil Conservation Services-Curve Number (SCS-CN) Loss method for all the return periods. It also indicated that, by considering both Routing and Loss methods, initial and constant loss method gives lower stream flows.

Prajapati (2015) assessed the run of river hydropower potential of the Karnali Basin by using GIS (Geographical Information System) and Continuous Semi-distributed Hydrological Model (Hydrological Modeling System – HMS). The digital Elevation model (DEM) was used to calculate the elevation data of upstream and downstream ends of the reaches and daily discharges of the reaches were derived from precipitation data using HEC-HMS model with Nash efficiency ranging from 61.7 % to 82.02 % and the volume deviation -1.52 % to 17.3 % for calibration and validation period. Using design discharge corresponding to 40^{th} percentile flow with the hydraulic head, total power potential of 14150.80 MW was determined.

CHAPTER III
MATERIALS AND METHODS

This chapter deals with the description of the study area selected, details of data collected, generated, and used for rainfall runoff modelling along with details of the models applied. A theoretical consideration of various models, and methods applied are also presented in this chapter.

3.1 Description of the Study Area

Hadaf River is tributary of Panam river. Hadaf river basin is the case study area in this research which is located in Panchmahals, Gujarat, India. Hadaf dam site is situated at 43 km far from Godhra, headquarter of Panchmahals district, Gujarat. This location is situated at N latitude 22° 53' 26.327" and E longitude 73° 52' 43.714" with elevation of 164 m mean sea levels. The Study area is located in between E longitude 73° 52' 9.064" to 74° 11’ 8.536" and N latitude 22° 40' 33.039" to 22° 57' 48.301". The catchment lies in semi-arid region located in middle Gujarat having area of 502.7 km^2. As the watershed being situated in semi-arid region and dominated with agriculture and forest land, water availability in the region is an important and critical issue. One rainwater harvesting structure (Umaria reservoir) has been put in place over the past years located at N latitude 22° 46' 00" and E longitude 74° 04' 12" and having an area of 72.52 km^2, having a bit success in improving the water availability for Agricultural production. There is huge scope of improving the potential of the watershed for increasing the availability of water for agriculture.

The area has semi-arid type of weather condition with winters, summers and rainy season with average annual rainfall of about 843 mm. It is characterized by three distinct seasons: rainy season (June to September), and winter (October to February) and hot spring (March to May). The winter temperature ranges between 15℃ - 30℃. In the hottest months of the year (April, May and June), the maximum temperature goes as high as 42℃ and minimum temperature 30℃. In general, the site receives ample rainfall during the rainy season, which starts from June and continues up to September. June and July receive the highest amount of rainfall.

The water need and availability especially for agriculture in the area is completely dependent on rainfall. The rainfall is highly lacking in amplitude or

quality which has resulted in recurrent phenomenon of draught. Lack of surface water sources and limited availability of ground water in the area causing hindrance in the irrigation and drinking water requirement. The average land holding is about 1 ha in the area and lack of irrigation source forces the majority of these farmers to migrate to ensure their livelihood. This affects directly the demographic profile of the village. The major crops cultivated in the area are Makai (Maize), Danger (Peddy), Soyaben, Ghau (Wheat), Tuver (Pigean Pea), and Chana (Gram) in the study area. If rain is good and proper irrigation source is available then the farmer can not only improve the agriculture production in the kharif season but can also cultivate rabi crops viz. Wheat, and Gram. The productivity is low not because of the land is unproductive or the farmer's lack of skills to manage their agriculture crop but it is due to the lack of irrigation sources availability and scarcity of rainfall. Agriculture could be effective only when it gets sufficient water at the right time. Therefore, to ensure sustainable agricultural development, there should be reliable supply of water as well as proper land and water management systems to effectively utilise the available land and water resources in the area. Hence, one of the important aspects in this process is to understand the underlying hydrological processes and rainfall runoff relationship of the watershed.

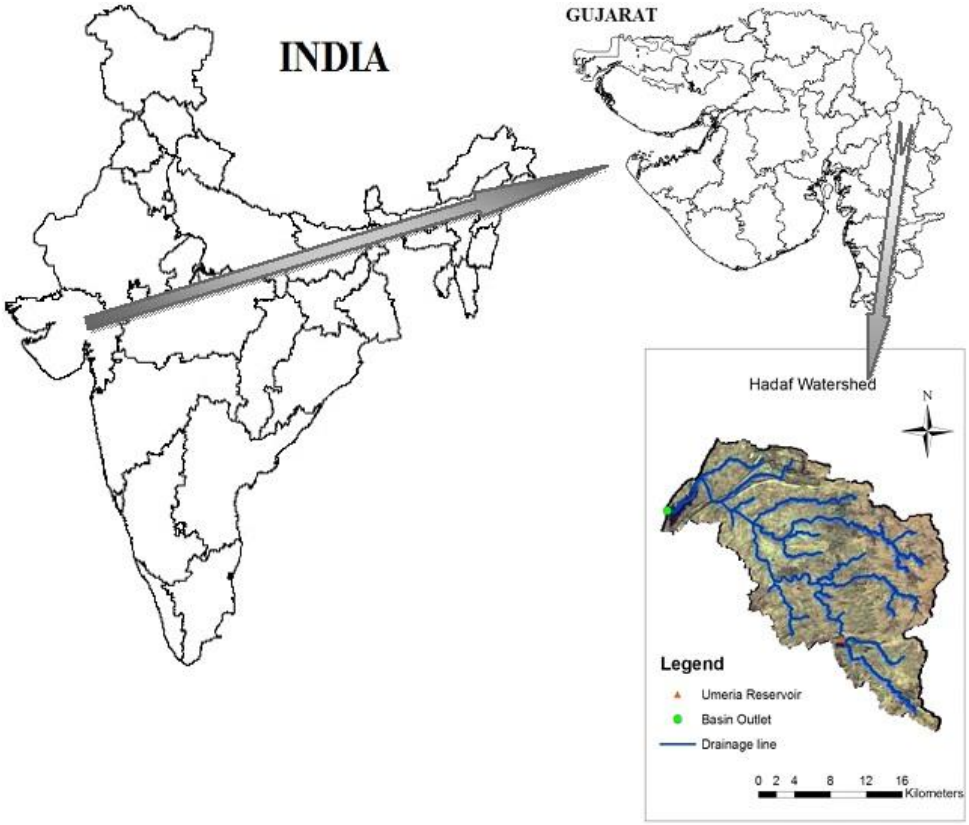

Fig. 3.1 Geographical location of study area

3.2 Data Applied for Model Development

For rainfall runoff simulation different hydro-climatic and remote sensing data are collected as presented in Table 3.1 (a) & (b).

Table 3.1 (a): Hydro-meteorological and remote sensing data

Data	Description	Source of Data
Hydrological and meteorological data	Rainfall, Discharge.	➢ Hadaf Irrigation Project, Morava, Godhra ➢ Umariya Irrigation Project, Umariya, Dahod. ➢ Sevasadan Department, Godhra. ➢ Panam Dam Circle Office, Godhra
Remote Sensing data	Landuse/cover map, soil map, slope map, drainage map.	➢ National Remote Sensing Center, Hyderabad. ➢ Bhaskaracharya Institute for Space Application and Geo-informatics (BISAG), Gandhinagar. ➢ Downloaded from Global Land Cover Facility Data Centre of

		Maryland University, USA.
	Digital elevation model (DEM)	➢ SRTM (Shuttle Radar Topography Mission) united states geological survey. ➢ ASTER Download from USGS site
	Base map/ Topography sheet	➢ Survey of India.

Table 3.1 (b): Details of satellite imageries

Sr. No	Date of pass	Remote Sensing Imageries
1	13-10-2008	LISS-III 2008
2	21-11-2012	LISS-III 2012
3	08-01-2013	LISS-IV 2013

3.3 Software's Used

- **ERDAS Imagine:** The ERDAS (Earth Resources Data Analysis System) imagine, an image processing software has been extensively used for importing and exporting of different remote sensing images from one format to another, rectification of imageries, sub setting of images, classification of images and preparation of thematic maps.
- **ArcMap:** In the present study ArcMap software developed by ESRI (Environmental Systems Research Institute) has been used extensively for arranging all the thematic layers in proper sequence, and to perform different operations such as overlaying, intersection etc. to generate Hec-GeoHMS compatible input file
- **HEC-GeoHMS Version 5.0:** It is a geospatial hydrology toolkit for engineers with limited GIS experience. It is an extension package used in ArcMap software. In this study, HEC-GeoHMS is used to derive river network of the basins and to delineate sub basins of the basins from the digital elevation model (DEM) of the basins. It is also used to calculate different geo-morphological characteristics of the watersheds.
- **HEC-HMS Version 3.5:** It is hydrologic modelling software developed by US Army Corps of Engineers Hydrologic Engineering Center. It includes

many of the well-known and well applicable hydrologic methods to be used to simulate rainfall-runoff processes in river basins.

3.4 Extraction of Morphological Parameters

The morphological characteristics of a basin govern its hydrological response to a considerable extent **(Singh *et al.*, 2003)**. The morphological characteristics of a basin represent its attributes, which may be employed in synthesizing its hydrological behavior. Basin characteristics when measured and expressed in quantified morphometric parameters can be studied for their influence on runoff. In the present study, the important morphological parameters for Hadaf watershed have been derived using ArcMap GIS software. Various formulae to calculate the morphometric parameter are listed in Table 3.2.

Table 3.2: Mathematical formula to calculate morphometric parameters

Sr. No.	Morphometric Parameters	Formula	Reference
1	Stream order (N_u)	Hierarchical rank	Horton (1945)
2	Stream Length ratio (R_L)	$R_L=L_u-L_{u-1}$	Horton (1945)
3	Bifurcation ratio (R_b)	$R_b=N_u/N_{u+1}$	Schumm (1956)
4	Drainage Density (D_d)	$D_d=L_u/A$	Horton (1932)
5	Length of over Land flow (L_g)	$L_g=1/D_d*2$	Horton (1945)
6	Fitness ratio (R_{fn})	$R_{fn}=L_b/p$	Melton (1957)
7	Circularity Ratio (R_c)	$R_c=4*pi*A/P^2$	Miller (1953)
8	Elongation Ratio (R_e)	$R_e=(2/L_b)X(A/pi)^{0.5}$	Schumn (1956)
9	Form factor (R_f)	$R_f=A/L_b^2$	Horton (1932)
10	Unity Shape factor (R_u)	$R_u=L_b/A^{0.5}$	Horton (1945)
11	Watershed Shape factor (W_s)	$W_S=L_m/D_c$	Wu *et al.* (1964)
12	Compactness Coefficient (C_c)	$C_c=0.2821*P/A^{0.5}$	Strahler(1964)
13	Drainage texture (R_t)	$Rt=N_u/P$	Horton (1945)

14	Total Relief (H)	$H=h_1-h_2$	Hardley and Schumn (1961)
15	Relief Ratio (R_h)	$R_h=H/L_b$	Schumn (1956)
16	Relative relief (R_p)	$R_p=H/P$	Melton (1957)

Where, A = area of basin (km^2), N_u = total number of stream segment of order 'u', L_u = total stream length of all order (km), P = perimeter of basin (km), L_b = Basin length (km), D_c = Diameter of circle having same area as that of watershed, L_m = Length of main channel (km), N_u = Total No. of Stream of all orders, h_1 and h_2 = Highest and lowest points on the valley floor of a watershed.

3.5 HEC-HMS Model

The HEC-HMS model was developed by the US Army Corps of Engineers (USACE) Hydrologic Engineering Center's (HEC) and is well known hydrological model of the most widely used rainfall-runoff models. HEC-HMS was designed to simulate the rainfall-runoff process of a dendritic watershed system (USACE, 2000). The model is suitable for small and larger catchment hydrologic applications in addition to lumped and distributed rainfall-runoff modelling such as water balance studies, flood studies, impact of land use and climate change on runoff generation and flooding. Before going to HEC-HMS the input data files are prepared using HEC-GeoHMS, ERDAS Imagine and Arc-GIS which are describe below.

3.5.1 Input data for HEC-HMS

The input data for HEC-HMS model setup includes Digital Elevation Model (DEM), rainfall, stream-flow gauge data, soil types, land-use/land-cover data, etc. Data describing the terrain should be in ESRI's ARC Grid Format while vector data, such as stream alignments and stream flow gauge locations, should be in the shapefile format.

In the present study performance of two DEM remote sensing images viz., SRTM with 90 m resolution and ASTER with 30 m resolution is assessed in watershed delineation and drainage network generation. This SRTM 90 m and ASTER 30 m DEM in ESRI Arc Grid format has been used to develop HEC-HMS

basin model. Hydro-meteorological parameters like rainfall, discharge, temperature are collected from the different gauging station in the watershed. Land-use/land-cover data are prepared using superwised classification in ERDAS Imagine and soil data is prepared in Arc GIS environment.

3.5.2 HEC-GeoHMS Model

The Geospatial Hydrologic Modelling Extension (HEC-GeoHMS) has been developed in year 2000 by Hydrologic Engineering Centre (HEC), California, USA, as a geospatial hydrology toolkit for engineers and hydrologists with limited GIS experience. HEC-GeoHMS uses ArcView and the Spatial Analyst extension to visualize spatial information, document watershed characteristics, perform spatial analysis, and delineate sub basins, streams and develop a number of hydrologic modelling inputs for the HEC-HMS. The following steps describe the major steps in starting a HEC-HMS project and taking it through the HEC-GeoHMS process.

3.5.2.1 Terrain Preprocessing

Using the terrain data as input, terrain pre-processing is a series of steps to derive the drainage network. The steps consist of computing the fill sinks, flow direction, flow accumulation, stream definition, and watershed delineation.

(a) Fill DEM: The Fill DEM is created by filling the depressions or pits by increasing the elevation of the pit cells to the level of the surrounding terrain. The pits are often considered as errors in the DEM due to re-sampling and interpolating the grid.

(b) Flow Direction: Flow direction map generated using Hydro DEM as input data, which defines the direction of the steepest descent for each terrain cell. Similar to a compass, the eight point pour algorithm specifies the following eight possible directions as shown in Figure 3.2

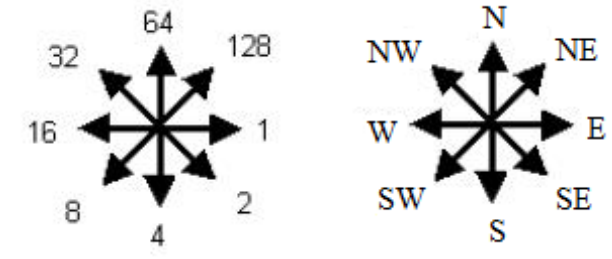

Fig. 3.2: Eight-point pour algorithm for flow direction

(c) Flow Accumulation: Flow accumulation map determines the number of upstream cells draining to a given cell, using flow direction data as input. Upstream drainage area at a given cell can be calculated by multiplying the flow accumulation value by the grid cell area.

(d) Stream Definition: This step classifies all cells with a flow accumulation greater than the user-defined threshold as cells belonging to the stream network. The user specified threshold may be specified as an area in distance units squared. e.g., square kilometres, or as number of cells. The flow accumulation for a particular cell must exceed the user-defined threshold for a stream to be initiated. The default is one percent (1 %) of the largest drainage area in the entire DEM.

(e) Stream Segmentation: Flow direction and stream grids are used to divide the stream grid into segments. Streams segments, or links, are the sections of a stream that connect two successive junctions, a junction and an outlet, or a junction and the drainage divide.

(f) Catchment Grid Delineation: The watershed is delineated in subbasins for every stream segment using flow direction and stream link grids.

(g) Catchment Polygon Processing: A vector layer (polygon subbasin layer) of subbasin is created using the catchment grid.

(h) Drainage Line Processing: A vector stream layer is generated using stream link and flow direction grid.

(i) Watershed Aggregation: This step aggregates the upstream subbasin at every stream confluence using drainage line and catchment layer. This is a required step and is performed to improve computational performance for interactively delineating subbasins and to enhance data extraction when defining a HEC-GeoHMS project.

(j) Hydrological Processing: Hydrologic process is generally responsible for hydrological model construction and setup. HEC-HMS project area is generated defining the outlet of the watershed. After defining the downstream outlet new datasets Main ViewDEM, RawDEM, HydroDEM, flow direction grid, Flow accumulation grid, stream grid, stream link grid, catchment grid, subbasin, project point and river are created for new project.

3.5.3 HEC-HMS Overview

After that we need to define in detail the study area and develop input files for HEC-HMS project. To this end, a new project has to start through the module "HMS Project setup", so that a directory for the extracted data will be created. Next step is the definition of a project point. This point is situated at the downstream end of the Hadaf River Basin. After defining the downstream outlet, a tool named "Generate Project" is applied, and the area upstream the outlet is defined. Necessary data for the drainage area are extracted from the "Terrain Pre-processing" and a Project for the study area is created.

3.5.3.1 Basin Processing

After the terrain preprocessing is completed and a new project has been created, basin processing is used to revise the sub-basin delineations. Basin processing includes basin merge, basin subdivision, river merge, river profile, extract physical characteristics of streams sub-basins, develop hydrologic parameters and develop HMS inputs.

(a) Basin Merge: Multiple sub-basins are merged together into one sub-basin. There are following rules for sub-basins merge:

i. The sub-basin must share a common confluence

ii. The sub-basin must be adjacent in an upstream and downstream manner.

iii. More than two sub-basins are permitted.

(b) River Profile: The river profile is created by extracting elevation values from the terrain model along the stream line which provides information on slopes and grade breaks that can be useful for selecting delineation points.

(c) Stream and Watershed Characteristics: When the stream and sub-basin delineation has been finalized, physical characteristics for a stream line such as length, upstream and downstream elevations, and slope are extracted from the terrain data. Similarly, physical characteristics for a sub-basin, such as longest flow length, centroidal flow lengths, and slopes are extracted from the terrain data.

(i) River Length: River length is computed using river layer for selected or all routing reaches in the river layer.

(ii) River Slope: Upstream and downstream elevation and slope of a river is computed using RawDEM and River layer as input data.

(iii) Basin Slope: Average basin slope in the watershed is computed using sub-basin and slope grid. Basin slope is used for the computation of the CN Lag time parameter.

(iv) Longest Flow Path: A number of physical characteristics such as the longest flow length, upstream/downstream elevation and slope between endpoints are computed using RawDEM, flow direction grid and sub-basin.

(v) Basin Centroid: Basin centroid is identified for each sub-basin. There are three algorithm Center of gravity method, longest flow path method and 50% area method.

(vi) Basin Centroid Elevation: Elevation for each centroid point is calculated using RawDEM.

(vii) Centroidal Flow Path: Centroidal flow path is calculated using sub-basin, centroid and longest flow path. It is measured from the projected point on the longest flow path to the sub-basin outlet.

(d) Hydrologic Parameters: After the physical characterises of streams and sub-basins, hydrologic parameters are defined such as HMS process (loss method, transform method, base-flow type, and routing method), river auto name, basin auto name, time of concentration, CN Lag method, etc.

(e) Develop HEC-HMS Model Files: HEC-GeoHMS produces a number of files that can be used directly by HEC-HMS. These files include background map files, the basin model file, the meteorological model file and a project file.

(i) Map to HMS Units: Physical characteristics of RawDEM, Sub-basin, Longest flow path, centroidal longest flow path, river and centroid are converted to English or International System (SI) units.

(ii) HMS Data Check: Data check is necessary to keep track of the relationship between the stream segments, sub-basins, and outlet points.

(iii) HEC-HMS Basin Schematic: The HMS basin schematic is the GIS representation of the HEC-HMS model. It shows the network of basin elements (nodes/links or junctions/edges) and their connectivity.

(iv) HMS Legend: Point and line features in the HMS Node and HMS Link layers are presented.

(v) Add Coordinates: Geographic coordinates are attached to features in the HMS Node and HMS Link layers using RawDEM. The coordinates are added to attribute tables.

(vi) Prepare Data for Model Export: Basin model file is exported with hydrologic elements, their connectivity, and related parameters using sub-basin and river layers.

(vii) Background Map File: Background map layers capture the geographic information of the sub-basin boundaries and stream reaches in ASCII text file or shape file format.

(viii) Basin File: The basin model captures the hydrologic elements, their connectivity, and related geographic information in ASCII text file that can be loaded into an HEC-HMS project.

3.5.3.2 HEC-HMS Features: Data entry can be performed for individual basin elements such as sub-basins and stream reaches or simultaneously for entire classes of similar elements. Tables and forms for entering necessary data are accessed from a visual schematic of the basin. Each HEC-HMS project requires three data components: a Basin Model, a Meteorological Model, and Control Specifications.

3.5.3.3 Basin Model Data: The basin model contains data, which represents the physical system. The descriptive data is entered by the user or imported from GIS and can be edited. Such data includes specification of the hydrologic elements of which the basin model is comprised, information on how the hydrologic elements are connected, and values of parameters for the hydrologic elements. A basin model consists of hydrologic elements, of which there are seven types: sub basin, routing reach, junction, reservoir, diversion, source, and sink. The development of a basin model requires the specification of such elements and data that controls their 'behaviour'.

Table 3.3: Hydrologic elements used in HEC-HMS model

Element/Symbol	Description
Sub-basin 	A physical watershed or a region of space enclosed by a single boundary line following natural drainage divides which precipitation falls and only one outflow (i.e. excess precipitation) is transforming to outlet which located at the most downstream point in the basin.

Reach 	A single line which carries flow downstream from one or many upstream hydrologic elements in the basin model. All inflow is added together and the outflow terminates at the watershed outlet.
Junction 	A location where multiple stream flow from upstream hydrologic elements are joint together (i.e. at a confluence) to form one downstream reach, or where the drainage from a sub-basin enters a channel reach.
Diversion 	A location where one upstream reach splits to form two downstream reaches, or where water is withdrawn from the channel and may be discharged to a canal or downstream.
Reservoir 	An area of impounded water bounded by lines, which have one or more inflow (which add together) and only one computed outflow. It is normally used to model the detention and attenuation of a hydrograph caused by a reservoir or detention pond.
Source 	An inlet location where a river discharges water derived from a drainage area lying outside the study watershed. Source elements are particularly useful for partitioning a large region into smaller study areas using gauged flows at the source locations to describe the contribution of upstream tributary areas, thus outflow from the source element is defined by the user.
Sink 	An outlet location where a river discharge leaves the watershed. There is one or many inflows that come from upstream hydrologic elements and no outflow from the sink element.

3.5.3.4 Meteorological Model: The Precipitation Model is a set of information required to define historical or hypothetical precipitation to be used in conjunction with a basin model. Types of hypothetical storm include frequency-based and the Corps of Engineers' Standard Project Storm. Frequency-based storms require that the user provide rainfall depths for various durations. Gauge weights of each rain gauge station are defined in meteorological model manager.

3.5.3.5 Control Specifications: Lastly, the Control Specifications define time-related information for a simulation, including the starting and ending dates and the time

interval for computations. The function of control specifications is to set the starting and ending dates and times and time (computation) interval.

3.5.4 HEC-HMS Model Set-up

The HEC-HMS model provides a variety of options for simulating precipitation-runoff processes. The hydrologic elements are arranged in a dendritic network, and computations are performed in an upstream-to-downstream sequence. Computations are performed in SI units. A schematic flowchart of different processes involved in rainfall-runoff transformation processes are shown in Fig. 3.3.

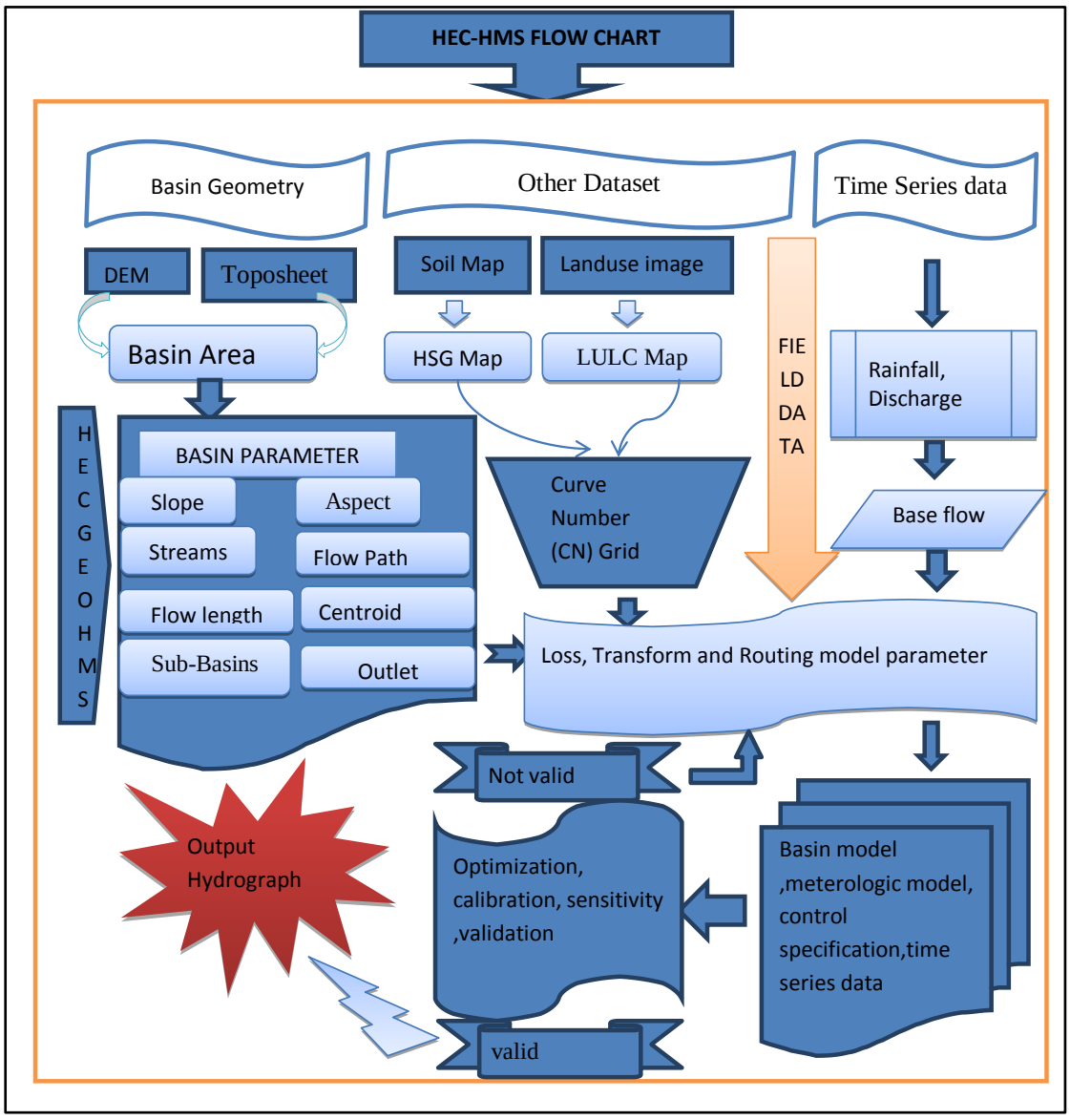

Fig. 3.3: HEC-HMS Flow Chart

3.5.5 Loss Rate Method

Precipitation loss is the main factor that influences direct runoff in the basin. Usually precipitation loss is used to estimate the relationship between precipitations and exceeding or effective precipitation. Normally, after rainfall, precipitation loss is caused by interception, storage, evaporation, and infiltration. When the storm events are simulated, only influences caused by infiltration, evapotranspiration, and interception are considered, and storage is ignored in storm simulation; thus, infiltration is the main factor for estimating precipitation loss.

Sub-basin soil types can be divided into pervious surface and directly-connected impervious surface in HEC-HMS. With impervious surface, all the precipitation transforms to the runoff and is expressed in the percentage of basin area. Out of twelve different loss methods available in this research, the SCS-CN method, which was developed by U.S. Soil Conservation Service to estimate direct runoff, is applied. The SCS-CN method is a simple, widely used and efficient method for determining the approximate amount of runoff from a rainfall. Although the method is designed for a single storm event, it can be scaled to find average annual runoff values. The data requirements for this method are very low i.e. rainfall amount and curve number, where curve number is a function of land use, soil type and slope.

3.5.5.1 SCS-CN Method

In the early 1950s, the United States Department of Agriculture (USDA) Natural Resources Conservation Service (NRCS) (then named the Soil Conservation Service (SCS)) developed a method for estimating the volume of direct runoff from rainfall. This method, which is often referred to as the CN method, was empirically developed for small agricultural watersheds. Analysis of storm event rainfall and runoff records indicates that there is a threshold that must be exceeded before runoff occurs. The storm must satisfy interception, depression storage, and infiltration volume before the onset of runoff. The rainfall required to satisfy the above volumes is termed initial abstraction. Additional losses will occur as infiltration after runoff begins, whereas accumulated infiltration increases with rainfall up to some maximum retention amount. Runoff also increases with rainfall. The standard SCS-CN method is based on the following relationship between rainfall, P (mm), and runoff, Q (mm) (Soil conservation service engineering division, 1986; Schulze *et al.* 1992):

$$Q = \begin{cases} \dfrac{(P - I_a)^2}{P - I_a + S} & P > I_a \\ 0 & P \le I_a \end{cases} \quad (3.1)$$

Where, *S* (mm) is potential maximum retention after runoff begins.

I_a is all loss before runoff begins. It includes water retained in surface depressions, water intercepted by vegetation, evaporation, and infiltration. I_a is highly variable but generally is correlated with soil and land cover parameters. To remove the necessity for an independent estimation of I_a, a linear relationship between I_a and *S* was suggested by Soil conservation service engineering division (1986) as: $I_a = S\lambda$, where λ is an initial abstraction ratio. The values of λ vary in the range of 0 to 0.3 and have been documented in a number of studies encompassing various geographic locations in the United States and other countries (Shrestha 2003). Through studies of many small agricultural catchments, I_a was found to be approximated by empirical equations such as Ia= 0.2*S*.

By removing I_a as an independent parameter, a combination of *S* and *P* to produce a unique runoff amount can be approximated. Substituting $I_a = 0.2S$ give

$$Q = \frac{(P - 0.2S)^2}{P + 0.8S} \quad (3.2)$$

The variable *S*, which varies with antecedent soil moisture and other variables, can be estimated as

$$S = \frac{25400}{CN} - 254 \quad (3.3)$$

Where, *CN* is a dimensionless catchment parameter ranging from 0 to 100. A *CN* of 100 represents a limiting condition of a perfectly impermeable catchment with zero retention, in which all rainfall becomes runoff. A *CN* of zero conceptually represents the other extreme, with the catchment abstracting all rainfall and with no runoff regardless of the rainfall amount. The curve number can be determined from empirical information. The SCS has developed standard tables of curve number values as functions of catchment land use/cover conditions and HSG (hydrologic soil

group). These are listed in the *SCS User Manual* (Soil conservation service engineering division,1986).

The HSG refer to the standard SCS soil classifications based on water infiltration capacity. Water infiltration capacity of the soil was classified by the USDA-SCS into four classes called hydrologic soil groups (Mihalik *et al.,* 2008; Matziaris *et al.,* 2005) Every type of soil has a HSG that indicates an infiltration capacity and a rate of water transmission through the soil. The four types of HSGs are presented in Table 3.4. The HSG values are based on the intake and transmission of water under the conditions of maximum yearly wetness (thoroughly wet) and are valid for unfrozen soil. When assigning a HSG to a soil, bare soil surface is considered. The land cover and land use are used in conjunction with these HSGs in order to obtain the final value of the Curve Number (CN) parameter.

In this classification, A, refers to sand and aggregated silts with high infiltration rates, classification D,

Corresponds to soils that swell significantly when wet and have low infiltration rates. The HSG reflects a soil's permeability and surface runoff potential.

Table 3.4: Classification of hydrologic soil groups (USDA-NRCS 2007)

Hydrologic Soil Group (HSG)	**Surface runoff potential**	**Final infiltration rate (mm/h)**	**Permeability rate (mm/h)**
A	Soils in this group have low runoff potential when thoroughly wet. Water is transmitted freely through the soil. Group A soils typically have less than 10 percent clay and more than 90 percent sand or gravel and have gravel or sand textures.	25	> 7.6
B	Soils in this group have moderately low runoff potential when thoroughly wet. Water transmission through the soil is unimpeded. Group B soils typically have between 10 percent and 20 percent	13	3.8 to 7.6

	clay and 50 percent to 90 percent sand and have loamy sand or sandy loam textures.		
C	Soils in this group have moderately high runoff potential when thoroughly wet. Water transmission through the soil is somewhat restricted. Group C soils typically have between 20 percent and 40 percent clay and less than 50 percent sand and have loam, silt loam, sandy clay loam, clay loam, and silty clay loam textures.	6	1.3 to 3.8
D	Soils in this group have high runoff potential when thoroughly wet. Water movement through the soil is restricted or very restricted. Group D soils typically have clay textures. Soils in this group may have high shrinks well potential, a water table or a water impermeable layer close to the surface.	3	< 1.3

Landuse and land cover maps are generated using remote sensing imageries. LISS-III and LISS-IV and remote sensing imageries are applied in this study. These imageries are applied to calculate CN values for different years to further assess the impact of land use on runoff generation. The categories of landuse are determined according to the required level of detail in the results. Table 3.5 (a) presents an example of standard CN values associated to the most frequent landuse categories for each of the four hydrologic soil groups. The landuse categories are the main landuse categories used in hydrologic analysis with the SCS method.

Table 3.5 (a): Curve numbers for hydrologic cover complexes for watershed condition II, and Ia = 0.2 S_M (USSCS, 1964; Das, 2009).

Sr. No.	**Land use cover**	**Treatment**	**Hydrologic condition**	**Hydrologic soil group**			
				A	**B**	**C**	**D**
1.	Fallow	Straight row	Poor	77	86	91	94

2.	Row crops	Straight row	Poor	72	81	88	91
			Good	67	78	85	89
		Contoured	Poor	70	79	81	86
			Good	65	75	82	86
		Contoured and terraced	Poor	66	74	80	82
			Good	62	71	78	81

Table 3.5 (b): Runoff curve numbers for (AMC II) for the Indian conditions.

Sr. No.	**Land use cover**	**Treatment**	**Hydrologic condition**	**Hydrologic soil group**			
				A	**B**	**C**	**D**
1.	Cultivated	Straight Row	……	76	86	90	93
		Contoured	Poor	70	79	84	88
			Good	65	75	82	86
		Contoured and Terraced	Poor	66	74	80	82
			Good	62	71	77	81
		Bunded	Poor	67	75	81	83
			Good	59	69	76	79
		Paddy (rice)	……	95	95	95	95
2.	Orchards	With under stony cover	……	39	53	67	71
		Without under stony cover	……	41	55	69	73
3.	Forest	Dense	……	26	40	58	61
		Open	……	28	44	60	64
		Shrubs	……	33	47	64	67
4.	Pasture	……..	Poor	68	79	86	89
			Fair	49	69	79	84
			Good	39	61	74	80

5.	Wasted land	……...	……	71	80	85	88
6.	Hard Surface	……	……	77	86	91	93
7.	Water	……	Deep	100	100	100	100

http://www.gisdevelopment.net/application/nrm/water/watershed/watws0015pf.htm

The Curve Numbers presented in Table 3.5 (b) correspond to Antecedent Moisture Condition II (AMC II). The AMC is the moisture state of the soil before the studied rainfall starts.

Due to spatial and temporal variability of rainfall, quality of measured rainfall-runoff data, the variability of antecedent rainfall and the associated soil moisture amount, the SCS-CN method has sufficient room for variability (Ponce and Hawkins 1996). A source of variability is also the antecedent moisture condition (AMC). Though the term antecedent is taken to vary from previous 5 days to 30 days (Soil conservation service engineering division, 1986), there is no explicit guideline for varying the soil moisture with the antecedent rainfall of certain duration.

The SCS methodology represents this parameter based on the cumulated precipitation over the previous five days in the following way (McCuen 1982):

1. AMC I represents dry soil, with cumulated precipitation < 12.7 mm in the dormant season and < 35.6 mm in the growing season.

2. AMC II represents medium soil moisture, with cumulated precipitation of 12.7 - 28 mm in the dormant season and 35.6 – 53.4 mm in the growing season.

3. AMC III represents moist or saturated soil, with cumulated precipitation > 28 mm in the dormant season and > 53.4 mm in the growing season.

These values of AMC correspond, respectively, to 90, 10, and 50% cumulative probability of exceedance of runoff depth for a given rainfall (Hjelmfelt *et al.*, 1991).

Table 3.6 presents values corresponding to each AMC according to rainfall and season.

Table 3.6: Antecedent moisture conditions

AMC	Five day Precipitation	
	Dormant Season	**Growing season**
I	< 12.7 mm	< 35.6 mm
II	12.7 -28 mm	35.6-53.4 mm
III	> 28 mm	>53.4 mm

The Curve Numbers are calculated for AMC II and then adjusted by addition to simulate AMC III or subtraction to simulate AMC I. Different formulas can be used to adapt the AMC II curve number values to another AMC.

For a catchment with sub-areas that have different soil types and land covers, a composite curve number CN_C is determined by weighting the curve number values for the different sub-areas in proportion to the land area associated with each:

$$CN_c = \frac{CN_1A_1 + CN_2A_2 + \cdots CN_iA_i + \cdots + CN_nA_n}{\sum_{i=1}^{n} A_i} \tag{3.4}$$

Where CN_{i} is the curve number of the sub-area i, *Ai* is the area of the sub-area *i*, and *n* is the total number of sub-areas. CN_{II} is considered the base *CN*, and is applied for moderate antecedent moisture condition (AMC-II). It can be adjusted for calculating CN_{III} , which is applied for near-saturated antecedent moisture condition (AMC-III), or, CN_I, which is applied for dry antecedent moisture condition (AMC-I), as shown below (Chow *et al.,* 1988):

$$CN_I = \frac{CN_{II}}{2.334 - 0.01334CN_{II}} \tag{3.5}$$

$$CN_{III} = \frac{CN_{II}}{0.4036 + 0.059CN_{II}} \tag{3.6}$$

3.5.6 Unit Hydrograph Transforms Methods

When rainfall occurs it satisfies all the basin requirement such as infiltration, initial abstraction, storage, etc. and the remaining portion is drained through the watershed outlet and is called as direct runoff. To calculate the direct runoff there are 7 different methods viz., Kinematic Wave Method, Modclark Method, User -

Specified Unit Hydrograph Method, Clark's Unit Hydrograph Method, Snyder's Unit Hydrograph, SCS Unit hydrograph Method, and User-specified S-Graph.

3.5.6.1 SCS Unit Hydrograph

The Soil Conservation Service (SCS) proposed a parametric UH model; this model is included in HEC-HMS. The model is based upon averages of UH derived from gauged rainfall and runoff for a large number of small agricultural watersheds throughout the US. Soil Conservation Service,*Technical Report 55* (1986) and the *National Engineering Handbook* (1971) describe the UH in detail.

3.5.6.2 Basic Concepts and Equations of SCS Unit Hydrograph

At the heart of the SCS UH model is a dimensionless, single-peaked UH. This dimensionless UH, which is shown in Figure 3.4, expresses the UH discharge U_t, as a ratio to the UH peak discharge, *Up*, for any time *t*, a fraction of T_p, the time to UH peak.

Research by the SCS suggests that the UH peak and time of UH peak are related by:

$$U_P = C\frac{A}{T_P} \tag{3.7}$$

Where, *A* = watershed area; and *C* = conversion constant (2.08 in SI and 484 in foot-pound system). The time of peak (also known as the time of rise) is related to the duration of the unit of excess precipitation as:

$$T_P = \frac{\Delta t}{2} + t_{lag} \tag{3.8}$$

Where, Δt = the excess precipitation duration (which is also the computational interval in HEC-HMS); and t_{lag} = the basin lag, defined as the time difference between the center of mass of rainfall excess and the peak of the UH. [for adequate definition of the ordinates on the rising limb of the SCS UH, a computational interval, Δt, that is less than 29 % of t_{lag} is used (USACE, 1998).]

When the lag time is specified, HEC-HMS solves Equation 3.8 to find the time of UH peak, and Equation 3.7 to find the UH peak. With U_p and T_p known, the UH can be

found from the dimensionless form, which is included in HEC-HMS, by multiplication.

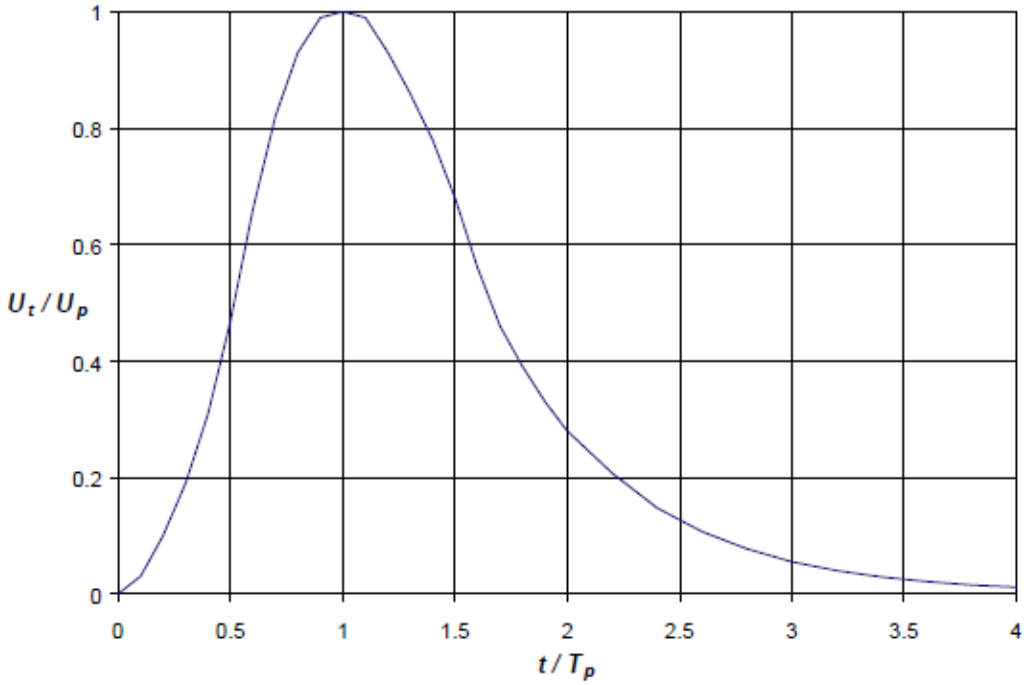

Fig. 3.4: SCS Unit Hydrograph

3.5.6.3 Estimating the SCS UH Model Parameters

The SCS UH lag can be estimated via calibration for gauged headwater sub watersheds. For ungauged watersheds, the SCS suggests that the UH lag time may be related to time of concentration, t_C as:

$$t_{lag} = 0.6 t_C \tag{3.9}$$

Time of concentration is a quasi-physically based parameter that can be estimated as

$$t_C = t_{sheet} + t_{shallow} + t_{channel} \tag{3.10}$$

Where, t_{sheet} = sum of travel time in sheet flow segments over the watershed land surface; $t_{shallow}$ = sum of travel time in shallow flow segments, down streets, in gutters, or in shallow rills and rivulets; and $t_{channel}$ = sum of travel time in channel segments.

For channel flow the velocity is estimated by Manning's equation:

$$V = \frac{CR^{\frac{2}{3}}S^{\frac{1}{2}}}{n} \tag{3.11}$$

Where, V = average velocity; R = the hydraulic radius (defined as the ratio of channel cross-section area to wetted perimeter); S = slope of the energy grade line (often approximated as channel bed slope); and C = conversion constant (1.00 for SI and 1.49 for foot-pound system.) Values of n, which is commonly known as Manning's roughness coefficient, can be estimated from textbook tables, such as that in Chaudhry (1993). Once velocity is thus estimated, channel travel time is computed as:

$$t_{channel} = \frac{L}{V} \tag{3.12}$$

Where, L = channel length.

Sheet flow is flow over the watershed land surface, before water reaches a channel. Distances are short—on the order of 10-100 meters (30-300 feet). The SCS suggests that sheet-flow travel time can be estimated as:

$$t_{sheet} = \frac{0.007(NL)^{0.8}}{(P_2)^{0.5}\,S^{0.4}} \tag{3.13}$$

Where, N = an overland-flow roughness coefficient; L = flow length; P_2 = 2-year, 24-hour rainfall depth, in inches; and S = slope of hydraulic grade line which may be approximated by the land slope

Sheet flow usually turns to shallow concentrated flow after 100 meters. The average velocity for shallow concentrated flow can be estimated as:

$$V = \begin{cases} 16.1345\sqrt{S} & for\ unpaved\ surface \\ 20.3282\sqrt{S} & for\ paved\ surface \end{cases}$$

From this, the travel time can be estimated with Equation 3.12.

3.5.6.4 The Clark Unit Hydrograph Method

The Clark Unit Hydrograph Method requires a specified duration, the Clark Unit Hydrograph (CUH) was developed using a time-area method (Viessman and Lewis 2003). This method considers an instantaneous unit hydrograph, which is

similar to a regular unit hydrograph except that it is assumed that effective precipitation is applied to a drainage basin in an infinitely short period of time.

Essentially, the technique acknowledges the fact that runoff at any point in time relates directly to characteristics of a given watershed. These characteristics include both storage and translation characteristics, which includes the combination of overland and channel travel times with the watershed's storage (Viessman and Lewis 2003). Translation through the watershed is accounted for with the watershed's travel time or T_c (Eq. 3.9)

Storage effect or attenuation is accounted for by a built-in storage coefficient. Many studies have found that the storage coefficient, divided by the sum of time of concentration and storage coefficient, is reasonably constant over a region (HEC-HMS User's Manual 2008)shows this relationship.

$$\frac{R}{R+T_C} \tag{3.14}$$

The storage coefficient (R) measures the storage of rainfall in the watershed before it can drain to the outlet point. It is measured in units of time. The higher the storage coefficient in comparison to the time of concentration, the higher the storage within the watershed (Sabol 1988).

While there are numerous methods for determining Clark's storage coefficient, there is an acceptable way to estimate this parameter. According to Viessman and Lewis (2003), this coefficient can be estimated by multiplying *Tc* by a constant, which generally ranges from 0.6- 2.0. This calculation yields a ratio that can be used in equation to find the storage coefficient, R. From this estimation one can require a range of storage coefficients, which is useful in determining the best coefficient to use for a particular watershed.

$$R = \frac{Ratio \times T_C}{1 - Ratio} \tag{3.15}$$

The CUH method is also easily implemented into computer programs. This easy is due to the fact that the CUH technique already accounts for hydrologic routing procedures, meaning that "a unit hydrograph need not be developed as an

intermediate step in converting rainfall excess to a storm hydrograph" (Sabol, 1988). This process makes it easy for computerized models to create an outflow hydrograph.

The storage coefficient relates the effects of direct runoff storage in the watershed to unit hydrograph shape. The equation for estimating the storage coefficient (R) is (Russell *et al.*, 1979):

$$R = cT_c \tag{3.16}$$

Where, R = Clark's UH storage coefficient, in hours, T_c = time of concentration, in hours, c = calibration parameter (for forested catchments = 8 - 12, for agricultural catchments = 1.5 - 2.8, and for developed catchments = 1.1 - 2.1)

Because of its easy computerized application, the CUH procedure is used in several different modeling programs, including appearing as in the Hydrologic Engineering Center's Hydrologic Modeling System (HEC-HMS), as developed by the United States Army Corps of Engineers (USACE).

3.5.7 Flood Routing

When a watershed receives rainfall as an input and produce a runoff as output, the output or out flow hydrograph differs from the input or inflow hydrograph of rainfall in shape, duration and magnitude; these differences being attributable to storage properties of the watershed system. The procedure to compute the output hydrograph, when the input hydrograph and physical dimensions are known is called flood routing. Flood routing generally used for flood forecasting, design of spillways, reservoir and flood protection works, etc.

Flood routing procedure are classify in two broad categories: (1) Reservoir routing and (2) Channel routing. Reservoir routing considers the modulation effect of flood wave when it passes through a reservoir. Such events result in output or outflow hydrographs with attenuated peaks and enlarge time basis. By reservoir routing, variations in reservoir elevation and outflow (Discharge) are predicted with respect to time, when the relationships between elevation and volume, and elevation and outflow of the reservoir are known.

Channel routing considers the changes in the shape of the input hydrograph while the flood waves pass through a channel downstream. With the help of channel routing, flood hydrographs at various sections of the channel are predicted when the input hydrograph and channel-reach characteristics are known. The information generated on attenuation of the hydrograph peak and durations of high-water levels, assists in forecasting floods and taking preventive measures against floods.

Flood routing is modelled either by hydraulic routing or by hydrologic routing procedures. Hydraulic routing is based upon the equation of motion of unsteady flow, along with the equation of continuity. The differential equation which describes this flow is known as the St. Venant equation, whereas hydrologic routing is based on the equation of continuity. Generally, in hydrologic studies, the models of hydrologic flood routing are used.

3.5.7.1 Muskingum Method

The Muskingum channel routing method is based on two equations (Linsley*et al.*,1982). The first is the continuity equation or conservation of mass.

$$\frac{I_1 + I_2}{2}\Delta T - \frac{O_1 + O_2}{2}\Delta T = S_1 - S_2 \tag{3.17}$$

Where, and I_2 are inflow discharges at time 1 and time 2,

O_1 and O_2 are outflow discharges at time 1 and time 2,

ΔT = time difference between time 1 and time 2,

S_1 and S_2 are values of reach storage at time 1 and time

The second equation is a relationship of storage, inflow, and outflow of the reach.

$$S = K\left\{XI + (1 - X)O\right\} \tag{3.18}$$

Where, S = reach storage,

I = inflow discharge,

O = outflow discharge,

K = storage constant,

X = weighting factor

Combining equations 3.17 and 3.18 and simplifying results (Ponce, 1981):

$$O_2 = C_1 I_1 + C_2 I_2 + C_3 O_1 \tag{3.19}$$

Where, $C_1 = ((\Delta t / K) + 2X) / C_0$

$C_2 = ((\Delta t / K) - 2X) / C_0$

$C_3 = (2(1 - X) - \Delta t / K) / C_0$

$C_0 = \Delta t / K + 2(1 - X)$

C_0, C_1, C_2, and C_3 are dimensionless parameters.

An approximation for K is the travel time through the reach (length of reach divided by the average flow velocity). The value of X is between 0.0 and 0.5. A value of 0.0 gives maximum attenuation from the procedure and 0.5 provides the minimum attenuation. Linsley *et al.* (1982) describe a procedure to determine K and X from hydrographs.

3.5.8 Reservoir Routing

A reservoir mitigates adverse impacts of excess water by holding that water and releasing it at a rate that will not cause damage downstream. This is illustrated by the hydrographs shown in Fig. 3.5.To reduce this peak to the target level, storage is provided. Thus the volume of water represented by the shaded area is stored and then released gradually. The total volume of the inflow hydrograph and the volume of the outflow hydrograph (the dotted line) are the same, but the time distribution of the runoff is altered by the storage facility.

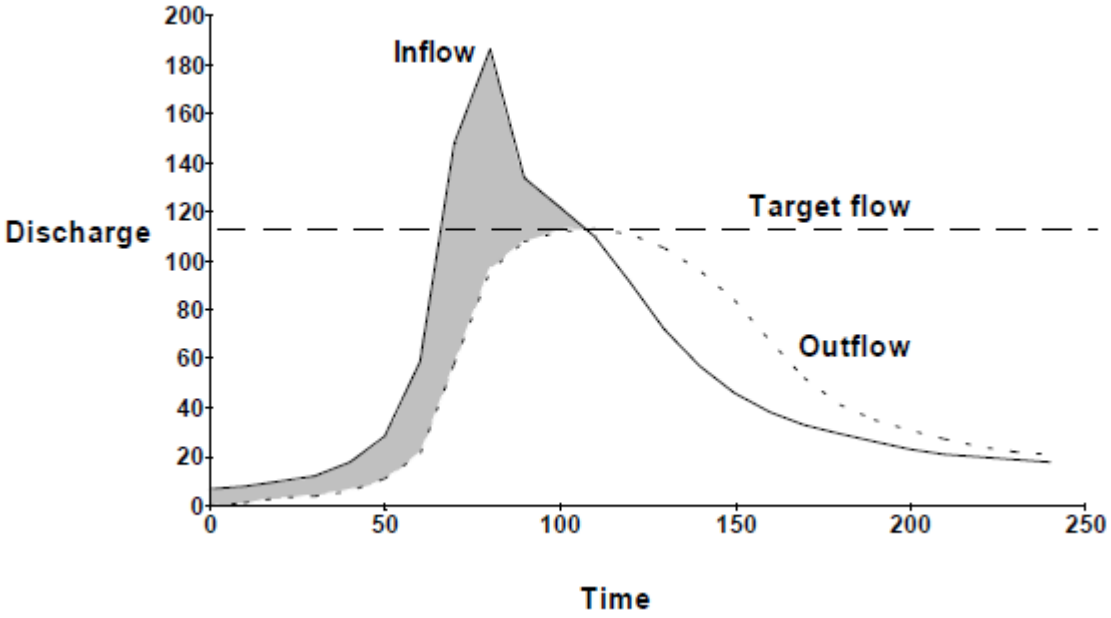

Fig. 3.5: Illustration of impact of reservoir

3.5.8.1 Basic Concepts and Equations

Outflow from an impoundment that has a horizontal water surface can be computed with the so-called level-pool routing model (also known as Modified Puls routing model). That model discretizes time, breaking the total analysis time into equal intervals of duration Δt. It then solves recursively the following one dimensional approximation of the continuity equation:

$$\left(\frac{2S_{t+1}}{\Delta t}+O_{t+1}\right)=\left(I_t+I_{t+1}\right)+\left(\frac{2S_t}{\Delta t}-O_t\right) \tag{3.20}$$

Where, I_{avg}= average inflow during time interval; O_{avg}= average outflow during time interval; ΔS = storage change. With a finite difference approximation, this can be written as:

$$\frac{I_t+I_{t+1}}{2}-\frac{O_t+O_{t+1}}{2}=\frac{S_{t+1}-S_t}{\Delta t} \tag{3.21}$$

Where, t = index of time interval; I_t and I_{t+1} = the inflow values at the beginning and end of the t^{th} time interval, respectively; O_t and O_{t+1}= the corresponding outflow values; and S_t and S_{t+1} = corresponding storage values. This equation can be rearranged as follows:

$$\left(\frac{2S_{t+1}}{\Delta t}+O_{t+1}\right)=\left(I_t+I_{t+1}\right)+\left(\frac{2S_t}{\Delta t}-O_t\right) \tag{3.22}$$

All terms on the right-hand side are known. The values of I_t and I_{t+1} are the inflow hydrograph ordinates, perhaps computed with models described earlier in the manual. The values of O_t and $S_t$are known at the t^{th} time interval. At t = 0, these are the initial conditions, and at each subsequent interval, they are known from calculation in the previous interval. Thus, the quantity ($2S_{t+1}/\Delta t+O_{t+1}$) can be calculated with Equation 3.22. For an impoundment, storage and outflow are related, and with this storage-outflow relationship, the corresponding values of O_{t+1} and S_{t+1}can be found. The computations can be repeated for successive intervals, yielding values O_{t+1},O_{t+2}, ...O_{t+n}, the required outflow hydrograph ordinates.

3.6 Computation of Hydrologic Parameters

The sub-basin parameters (area, lag-time, Time of concentration and average curve number) were calculated with the HEC-GeoHMS utility. Other parameters, needed for estimating the lag-time, such as length and slope of the longest flow path, were also calculated and stored in the sub-basin attribute table. These files, when opened in HEC-HMS, automatically create a topologically correct schematic network of sub-basins and reaches with hydrologic parameters.

The following procedure was adopted to construct the rainfall-runoff model for the Hadaf watershed. A schematic representation of the watershed network was created by dragging and dropping icons that represent hydrological elements, and connections between them were established. The hydrologic parameters for each sub-basin were entered using HEC-HMS subbasin editor; required data consist of sub-basin area, loss rate method (SCS-CN method was used), transform method (SCS Unit Hydrograph method and Clark Unit Hydrograph method were used), channel routing method (Muskighum method) and reservoir routing (Modified Puls routing method).

A precipitation model is the next component of the HEC-HMS model. Gage weighting. The watershed precipitation depth was inferred from the depths at gage using an averaging scheme.

The method that was used for determining the gage weighting factors for mean area precipitation depth computation is the thiessen polygon method. This is an area-based weighting scheme, based upon an assumption that the precipitation depth at any point within a watershed is the same as the precipitation depth at the nearest gage in or near the watershed. Thus, it assigns a weight to each gage in proportion to the area of the watershed that is closest to that gage.

3.7 Model Calibration and Optimization

Model calibration is an essential process needed to assure that the simulation outputs are close to real observations. Once a model was developed and simulated for the initial parameter estimates, it was calibrated against known discharge runoff rates measured at the gaging station during a storm event that occurred between selected time events. The available hydro-climatic records of 3 meteorological stations and 1 stream flow gage stations were analyzed for selection of calibration and validation data for the HEC-HMS model. The calibration was done using daily data for the time period 05-11 Sept 2006.

The model calibration was done by adjusting the method parameter values until the results matched the field data. The process was completed manually by repeatedly adjusting the parameters, computing, and inspecting the goodness of fit between the computed and observed hydrographs. The process can also be done automatically by using the iterative calibration procedure called optimization. The measure of the goodness of fit is the objective function (Kathol *et al.*, 2003). HEC-HMS allows the user to calibrate the model to the best-fit condition by selecting various objective functions to provide the best calibration results (HEC, 2005). The objective function measures the variation between computed and observed hydrographs, and is equal to zero when the hydrographs are identical.

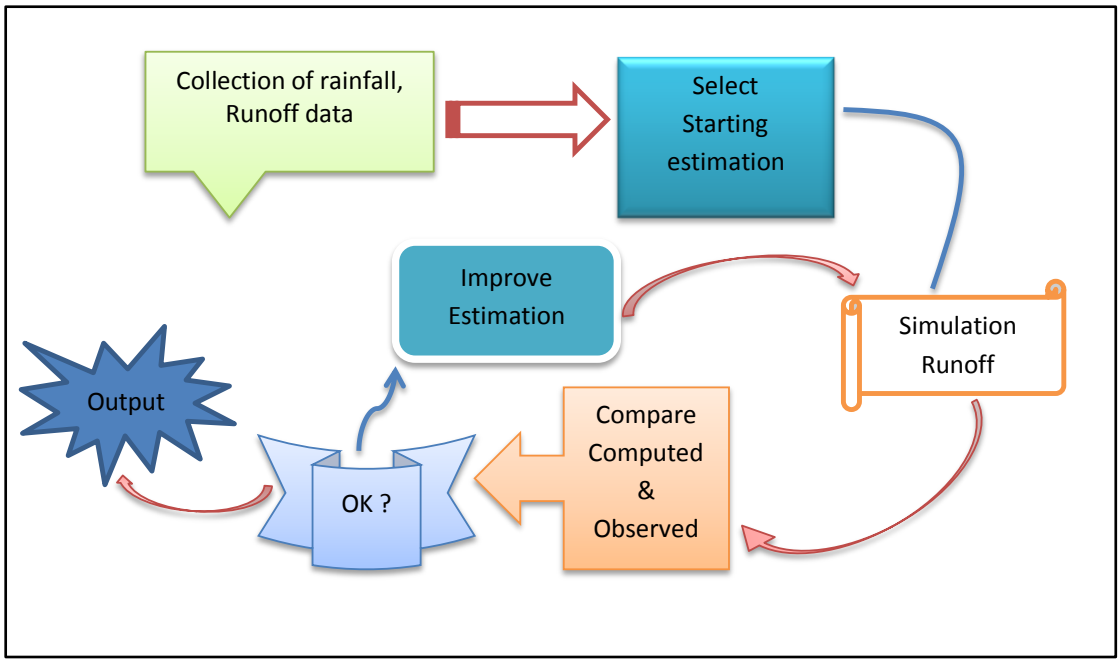

Fig. 3.6: Schematic of calibration procedure

The automated calibration was used to adjust initial losses, curve number and lag time to minimize the objective function value and to find optimal parameters. When manual validation of the observed and simulated hydrograph was not acceptable, initial parameters were adjusted to provide a better optimization target value for the optimization process (USACE, 2000). The objective function used was the simulated absolute error. This objective function gave greater weight to large errors and lesser weight to small errors, in addition of giving greater overall weight to error near the peak discharge. The optimization procedure required the use of a search method for minimizing an objective function and finding optimal parameters. The search method used for this calibration was the univariate gradient method. This method evaluated and adjusted one parameter at a time while holding all other parameters constant. The search method estimates the optimal parameters but do not indicates which parameters had the greatest impact on the solution (Kathol *et al.*, 2003). Besides evaluating the objective function for determining if the process produced an accurate calibration, graphical comparisons were made between the fit of the model and the actual measured data. Graphical comparisons of scatter plots and time series plots of residuals between computed and observed flow were used to visually inspect there sults of the calibration (Kathol *et al.*, 2003).

3.8 Performance Evaluation of HEC-HMS models

The performance of the HEC-HMS models was evaluated using five performance indices, namely: coefficient of determination (R2), Nash-sutcliffe efficiency (NSE), root mean square error (RMSE), peak percentage deviation (Pdv) and mean absolute error (MAE) as defined below.

3.8.1 Coefficient of determination (R^2)

The coefficient of determination (R^2) describes the proportion of the total variance in the measured data that can be explained by the model. It ranges from 0.0 to 1.0, with higher values indicating better agreement, and is given by,

$$R^2 = \left[\frac{\sum_{i=1}^{n} \left[O_i - O_{avg} \right] \left[S_i - S_{avg} \right]}{\left[\sum_{i=1}^{n} \left(O_i - O_{avg} \right)^2 \right]^{0.5} \left[\sum_{i=1}^{N} \left(S_i - S_{avg} \right)^2 \right]^{0.5}} \right] \quad (3.23)$$

Where, O_i is the i^{th} observed runoff, O_{avg} is the mean of the n observed runoff, S_i is the i^{th} simulated runoff value, S_{avg} is the mean of model simulated runoff values and n is the total number of data patterns.

3.8.2 Nash-sutcliffe efficiency (NSE)

$$E = 1 - \frac{\sum_{i=1}^{n} (O_i - P_i)^2}{\sum_{i=1}^{n} (O_i - \bar{O}_i)^2} \times 100 \quad (3.24)$$

Where, Pi is predicted runoff, respectively, $\overline{O}$ and $\overline{P}$ are the means of the observed and predicted runoff, respectively. The value of Nash–Sutcliffe efficiency varies between -∞ and 100. The closer the value to 100, the better is the model performance.

3.8.3 Root mean square error (RMSE)

$$RMSE = \sqrt{\frac{1}{n} \sum_{i=1}^{n} (O_i - P_i)^2} \quad (3.25)$$

RMSE is always greater than 0, and closer the values to 0 better the model performance.

3.8.4 Mean absolute error (MAE)

$$MAE = \frac{1}{n}\sum_{i=1}^{n}|O_i - P_i| \tag{3.26}$$

MAE is always a positive number, and a value 0 indicates a perfect model.

3.8.5 Percentage deviation (Pdv)

$$P_{dv} = \frac{P_p - O_p}{O_p} \times 100 \tag{3.27}$$

Where, O_p and P_p are the peak value of observed and predicted runoff, respectively.

CHAPTER IV
RESULTS AND DISCUSSION

4.1 HEC-HMS and HEC-GeoHMS Model

The input data required for HEC-HMS models setup were analysed and delineated using ERDAS Imagine and Arc-GIS. Digital Elevation Model (DEM) of the Hadaf Basin has been used as input data to delineate Hadaf watershed for HEC-HMS model setup after selection of appropriate DEM. Delineation of watershed using DEM requires a series of pre-processing including fill sinks, flow direction, flow accumulation, stream definition and catchment grid delineation, catchment polygon, watershed aggregation, project setup, stream and sub-basin characteristics.

4.1.1 Selection of appropriate DEM

DEMs are crucial in hydrological modelling as the topography controls the flow of water. DEMs are used in water resources planning and management work to identify drainage related features such as ridges, valley bottoms, channel networks and surface drainage patterns, and to quantify sub catchment and channel properties such as size, length, and slope. The accuracy of this topographic information is a function both of the quality and resolution of the DEM, and of the DEM processing algorithms used to extract this information. In this study two elevation dataset SRTM and ASTER are used. SRTM 90m Digital Elevation Model (DEM) and ASTER DEM 30m of the Hadaf Basin has been used in HEC-GeoHMS as input data to generate HEC-HMS model input files.

It can be observed that the drainage network generated using SRTM DEM is better compared to the ASTER DEM. Fig. 4.1 (a & b) clearly indicates that SRTM DEM gives better result because in the figures drainage line map prepared. The drainage map prepared using SRTM DEM in which drainage line is continuous from remote point of the watershed. While in the drainage map prepared using ASTER DEM, drainage line is not continuous from the remote point of the watershed. The drainage line of the both maps compared the toposheet and SRTM DEM found same drainage line as in the toposheet. This is demarked with the circle in the Fig. 4.9 (a & b).

Using terrain (SRTM and ASTER) data as an input, terrain processing is a series of step to derive the drainage network. The step consist of different terrain processing is shown in Fig. 4.1 (a & b) to 4.9 (a & b), all the ‘a’ figures are prepared using SRTM DEM while all the ‘b’ figures are prepared ASTER DEM for different processes i.e.,

clipped raw DEM of the Watershed, Fill sink map, Flow direction map, Flow accumulation map, Stream definition map, Stream segmentation map, Catchment grid delineation map, Catchment polygon map and Drainage line map. Fig. 4.10 shows the toposheet of the study area or watershed. Now after, terrain processing is done using the SRTM DEM as it proven better than the ASTER DEM.

After terrain processing is completed and a new project has been created, basin processing is used to revise sub-basin delineations. Basin processing is shown in the Figs. 4.11 to 4.17 include Sub-basin Merge and River Map, Longest Flow path Map, Sub-basin Centroid Map, Centroidal Longest Flow path, Thiessen Polygon Map, and HEC-HMS Schematics. This processes used for extract physical characteristics of streams and sub-basin, development of hydrological parameters and development of HEC-HMS inputs.

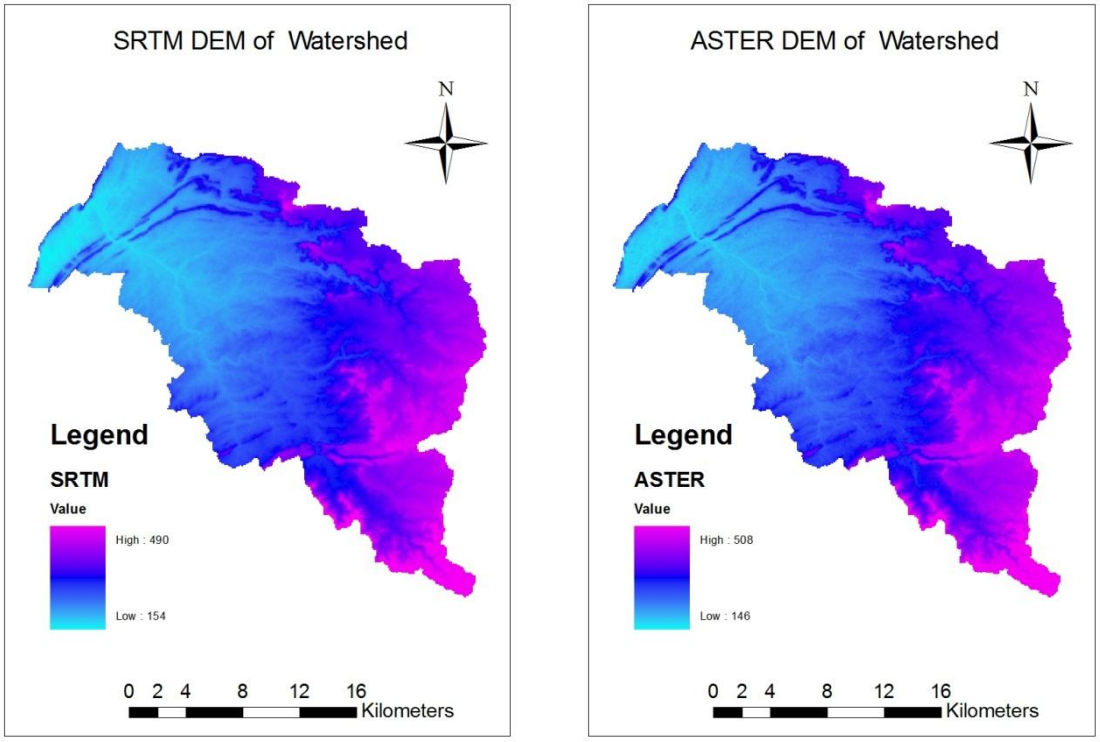

(a) SRTM **(b) ASTER**

Fig. 4.1: DEM of watershed

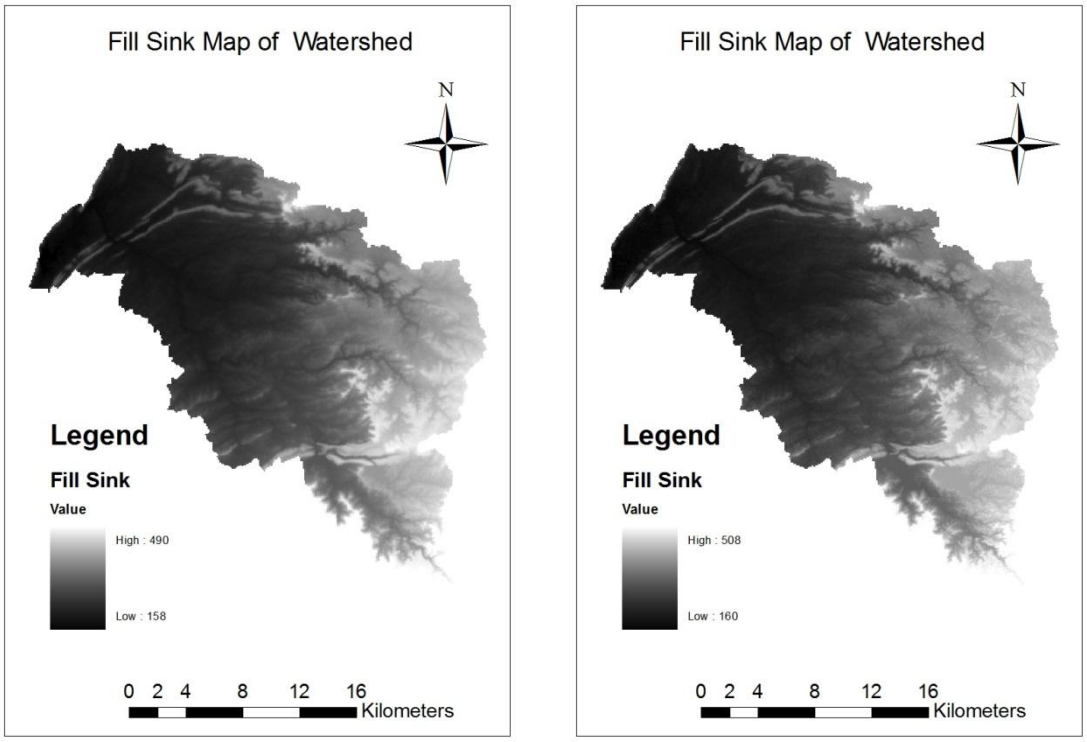

(a) SRTM **(b) ASTER**

Fig. 4.2: Fill sink map of watershed

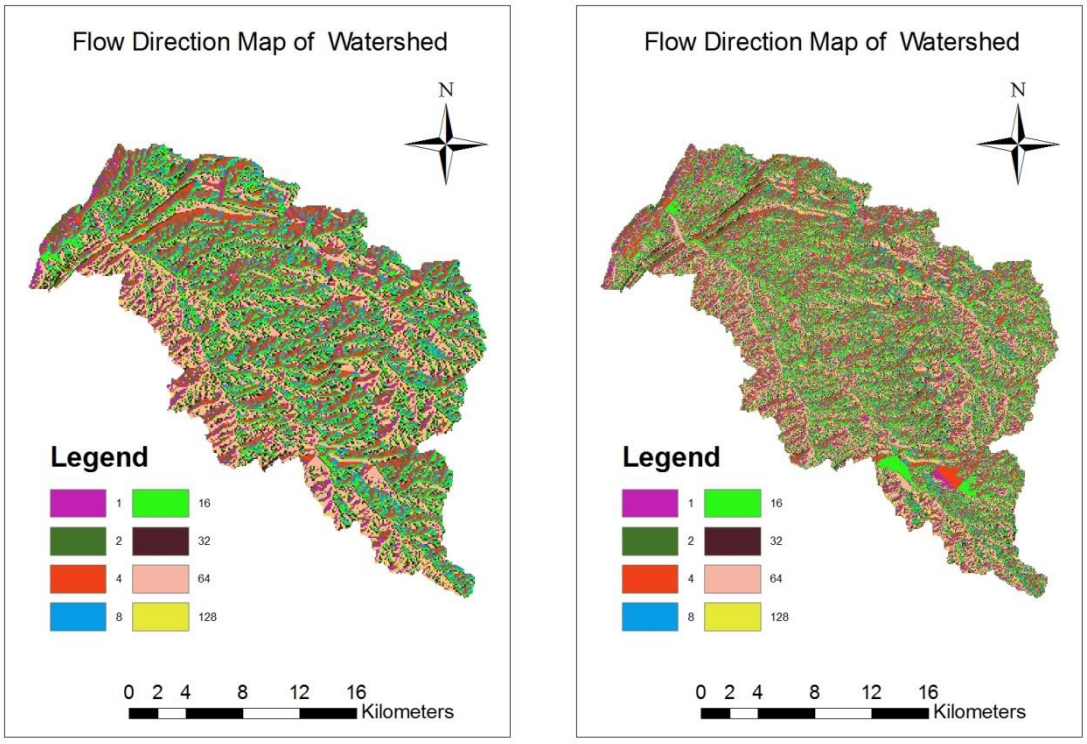

(a) SRTM **(b) ASTER**

Fig. 4.3: Flow direction map of watershed

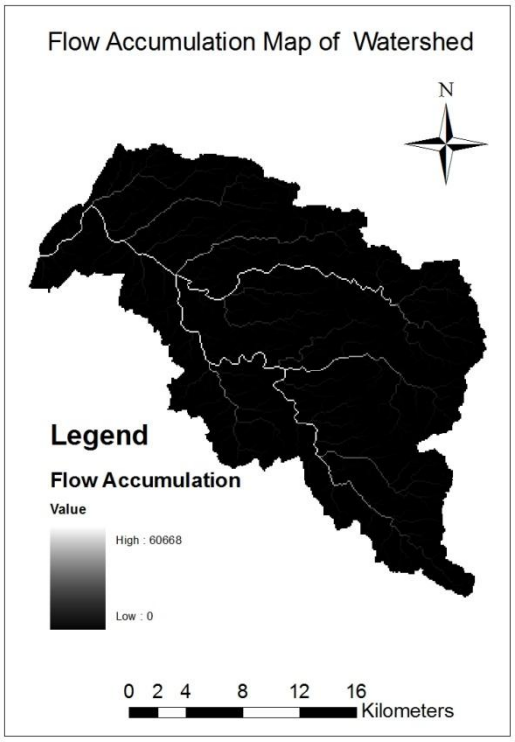

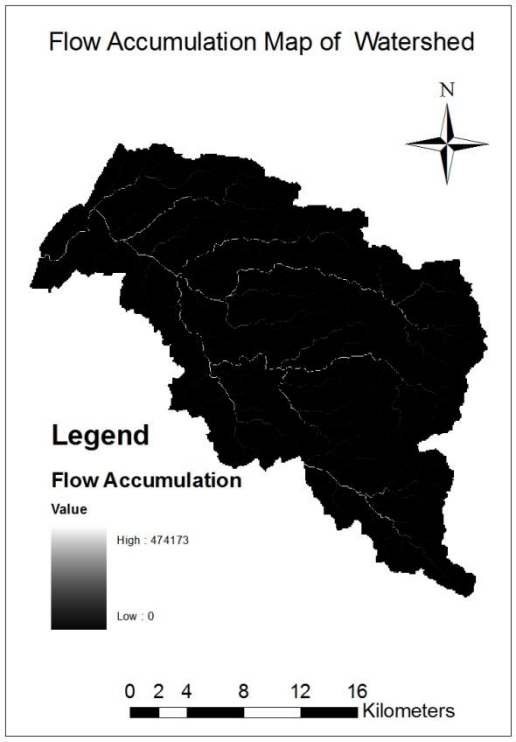

(a) SRTM **(b) ASTER**

Fig. 4.4: Flow accumulation map of watershed

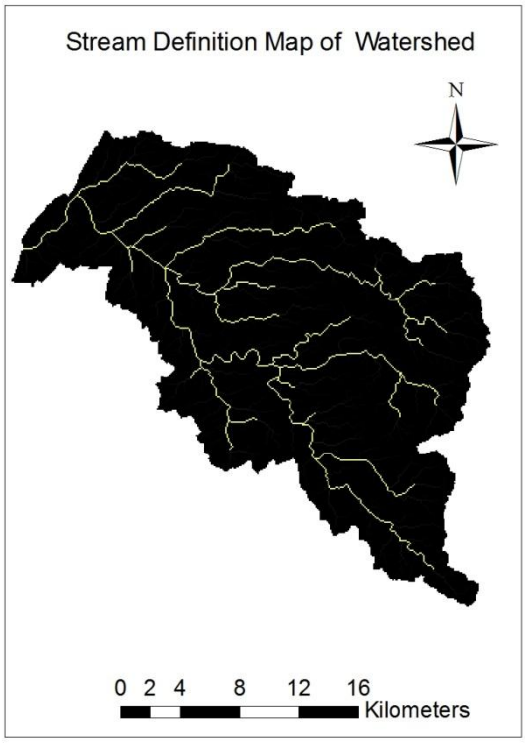

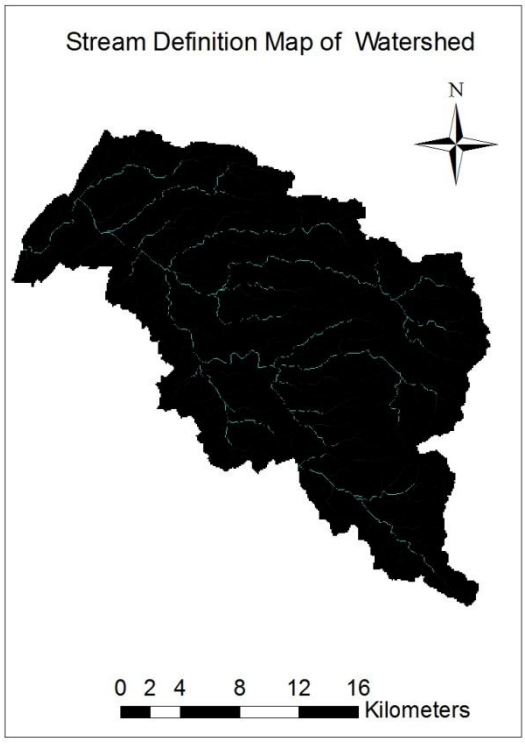

(a) SRTM **(b) ASTER**

Fig. 4.5 Stream Definition map of watershed

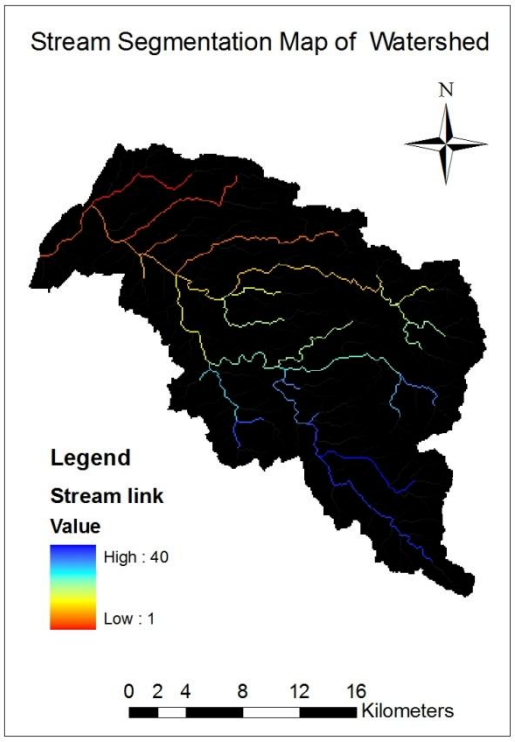

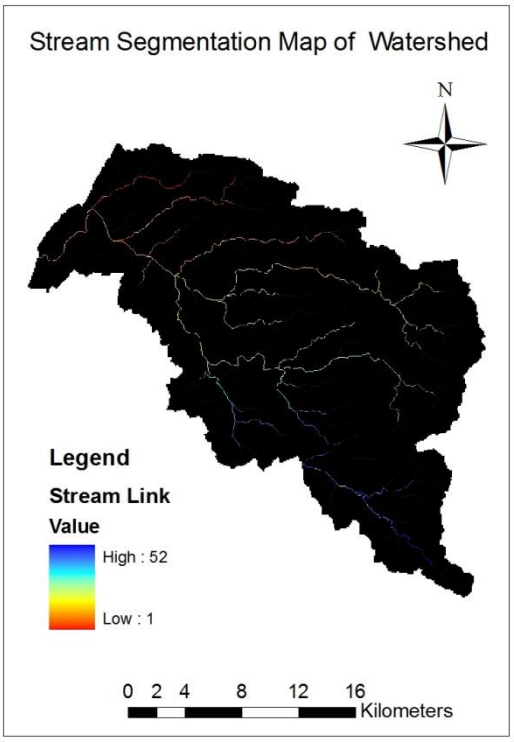

(a) SRTM **(b) ASTER**

Fig. 4.6: Stream segmentation map of watershed

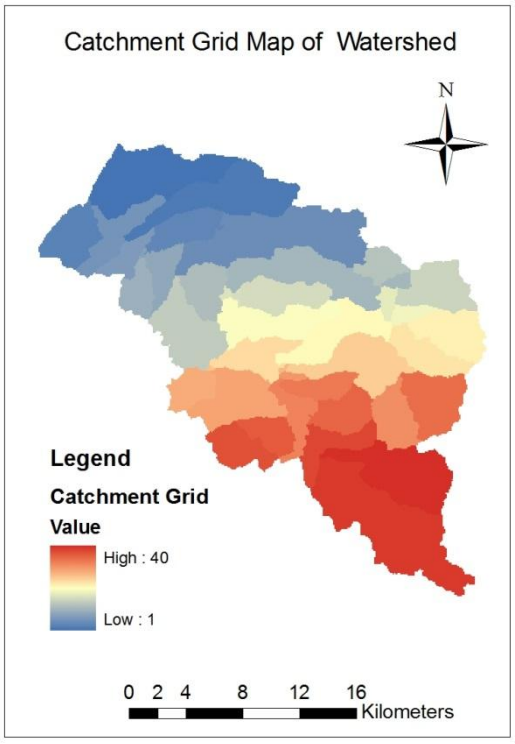

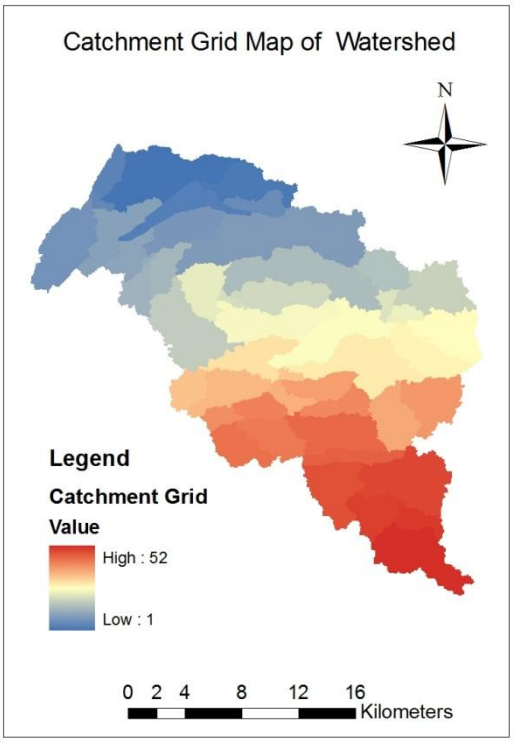

(a) SRTM **(b) ASTER**

Fig. 4.7: Catchment grid delineation map of watershed

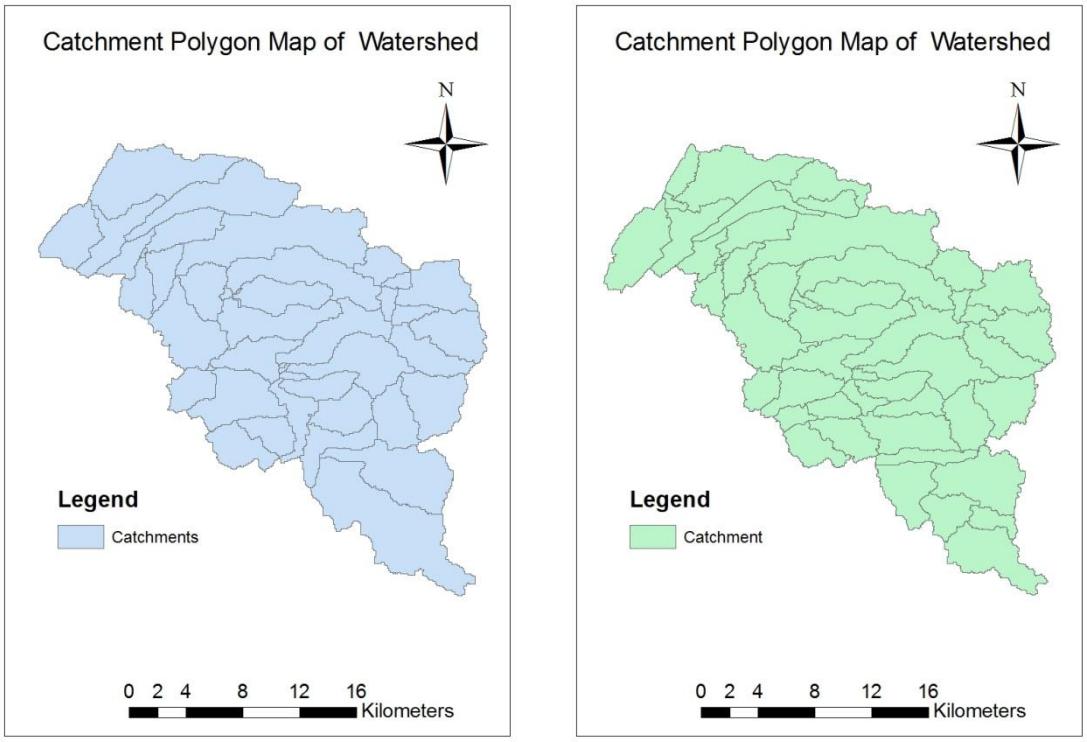

(a) SRTM **(b) ASTER**

Fig. 4.8: Catchment polygon map

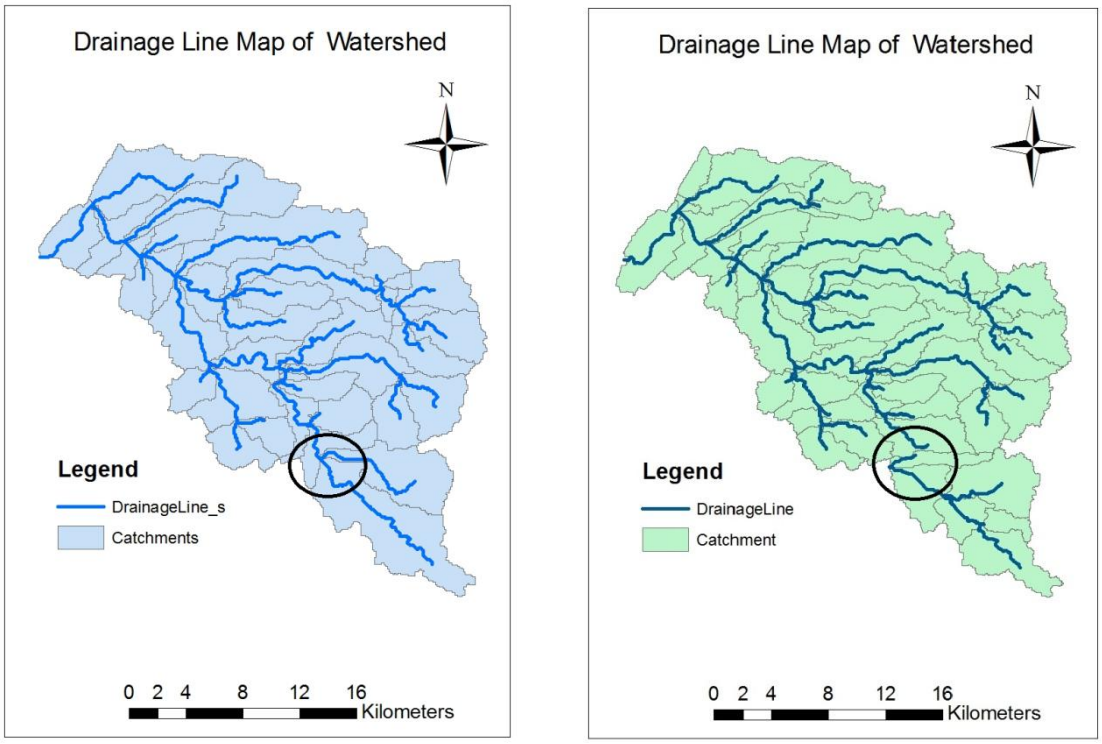

(a) SRTM **(b) ASTER**

Fig. 4.9: Drainage line map of watershed

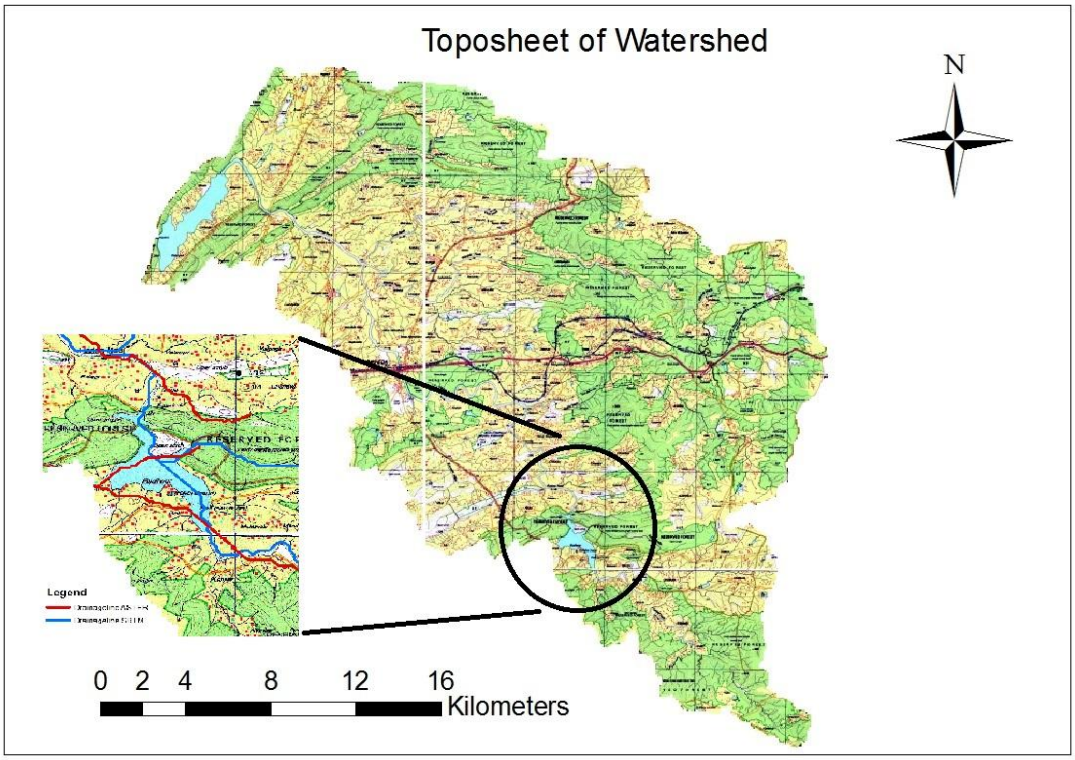

Fig. 4.10: Toposheet

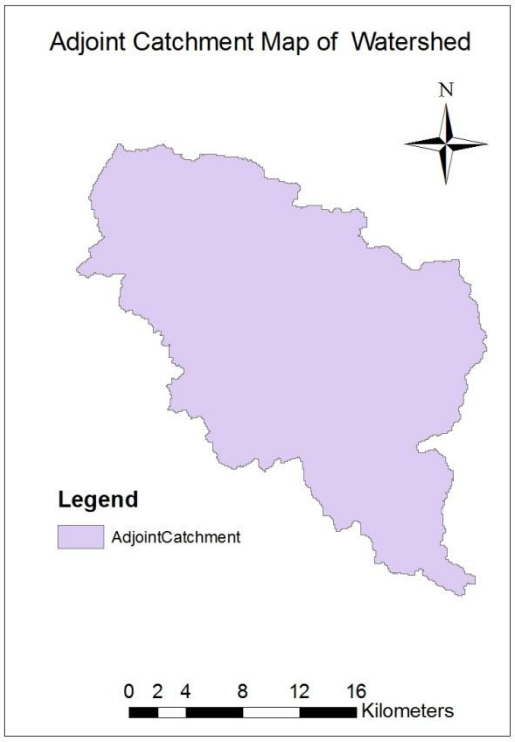

Fig. 4.11: Adjoint Catchment

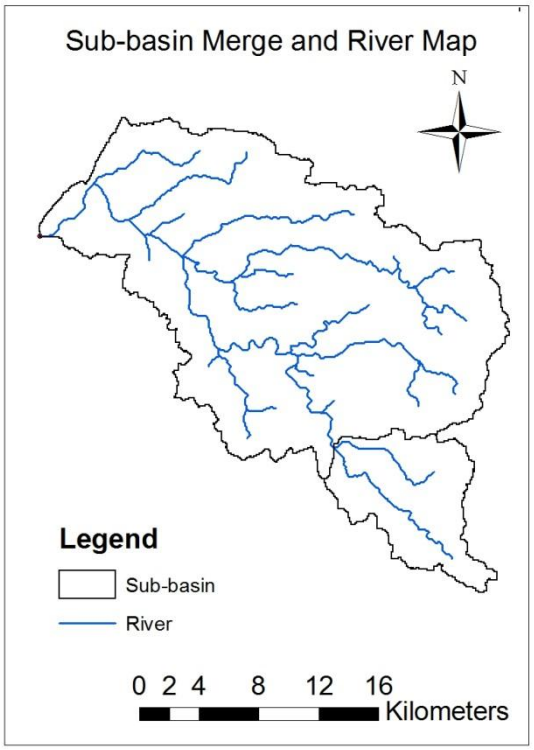

Fig. 4.12: Subbasin Merge and River Map

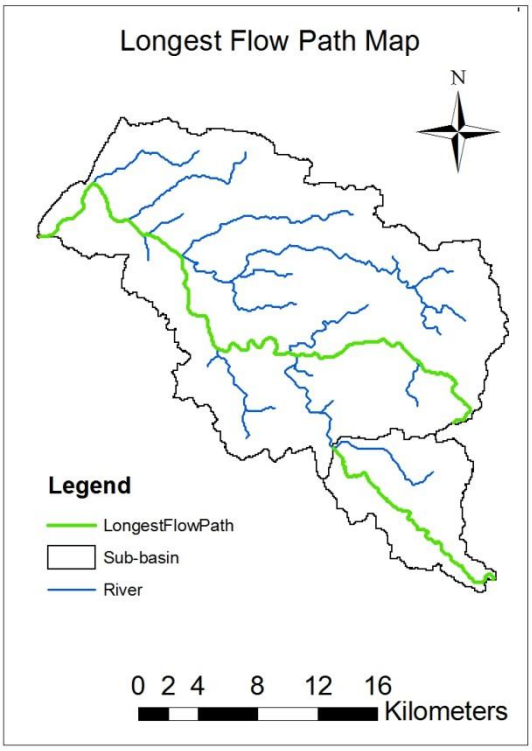

Fig. 4.13: Longest flow path map

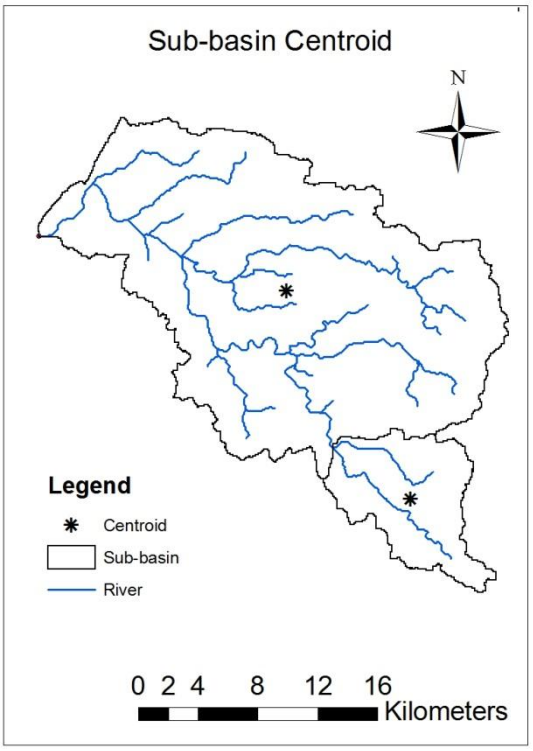

Fig. 4.14: Subbasin centroid map

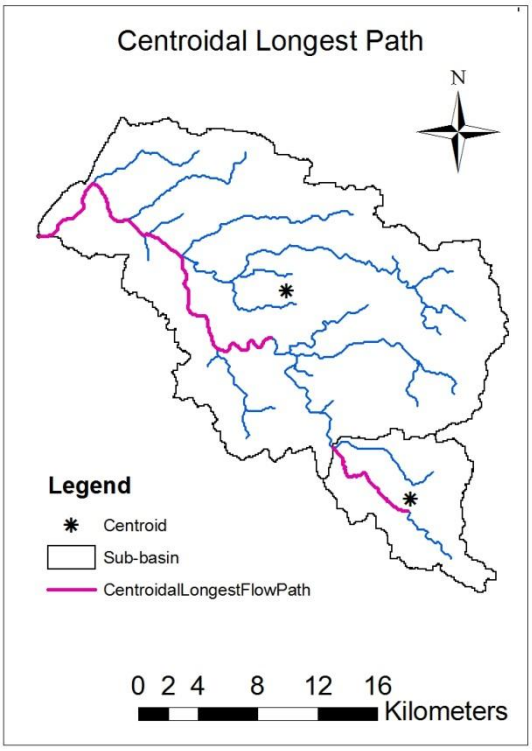

Fig. 4.15: Centroidal longest flow path

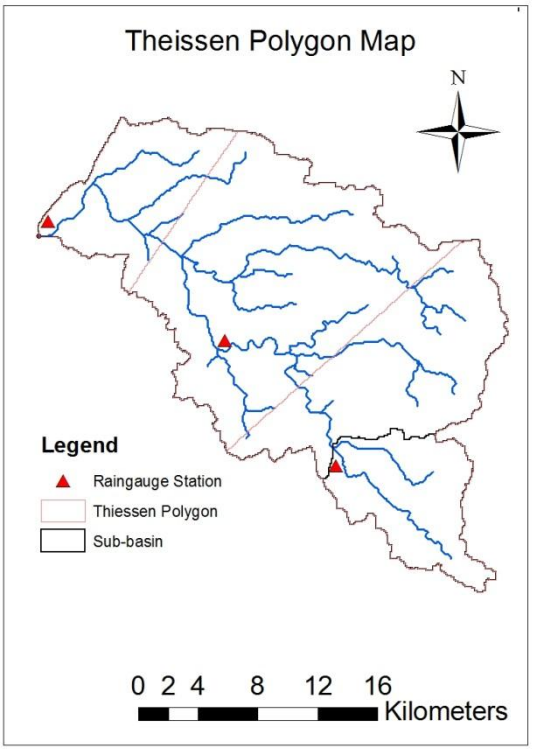

Fig. 4.16: Thiessen polygon map

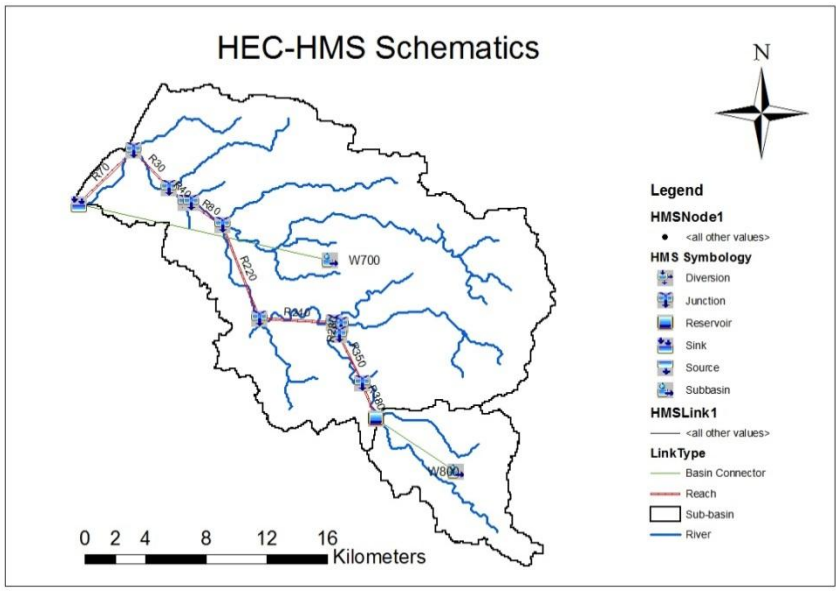

Fig. 4.17: HEC-HMS Schematics

4.1.2 Land use map

Land use is one of the most important parameters affecting the surface runoff generation process. To incorporate the effect of land use, the Hadaf watershed is classified into five dominant land use land cover categories viz. Agriculture, Forest, Water bodies, Waste land and Built up. Further to assess the effect of land use change on water harvesting potential and runoff generation in the watershed, land use maps for three different years 2008, 2012 and 2013 are considered in this study using corresponding remote sensing images. For land use maps remote sensing image LISS-III and LISS-IV is obtained from NRSC Hyderabad for the years 2008, 2012 and 2013, these images are then classified using supervised classification. ERDAS IMAGINE 11.0 is used to classify these remote sensing images in to different land use categories. Land use categories for the LISS-III year 2008 are presented in Fig. 4.18 (a), whereas Fig. 4.18 (b) shows the land use categories in the LISS-III year 2012 in the Hadaf watershed. Land use categories for the LISS-IV year 2013 are presented in Fig. 4.18 (c). The overall accuracy of the classification is found as 0.83, 0.80 and 0.90 for the LISS-III of year 2008, LISS-III of year 2012 and LISS-IV of year 2013, respectively. The area covered under different land use categories and the change in the area during year 2008 to 2012 is presented in Table 4.1. Table shows the area under different land use categories during year 2008 and 2012 classified using LISS-III remote sensing imagery. In year 2008 total agricultural land was 222.35 km^2 that has increased to 252.47 km^2 in year 2012. In year 2008 total forest land was 198.24 km^2 that has reduced to 157.91 km^2 in year 2012. In year 2008 total waste land was 51.11 km^2 that has increased to 71.75 km^2 in the year 2012.

.

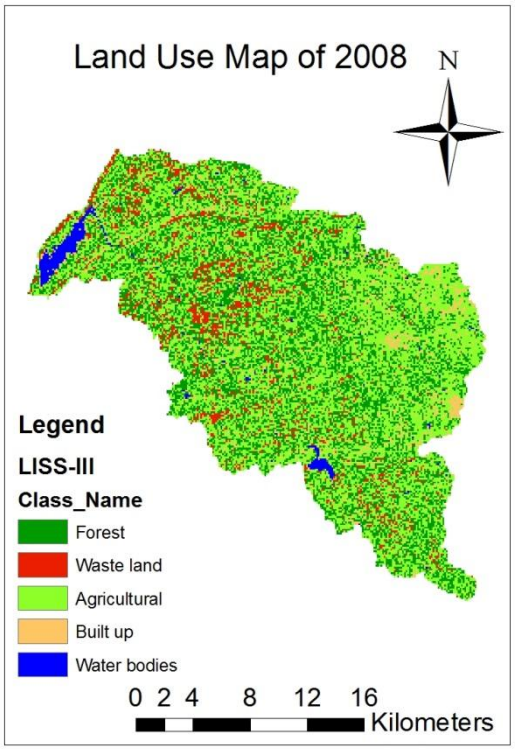

(a)

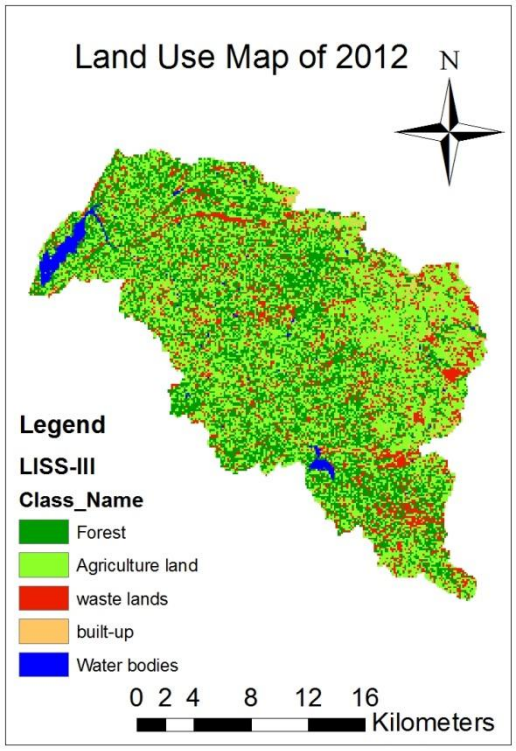

(b)

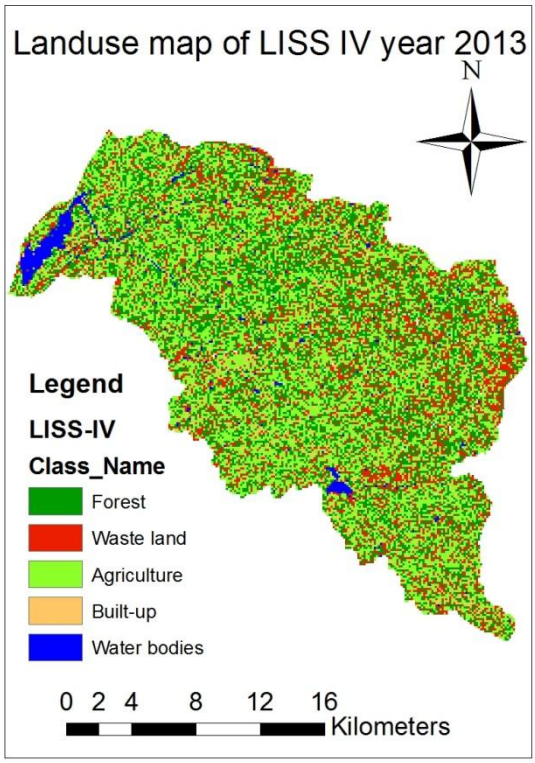

(C)

Fig. 4.18: Land use and land cover categories using (a) LISS-III for year 2008 (b) LISS-III for year 2012 and (c) LISS-IV for year 2013 of the watershed

Table 4.1: Changes in land use/land cover in Hadaf watershed

Land use class	Year 2008 (LISS-III)		Year 2012 (LISS-III)		Land use Changes	
	Area (km^2)	Area (%)	Area (km^2)	Area (%)		
Agricultural	222.35	44.69	252.47	50.72	30.12	6.04
Forest	198.24	39.84	157.91	31.73	-40.33	-8.12
Waste land	51.11	10.27	71.75	14.42	20.64	4.14
Built up	17.48	3.51	7.28	1.46	-10.20	-2.05
Water bodies	8.40	1.69	8.33	1.67	-0.07	-0.01
Total	497.57	100.00	497.74	100.00		

Land use class	Year 2013 (LISS-IV)	
	Area (km^2)	Area (%)
Agricultural	217.72	43.92
Forest	146.47	29.54
Waste land	98.96	19.96
Built up	21.33	4.30
Water bodies	11.26	2.27
Total	495.74	100.00

4.1.3 Soil map

Soil texture in the watershed is another factor affecting the conversion of rainfall into runoff. Soil series map at 1:250,000 scale for Gujarat state, published by National Bureau of Soil Survey & Land Use Planning (NBSS & LUP, 2005), is used as the source of soil database and soil grid in this study. After pre-processing of soil maps using GIS the soil types obtained for the study area are clayey, loamy and fine sand. In which the clayey, fine sand and loamy soil cover an area of 31.38, 164.22 and 302.14 km^2, respectively. The soil map and the area under different soil types are shown in Fig. 4.19 and Table 4.2, respectively.

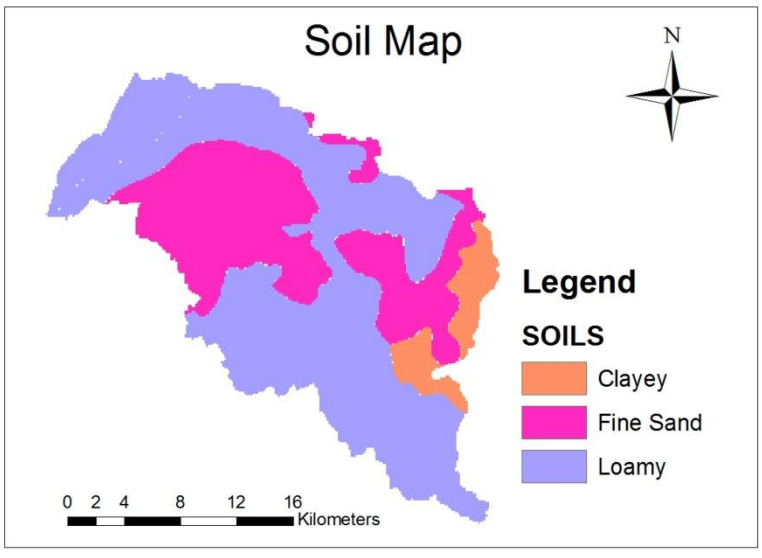

Fig 4.19: Soil map

Table 4.2: Percentage soil type in Hadaf watershed

Soil Type	Area (km^2)	Area (%)
Clayey	31.38	6.30
Fine Sand	164.22	32.99
Loamy	302.14	60.70
Total Area	497.74	100.00

4.1.4 Curve Number (CN) Generation

CN is used for loss model in HEC-HMS model. Primarily it is prepared from the combination of LULC and soil map. Then it is optimized in HEC-HMS using trial and error method. The following steps are done to get a Curve Number grid for the area of interest from LULC and HSG maps:

- Vectorization of both the LULC and HSG maps.
- Table or vector operation (Union) to get polygons of unique combination of both the maps in Arc-GIS.
- CN value generation from unique polygons by query operation in Arc-GIS and create the gridMap.
- CN value determination for each sub-basin.

The CN grid map of LISS-III year 2008, LISS-III year 2012 and LISS-IV year 2013 is presented in Fig. 4.20 (a), (b) and (c).

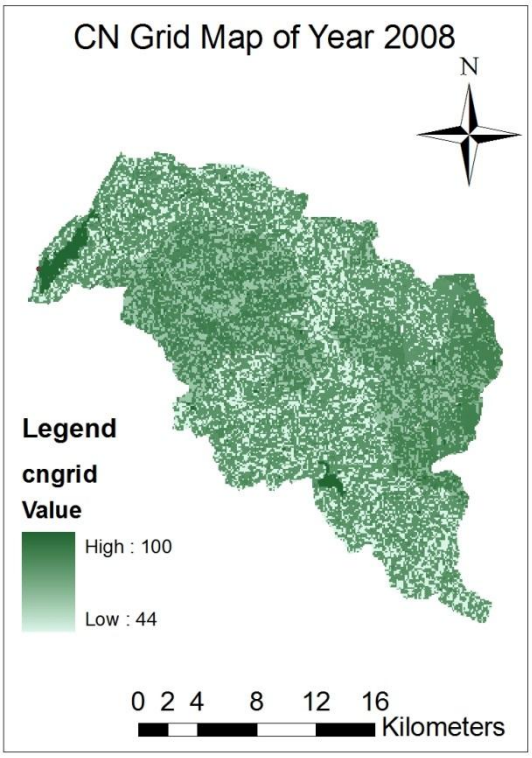

Fig. 4.20 (a): CN grid of LISS-III year 2008

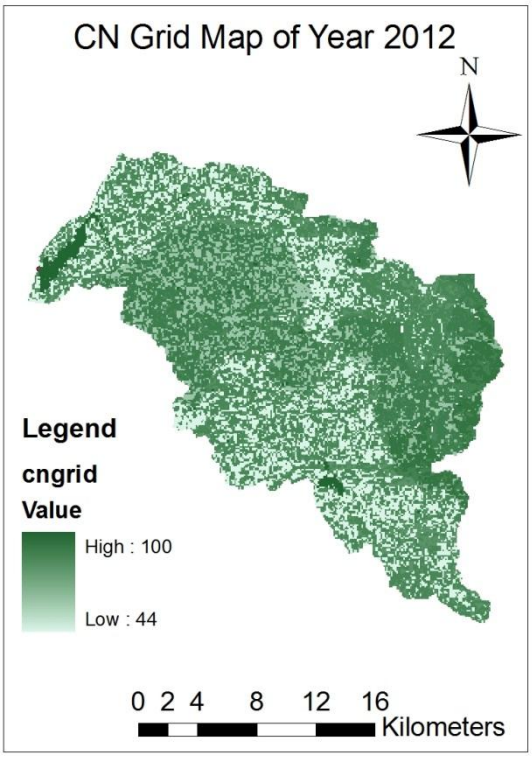

Fig. 4.20 (b): CN grid of LISS-III year 2012

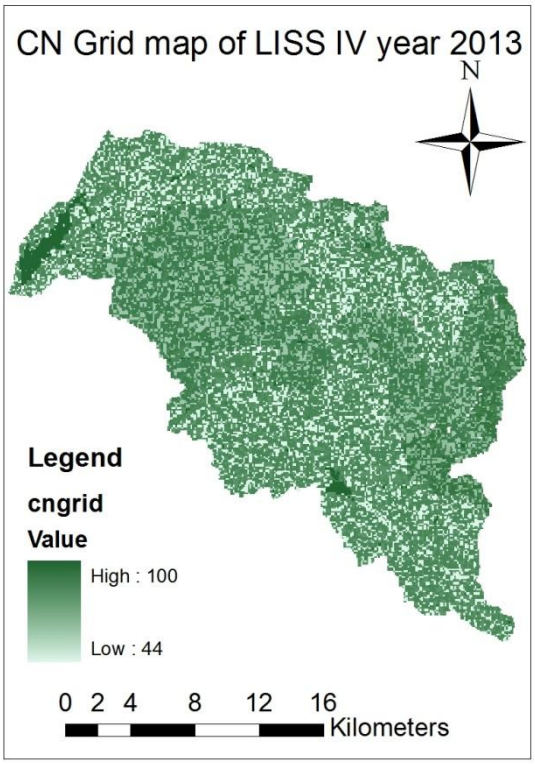

Fig. 4.20 (c): CN grid of LISS-IV year 2013

4.2 Calculations of Morphological Parameters for Hadaf Watershed

Some morphological parameter for the watershed are calculated and presented in Table 4.3. Descriptions of all the parameter are describes below.

Table 4.3: Calculated different morphological parameters

Sr. No.	Morphologic parameters	Parameter Values
1	Stream order	6
2	Total Stream length (L_u), (km)	1100.59
3	Mean stream length (L_{sm}), (km)	0.289
4	Mean Stream length ratio (R_L)	0.978
5	Mean Bifurcation ratio (R_{bm})	1.82
6	Length of main channel (L_m), (km)	47.96
7	Basin Area (A), (km^2)	496.55
8	Basin perimeter (P), (km)	168.45
9	Basin length (L_b), (km)	58.34
10	Drainage density (D_d)	2.18
11	Length of overland flow (L_g)	0.22
12	Fineness ratio (R_{fn})	0.34
13	Circulatory ratio (R_c)	0.219
14	Elongation ratio (R_e)	0.43
15	Form factor (R_f)	0.14
16	Unity shape factor (R_u)	2.61
17	Watershed Shape factor(W_s)	2.31
18	Compactness coefficient (C_c)	2.13
19	Drainage texture(R_t)	22.62
20	Total Relief (H), (km)	0.33
21	Relief Ratio (R_h)	0.0057
22	Relative relief (R_p)	0.0019

4.2.1 Stream order (N_u)

The designation of stream orders is the first step in drainage basin analysis. It is based on hierarchic ranking of streams proposed by (Strahler, 1964). The first order streams have no tributaries. The second order streams have only first order streams as tributaries. Similarly, third order streams have first and second order streams as tributaries and so on. Drainage patterns of stream network from the basin have been

observed as mainly dendritic type which indicates the homogeneity in texture and lack of structural control. In Hadaf watershed the stream orders is obtained as 6.

4.2.2 Stream length (Lu)

The stream length characteristics of the basin conform (Horton, 1945) second "law of stream length", which states that the average length of streams of each order in a drainage basin tends closely to approximate a direct geometric ratio. The numbers of streams of various orders in the basin are counted and their lengths are measured. In general, the total length of stream segments decreases with increasing stream order. The length is measured using the ArcGIS 10.0. The total stream length of Hadaf watershed is obtained as 1100.59 km. In which first order stream length is 538.23 km, second order stream length is 265.09 km, third order stream length is 139.97 km, fourth order stream length is 85.45 km, fifth order stream length is 47.91 km. and sixth order stream length is 23.91 km.

4.2.3 Mean stream length (L_{sm})

The mean stream length (L_{sm}) of a channel is a dimensional property revealing the characteristic size of components of a drainage network and its contributing basin surfaces (Strahler, 1964). In the Hadaf watershed the mean stream length is 0.28 km.

4.2.4 Stream length ratio (R_L)

Stream length ratio (R_L) is defined as the ratio of the mean length of an order to the next lower order of stream segment. The stream length ratio of the Hadaf watershed is obtained as 0.97.

4.2.5 Bifurcation ratio (R_b)

It is the ratio of the number of streams of a given order to the number of streams of the next higher order (Schumn, 1956). Horton (1945) considered bifurcation ratio (R_b) as an index of relief and dissections. Strahler (1957) demonstrated that R_b shows only a small variation for different regions on different environment except where powerful geological control dominates. Lower R_b values are the characteristics of structurally less disturbed watersheds without any distortion in drainage pattern (Nag, 1998). The mean bifurcation ratio (R_b) is defined as the average of bifurcation ratios of all order and the value of mean bifurcation for the Hadaf watershed is obtained as 1.82.

4.2.6 Length of main channel (L_m)

It is the length along the longest watercourse from the outflow point of designated Hadaf watershed to the upper limit to the watershed boundary. The main channel length computed by using ArcGIS 10.0 software is obtained as 47.96 km.

4.2.7 Basin area (A)

The area of the watershed is another important parameter like the length of the stream drainage. Schumm (1956) established an interesting relation between the total watershed areas and the total stream lengths, which are supported by the contributing areas. The computed basin area of the Hadaf watershed using ArcGIS 10.0 software is obtained as 502 km^2.

4.2.8 Basin perimeter (P)

Basin perimeter is the outer boundary of the watershed that encloses its area. It is measured along the divides between watersheds and is used as an indicator of watershed size and shape. The basin perimeter by using ArcGIS 10.0 software is obtained as 168.45 km.

4.2.9 Basin length (L_b)

It is the longest dimension of a basin parallel to the principal drainage line. In the study area basin length is computed using ArcGIS 10.0 software and it is obtained as 58.34 km.

4.2.10 Drainage density (D_d)

Horton (1932) introduced the drainage density (D_d) is an important indicator of the linear scale of land-form elements in stream eroded topography. It is the ratio of total channel segment lengths cumulated for all orders within a basin to the basin area, which is expressed in terms of km/km^2. The drainage density indicates the closeness of spacing of channels, thus providing a quantitative measure of the average length of stream channel for the whole basin. High drainage density is the result of weak or impermeable subsurface material, sparse vegetation and mountainous relief. Low drainage density leads to course drainage texture while high drainage density leads to fine drainage texture (Strahaler, 1964). The drainage density (D_d) of the study area is obtained as 2.18 km/km^2.

4.2.11 Length of overland flow (L_g)

It is the length of water over the ground before it gets concentrated into definite stream channels, (Horton, 1945). It is inversely related to the average slope of the channel and is quite synonymous with the length of sheet flow to a large degree. It approximately equals to half of reciprocal of drainage density (Horton, 1945). In the Hadaf watershed the L_g is estimated as 0.22.

4.2.12 Fineness ratio (R_{fn})

The ratio of main channel length to the length of the watershed perimeter is fitness ratio, which is a measure of topographic fitness. The fitness ratio for Hadaf watershed is 0.34.

4.2.13 Circulatory ratio (R_c)

It is ratio of the area of the basin to the area of circle having the same circumference as the perimeter of the basin (Miller, 1953). It is influenced by the length and frequency of streams, geological structures, land use/land cover, climate, relief and slope of the basin. In the present case R_c is 0.219. It indicates that all the sub-watersheds are characterized by low to moderate relief and drainage system is structurally uncontrolled and indicates that it is elongated.

4.2.14 Elongation ratio (R_e)

It is the ratio between the diameter of the circle of the same area as the drainage basin and the maximum length of the basin. A circular basin is more efficient in run-off discharge than an elongated basin (Singh and Singh, 1997). The value of elongation ratio (R_e) generally varies from 0.52 to 0.91 associated with a wide variety of climate and geology. Values close to 1.0 are typical of regions of very low relief whereas that of 0.6 to 0.8 are associated with high relief and steep ground slope (Strahler, 1964). These values can be grouped into three categories, namely circular (> 0.9), oval (09 - 0.8) and elongated (< 0.7). In the Hadaf watershed the elongation ratio is 0.43, indicating it as of elongated shape.

4.2.15 Form factor (R_f)

It is defined as the ratio of basin area to square of the basin length (Horton, 1932). The value of form factor would always be less than 0.78 (for a perfectly circular basin). Smaller the value of form factor, more elongated will be the basin. The basins with high form factors have high peak flows of shorter duration, whereas, elongated sub-

watershed with low form factors have lower peak flow of longer duration. R_f values of the study area is obtained as 0.14.

4.2.16 Unity shape factor (R_u)

It is the ratio of the basin length (L_b) to the square root of the basin area. The R_u values < 2 of sub-watersheds indicates that have weaker flood discharge periods, whereas R_u value > 2 indicates that have sharp peak flood discharge. In the present study area, unity shape factor is estimated as 2.61.

4.2.17 Watershed shape factor (W_s)

The ratio of main stream length (L_m) to the diameter (D_c) of a circle has the same area as the watershed. In the present study area the watershed shape factor is 2.31.

4.2.18 Compactness coefficient (C_c)

Compactness coefficient of a watershed is the ratio of perimeter of watershed to circumference of circular area, which equals the area of the watershed. The C_c is independent of size of watershed and dependent only on the slope. The compactness coefficient of Hadaf watershed is estimated as 2.13.

4.2.19 Drainage texture (R_t)

Drainage texture (R_t) is one of the important drainage parameters in morphometric analysis, which indicates relative spacing of drainage lines, which are more prominent in impermeable material compared to the permeable ones. Horton (1945) defined drainage texture as the total number of stream segments of all orders divided by the perimeter of the watershed. He also recognized infiltration capacity as the dominant factor influencing drainage texture which includes drainage density and stream frequency as well. Drainage texture (R_t) depends upon a number of natural factors such as climate, rainfall, vegetation, lithology, soil type, infiltration capacity, relief. In the Hadaf watershed the drainage texture is calculated as 22.62.

4.2.20 Total relief (H)

It is the maximum vertical distance between the lowest (outlet) and the highest (divide) points in the watershed. In the study area total relief is 0.33 km. if the vertical distance is more between these points, steepness will be more.

4.2.21 Relief ratio (R_h)

The elevation difference between the highest and lowest points on the valley floor of a watershed is its total relief, whereas the ratio of maximum relief to horizontal distance along the longest dimension of the basin parallel to the principal drainage line is Relief Ratio (R_h) (Schunm, 1956). It measures the overall steepness of a drainage basin and is an indicator of intensity of erosion processes operating on the slopes of the basin. The R_h normally increases with decreasing drainage area and size of a given drainage basin (Gottschalk, 1964). In the Hadaf watershed the relief ratio is 0.0057.

4.2.22 Relative relief (R_p)

The ratio of basin relief, Total relief to the length of the perimeter, Relative relief of the Hadaf watershed is 0.0019.

4.3 Prioritization of Sub watersheds based on Morphometric analysis

The morphometric parameters such as bifurcation ratio (R_b), basin shape (B_s), compactness coefficient (C_c), drainage density (D_d), drainage texture (R_t), length of overland flow (L_o), form factor (R_f), circularity ratio (R_c), and elongation ratio (R_e) are also termed as erosion risk assessment parameters and have been used for prioritizing sub-watersheds (Biswas et al. 1999). Calculated all Sub-watershed morphometric parameters have been shown in Appendix-1.

For prioritization of sub-watershed, Hadaf watershed is divided in to 16 sub-watersheds. Morphological parameter extraction drainage line map (Fig. 4.21), Stream order map (Fig. 4.22), slope map (Fig. 4.23) and sub watersheds map (Fig. 4.24) has been prepared using HEC-geoHMS software with input as SRTM 90 m DEM data.

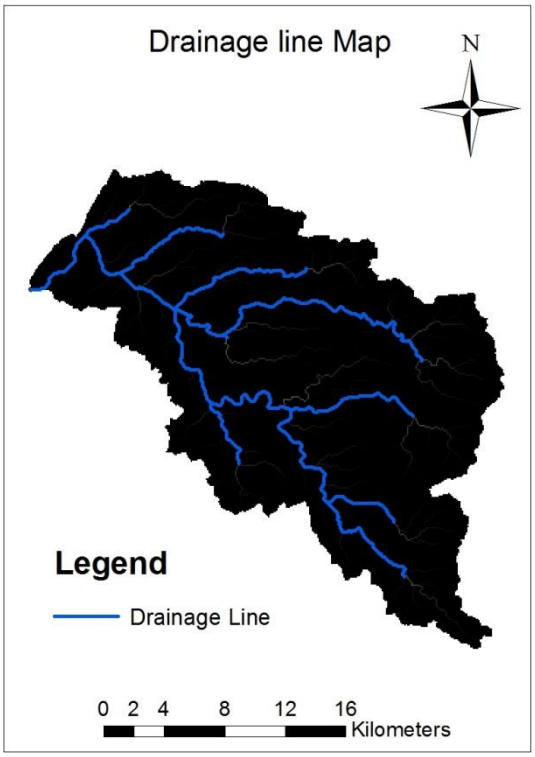

Fig. 4.21: Drainage line map

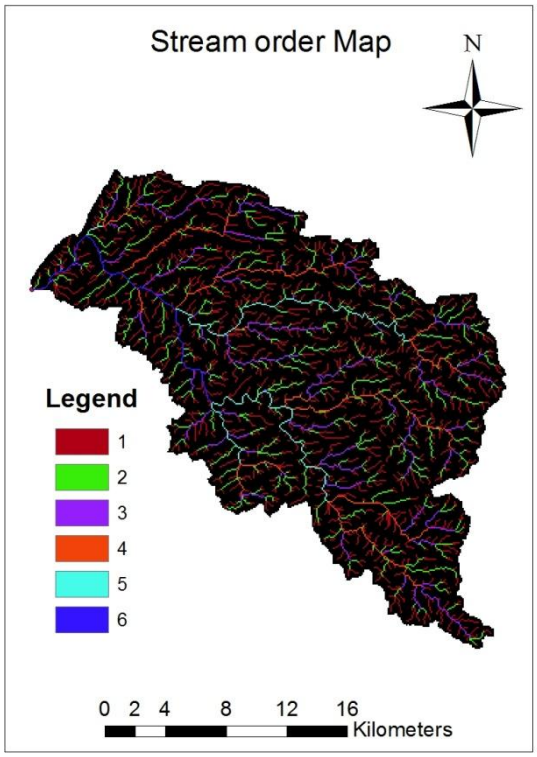

Fig. 4.22: Stream order map

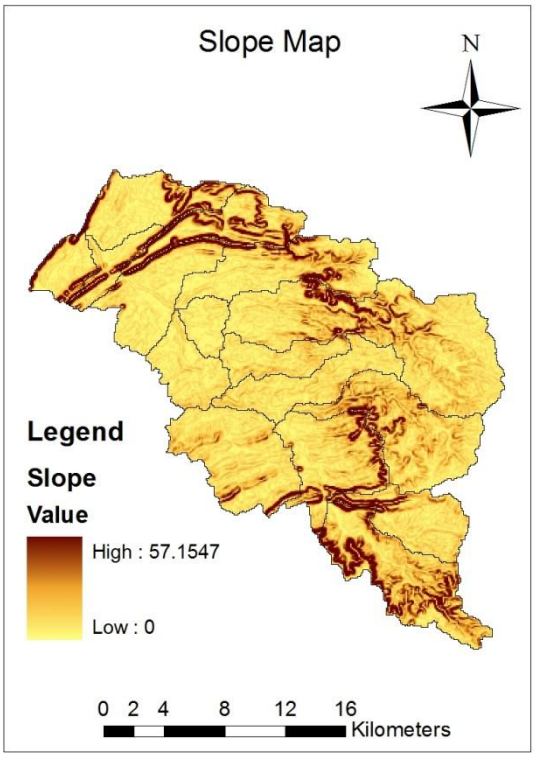

Fig. 4.23: Slope map

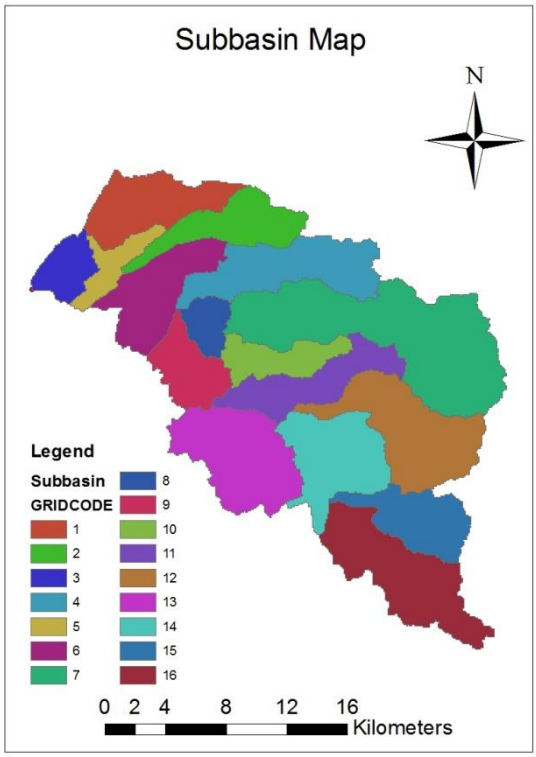

Fig. 4.24: Sub watersheds map

Shape parameters such as elongation ratio, compactness coefficient, circularity ratio, unity shape factor and form factor have an inverse relationship with erodibility

(Nookaratnam et al. 2005; Javed et al. 2009) lower the value more is the erodibility. Thus, the lowest value of shape parameters is rated as rank 1, next lower value is rated as rank 2 and so on and the highest value is rated last in rank. The linear parameters such as drainage density, stream frequency, bifurcation ratio, drainage texture, length of overland flow have a direct relationship with erodibility (Patel et al., 2013), higher the value, more is the erodibility. After the ranking has been done based on every single parameter, the ranking values for all the linear and shape parameters of each sub-watersheds are added up for each of the nine sub-watersheds to arrive at compound value (Cp). Based on average value of these parameters, the sub-watersheds having the least rating value was assigned highest priority, next higher value was assigned second priority and so on.

The compound parameter values of 16 sub-watersheds of Hadaf watershed are calculated and prioritization rating is shown in Table 4.4. Sub-watershed 11 with a compound parameter value of 7.429 receives the highest priority (one) with next in the priority list is sub-watershed 2 having the compound parameter value of 7.571. Highest priority indicates the greater degree of erosion potential associated in the particular sub-watershed and it becomes potential area for adaptation of soil conservative measure. Thus, in first glance, soil conservation measures should first be applied to sub-watersheds area 11 and then to the other sub-watersheds according to their ranking/priority. The subbasin priority map has been shown in Fig. 4.25.

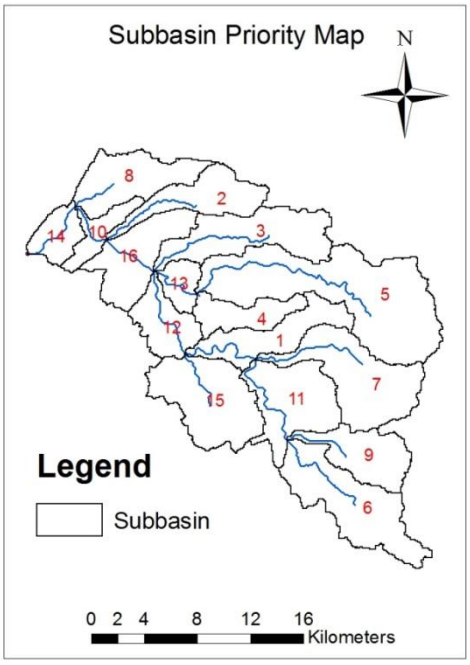

Fig. 4.25: Sub-basin priority map

Table 4.4: Priorities of sub-watersheds and their ranks

Sub basin	R_e	C_c	D_d	R_f	R_c	L_g	R_u	Compound parameters	Final Priority
1	8	8	4	8	9	13	9	8.429	8
2	2	14	15	2	3	2	15	7.571	2
3	14	1	1	14	16	16	3	9.286	14
4	3	13	12	3	4	5	14	7.714	3
5	10	16	16	10	1	1	7	8.714	10
6	16	6	11	16	11	6	1	9.571	16
7	5	12	6	5	5	11	12	8.000	5
8	13	2	2	13	15	15	4	9.143	13
9	12	4	5	12	13	12	5	9.000	12
10	4	11	8	4	6	9	13	7.857	4
11	1	15	7	1	2	10	16	7.429	1
12	7	9	14	7	8	3	10	8.286	7
13	15	3	9	15	14	8	2	9.429	15
14	11	5	10	11	12	7	6	8.857	11
15	9	7	3	9	10	14	8	8.571	9
16	6	10	13	6	7	4	11	8.143	6

4.4 Calibration and validation of HEC-HMS model

Once all the initial parameters are obtained the HEC-HMS model is calibrated to optimize the parameters using the hydro-meteorological dataset. The HEC-HMS model has a self- calibrating utility based on optimization techniques that allows the user to select different approaches of objective function. Hence, the selected gauged watershed is modelled and the results are presented for the selected events. To determine the accuracy of modeled results, the simulated hydrograph at outlet is compared to the historically observed hydrograph at outlet of the watershed.

The Hadaf watershed is divided into 2 subbasins: W700 and W800 as per the availability of hydro-meteorological data. Parameters of different hydrographs along with hydro-climatic data in each subbasin are provided and parameters are adjusted after calibration using the optimization method.

In the study four events used for calibration and validation of HEC-HMS model. The rainfall data is collected from three rain gauges namely Hadaf, Limkheda and Umaria Station. The weighted rainfall is calculated using thiessen polygon method. The HEC-HMS model is calibrated and validated using Event-I: 05-11 Sept 2006 and Event-II: 08-14 July 2007 respectively, for LISS-III imageries of the year 2008 and 2012. The model is also calibrated and validated using Event-III: 07-12 Sept 2010 and Event-IV: 04-12 Sept 2012 respectively, for the LISS-IV imagery of the year 2013. The graph plotted between weighted rainfall and observed discharge for all these four events is shown in Fig. 4.26 to Fig. 4.29.

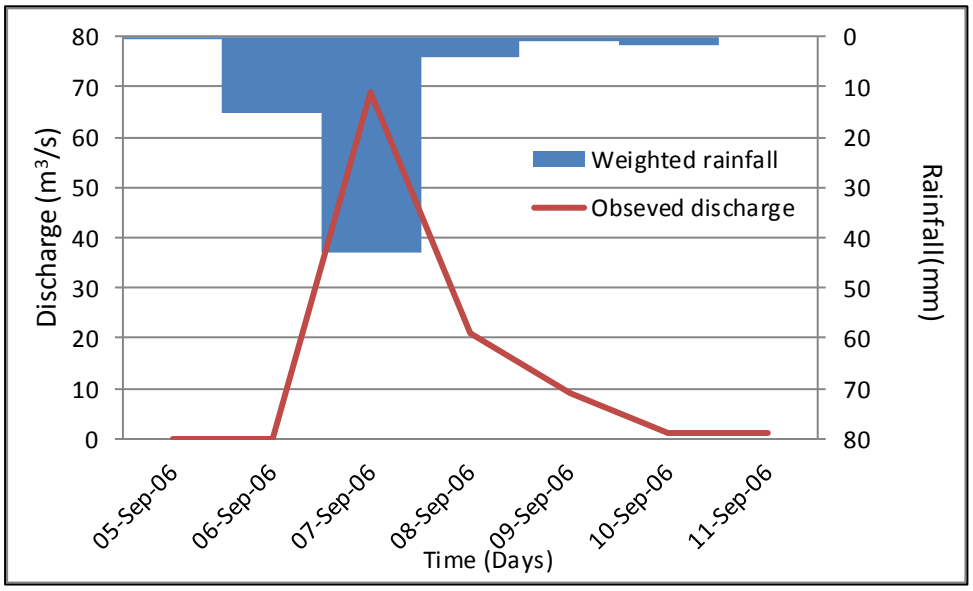

Fig. 4.26: Weighted rainfall versus observed discharge for event: I

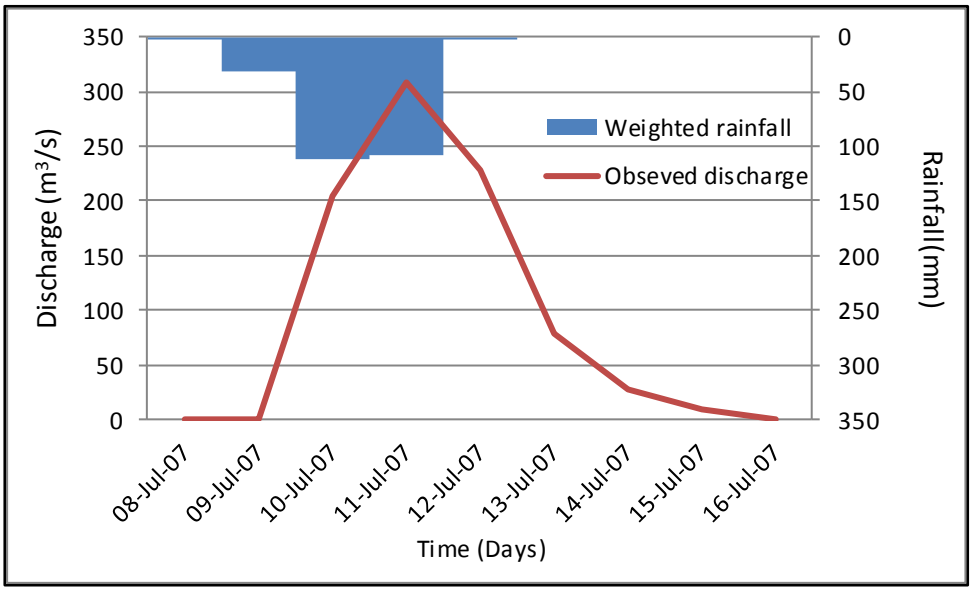

Fig. 4.27: Weighted rainfall versus observed discharge for event: II

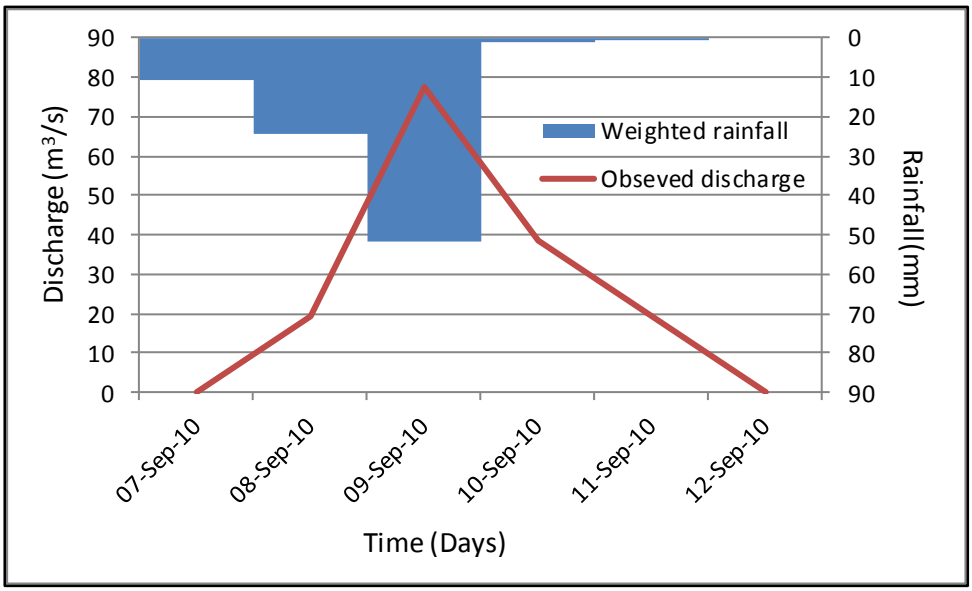

Fig. 4.28: Weighted rainfall versus observed discharge for event: III

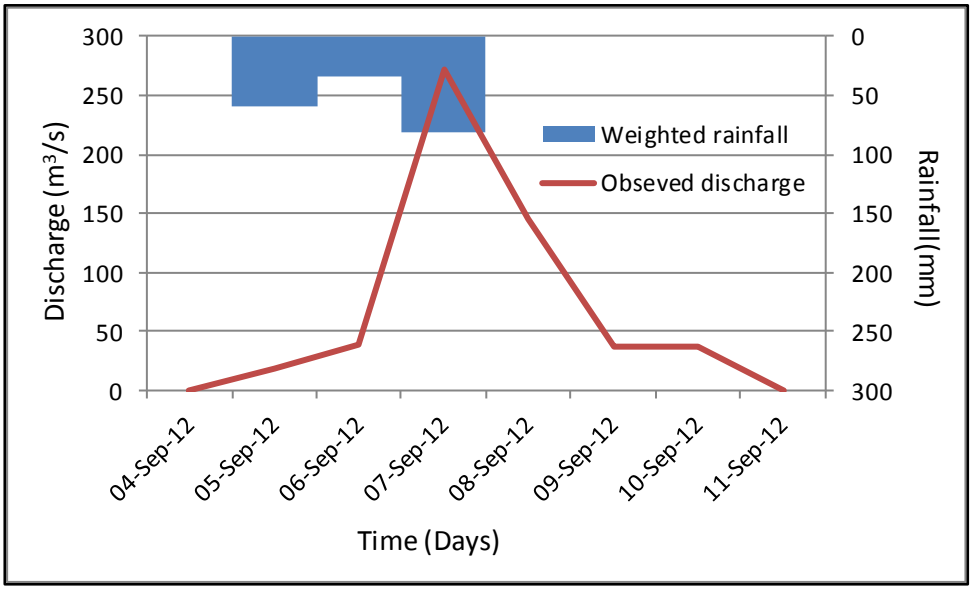

Fig. 4.29: Weighted rainfall versus observed discharge for event: IV

4.4.1 Calibration and validation of HEC-HMS model using LISS-III imagery of Year 2008

The HEC-HMS model is calibrated using the daily data set for the Event-I: 05-11 Sept 2006 and validated for the Event-II: 08-14 July 2007 for LISS-III Imageries of 2008. The calibration of HEC-HMS model is conducted using three methods namely (i) loss method (ii) Transform method (iii) Routing method. Different initial parameters of these three methods are presented in Table 4.5. It is to be noted that CN number is extracted using LISS-III imagery of year 2008.

Runoff simulation for calibration and validation of HEC-HMS model and evaluation of different unit hydrograph are made with two approaches as presented in the Table 4.5. In these two approaches the difference is only in the transform method used and remaining methods used are same in both the approaches. In the approach-1 SCS UH transformation method is applied whereas in the approach-2 Clark UH is applied as a transformation method.

Table 4.5: Simulation parameters of watershed using LISS-III 2008 for event: I

Method	Approach-1				Approach-2			
	Method Used	Parameter	Subbasin		Method Used	Parameter	Subbasin	
			W700	W800			W700	W800
Loss method	SCS CN	Initial Abstraction (mm)	20.74	28.57	SCS CN	Initial Abstraction (mm)	20.74	28.57
		Curve Number	71	64		Curve Number	71	64
		Impervious (%)	5	5		Impervious (%)	5	5
Transform method	SCS UH	Lag Time (min)	613.8	265.8	Clark UH	Time of Concentration (hr)	17.05	7.38
						Storage Coefficient (hr)	25.57	11.07
Channel Routing	Muskingum	Travel time (K)	2 hrs For all the reach's					
		Weighting Coefficient (X)	0.1 For all the reach's (for natural Channel)					
Resorvoir Routing	Modified Puls	Initial elevation	280 m					

Hydrograph and scatter plot between observed and simulated discharge using Approach-1 and Approach-2 without parameters optimization has been shown in the Fig. 4.30 (a) and Fig. 4.30 (b), respectively. The correlation co-efficient of approach-1 and approach-2 found 0.98 and 0.68, respectively. Therefore, it can be observed that approach-1 is found better compared to the approach-2.

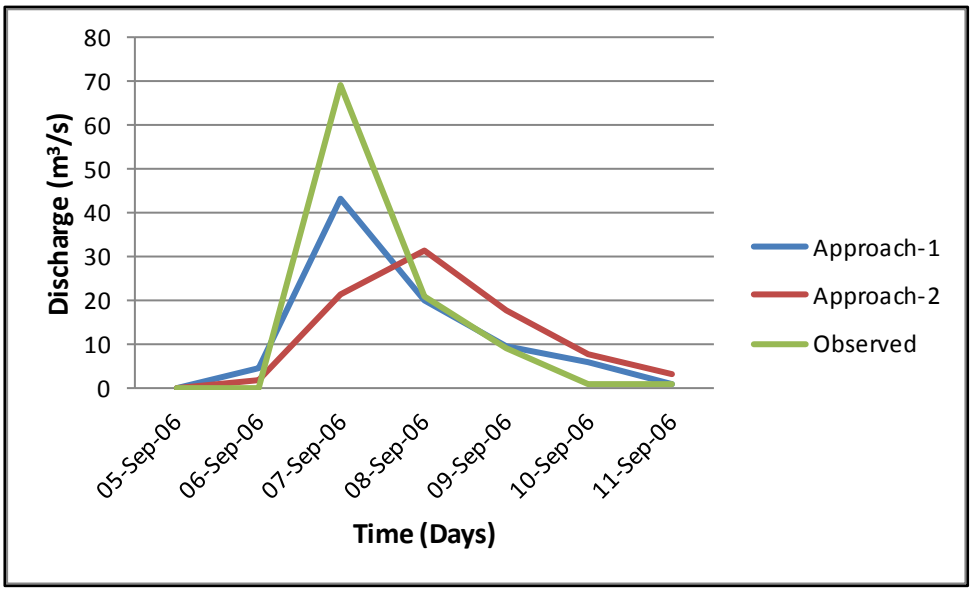

Fig. 4.30 (a): Hydrograph for observed and simulated discharge at outlet without parameter optimization using Approach-1 and Approach-2 for LISS-III 2008 imagery with event-I

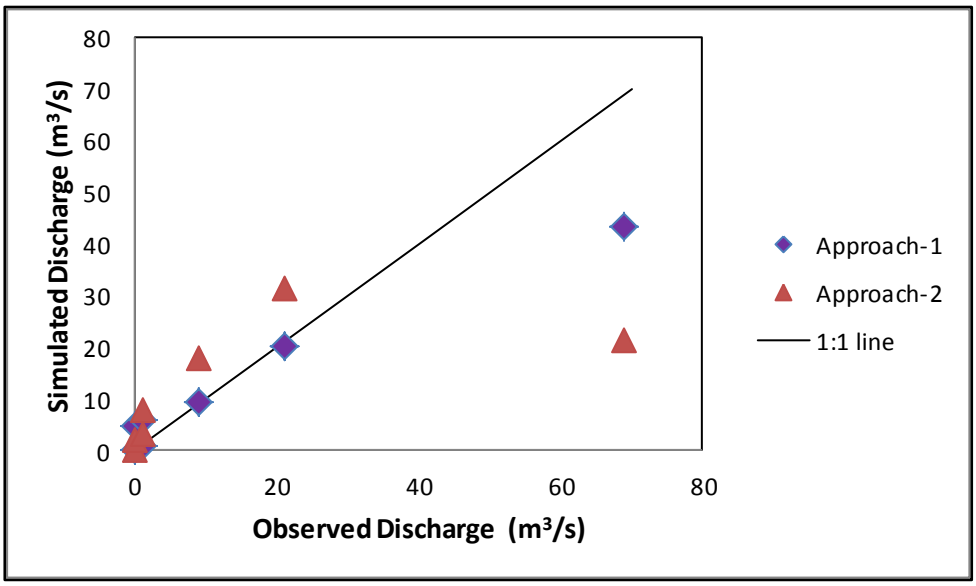

Fig. 4.30 (b): Scatter plot between observed and simulated discharge at outlet without parameter optimization using Approach-1 and Approach-2 for LISS-III 2008 imagery with event-I

The observed and modelled values of flood peak and flood volume for the Event-I using approach-1 & 2 without optimization have been shown in Table 4.6. It can be observed that the approach-1 produces better results comparatively.

Table 4.6: Comparison of simulated flood peak and flood volume with observed values before parameter optimization for LISS-III 2008

Event : I				
Method	**Flood Peak (m^3/s)**		**Flood Volume ($1000m^3$)**	
	Model	**Observed**	**Model**	**Observed**
Approach-1	43.4	69.0	7248.4	8683.20
Approach-2	31.5	69.0	7111.1	8683.20

4.4.1.1 Parameters optimization for Approach-1and Approach-2 using LISS-III 2008 imagery of Event-I

In the previous section rainfall runoff transformation applying the estimated parameters in the HEC-HMS model are applied. Now, the next step is to calibrate the parameters using a suitable optimization method applying the observed hydro-meteorological data to obtain most suitable parameters. HEC-HMS model offers seven different objective functions to measure the good of fitness. The objective function used in this study is the peak weighted RMS error method. This function is selected because it gives greater weight to matching the peak of the hydrograph. The peak weighted RMS error method focuses solely on the peak of the hydrograph. However, it takes in to account the volume and time of the peak as well. The univariate gradient method and nelder mead method are used to minimize the peak weighted RMS error-objective function. The univariate gradient method evaluates and adjusts one parameter at a time while holding others parameters constant. The nelder mead method uses a downhill simplex to evaluate all parameters simultaneously and determine which parameters to adjust. In optimization trials are done with changing the initial abstraction, lag time, time of concentration, storage coefficient and muskingum K using univariate gradient method and nelder mead method with peak weighted RMS error method. The optimized initial abstraction, lag time, time of concentration, storage coefficient and muskingum K parameter values for approach-1 and approach-2 are presented in Table 4.7 (a) & (b).

Table 4.7: The optimized values of parameters using Approach-1and Approach-2 for LISS-III 2008 Imagery

(a) Initial abstraction, lag time, time of concentration and storage coefficient

	Method	Parameter	Sub basin W700			Sub basin W800		
			Initial Value	Optimize Value		Initial Value	Optimize Value	
				Univariate	Nelder		Univariate	Nelder
Approach 1	SCS CN	Initial Abstraction (mm)	20.74	19.13	6.5242	28.57	17.927	28.346
	SCS UH	Lag Time (min)	613.8	613.8	612.42	265.8	265.8	267.45
Approach 2	SCS CN	Initial Abstraction (mm)	20.74	13.279	13.663	28.57	28.264	29.637
	Clark UH	Time of concentration	17.05	17.05	18.289	7.38	7.38	9.1343
		Storage coefficient	25.57	11.364	23.195	11.07	11.07	8.856

(b) Muskingum K parameter

Reach Element	Initial Value	Optimize Value			
		For Approach-1		For Approach-2	
		Univariate	Nelder	Univariate	Nelder
R220	2	0.39506	2.499	0.59259	0.49966
R240	2	0.59259	0.40557	0.59259	2.1248
R260	2	0.59259	1.4362	0.59259	2.158
R280	2	0.59259	0.041878	0.59259	2.231
R30	2	0.59259	0.29909	0.59259	0.7996
R350	2	0.59259	3.5172	0.59259	2.5478
R380	2	0.59259	2.0141	0.59259	1.9384
R40	2	0.59259	3.1317	0.59259	1.5808
R50	2	0.59259	3.9532	0.59259	0.58847
R70	2	0.59259	5.292	0.59259	1.5109
R80	2	0.59259	5.0203	0.88889	0.054315

After optimizing above tabulated parameters the resultant hydrograph and scatter plot between observed and simulated discharge using Approach-1 and Approach-2 after parameters optimization with univariate gradient method has been shown in the Fig. 4.31 (a) and (b), respectively and the result obtained by using nelder mead method is shown in the Fig. 4.32 (a) and (b). The correlation co-efficient obtained after optimization for approach-1 and approach-2 with univariate gradient method are 0.978 and 0.815 respectively. The correlation co-efficient obtained after optimization for approach-1 and approach-2 with nelder mead method are 0.979 and 0.682 respectively. Which are greater than without parameter optimization. The observed and simulated values of flood peak and flood volume for the event: I using approach-1 & 2 after optimization have been shown in Table 4.8. From the Tables 4.6 and 4.8 it shows the improvement in the result of flood peak and flood volume using the optimized parameter.

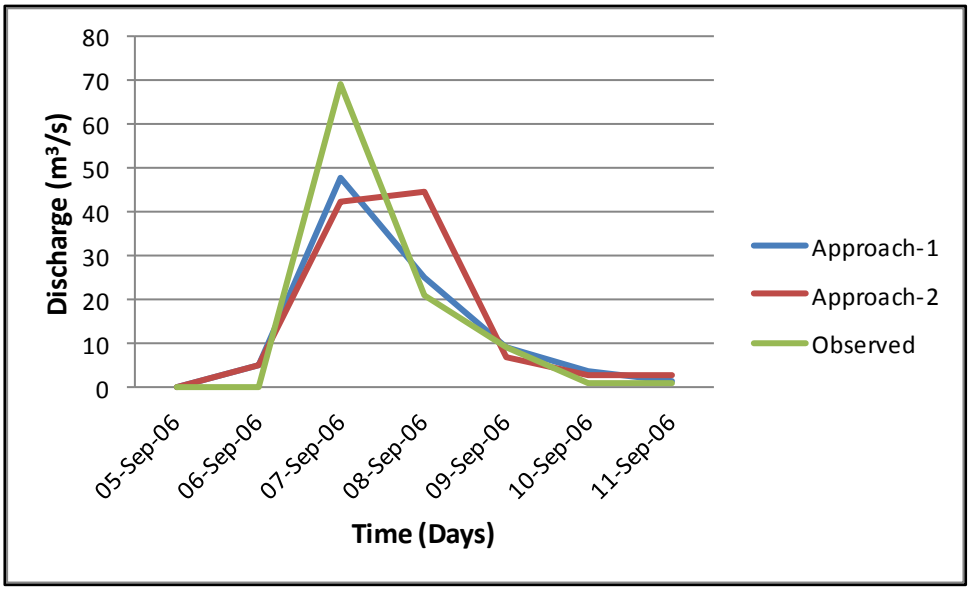

Fig. 4.31 (a): Hydrograph for observed and simulated discharge at outlet after parameter optimization using Approach-1, Approach-2 and univariate gradient method for LISS-III 2008 imagery with event-I

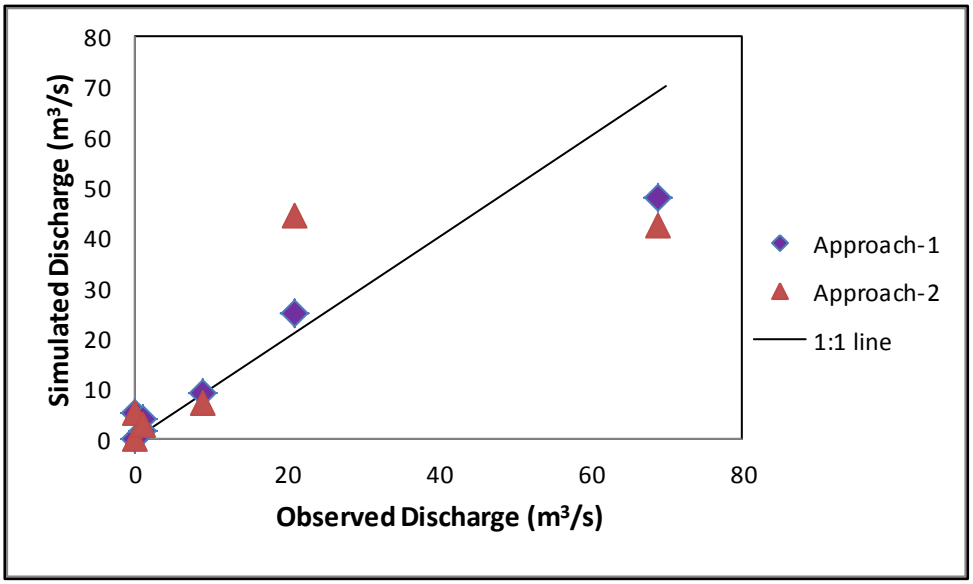

Fig. 4.31 (b): Scatter plot between observed and simulated discharge at outlet after parameter optimization using Approach-1, Approach-2 and univariate gradient method for LISS-III 2008 imagery with event-I

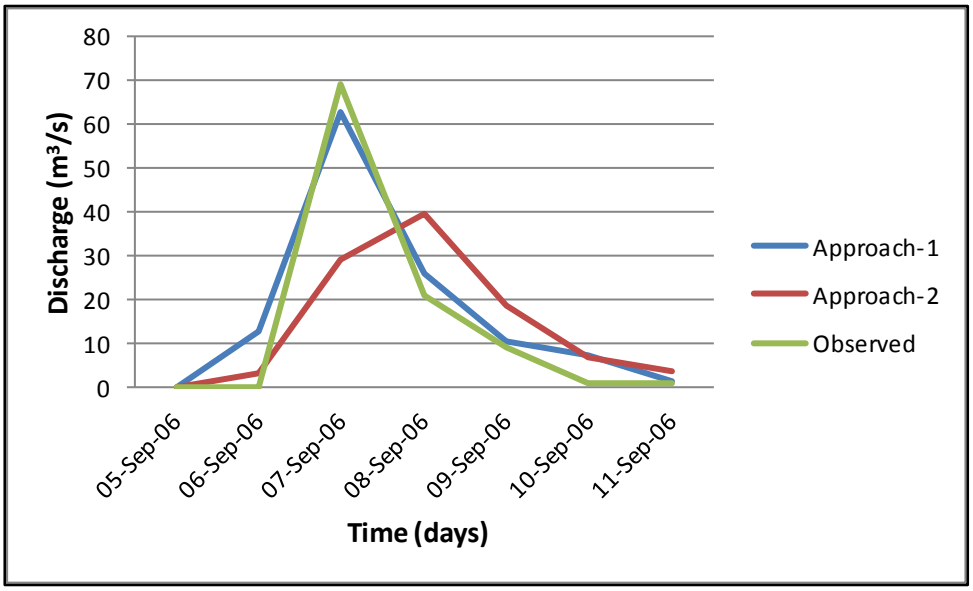

Fig. 4.32 (a): Hydrograph for observed and simulated discharge at outlet after parameter optimization using Approach-1, Approach-2 and nelder mead method for LISS-III 2008 imagery with event-I

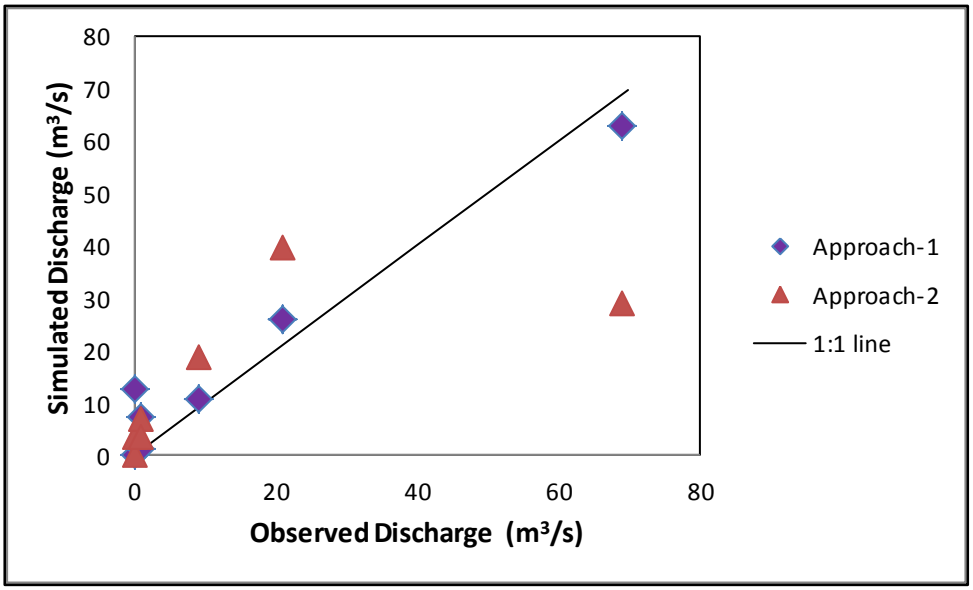

Fig. 4.32 (b): Scatter plot between observed and simulated discharge at outlet after parameter optimization using Approach-1, Approach-2 and nelder mead method for LISS-III 2008 imagery with event-I

Table 4.8: Comparison of simulated flood peak and flood volume with observed values after parameter optimization for LISS-III 2008 imagery

Method	Event : I					
	Flood Peak (m^3/s)			Flood Volume ($1000m^3$)		
	Univariate	Nelder	Observed	Univariate	Nelder	Observed
Approach-1	47.9	62.8	69.0	7892.9	10364.9	8683.20
Approach-2	44.5	39.6	69.0	8894.7	8589.9	8683.20

4.4.1.2 Validation of HEC-HMS model using LISS-III Imagery of year 2008

Model validation is processes of testing model ability to simulate observe data other than those use for calibration, with acceptable accuracy. During this process, calibrated model parameters are not subject to change, their values are kept constant. The quantitative measure of the match is again the degree of variation between computed and observed hydrograph. Here the parameters optimized by Event: I has been applied for validation of Event: II. Validation result of approach-1 and approach-2 using univariate gradient method has been graphically presented in Fig. 4.33 (a) and (b). The correlations co-efficient of approach-1 and approach-2 are obtained as 0.93 and 0.97, respectively. The resultant parameters optimized using nelder mead method has been also applied for validation of Event-II. Validation result of approach-1 and approach-2 using nelder mead method has been graphically presented in Fig. 4.34 (a) and (b). The correlations co-efficient of approach-1 and approach-2 are obtained as 0.94 and 0.95, respectively. The observed and modelled values of flood peak and flood volume for the Event: II using approach-1 & 2 during validation has been shown in Table 4.9.

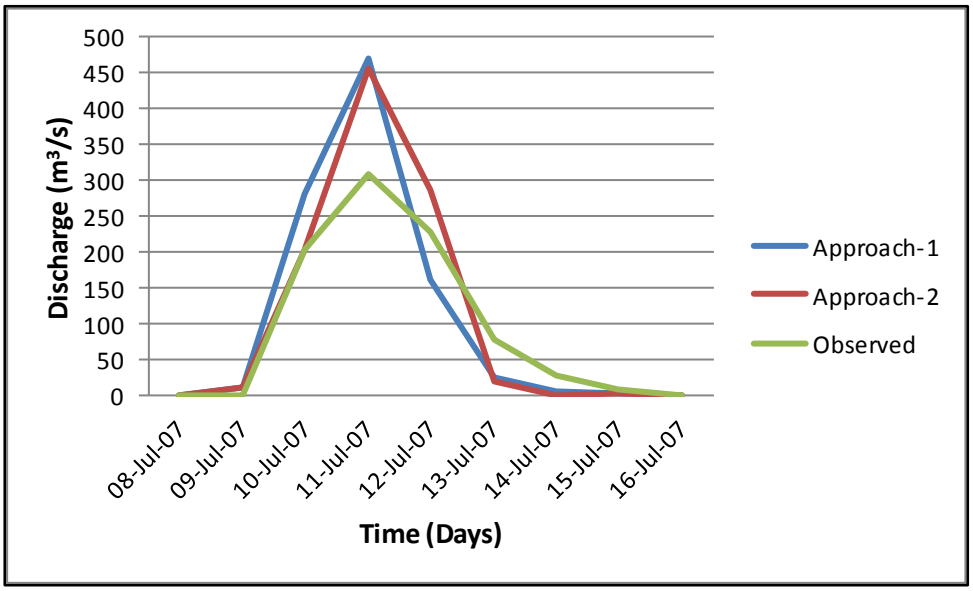

Fig. 4.33 (a): Hydrograph for observed and simulated discharge at outlet during validation using Approach-1, Approach-2 and univariate gradient method for LISS-III 2008 imagery with event-II

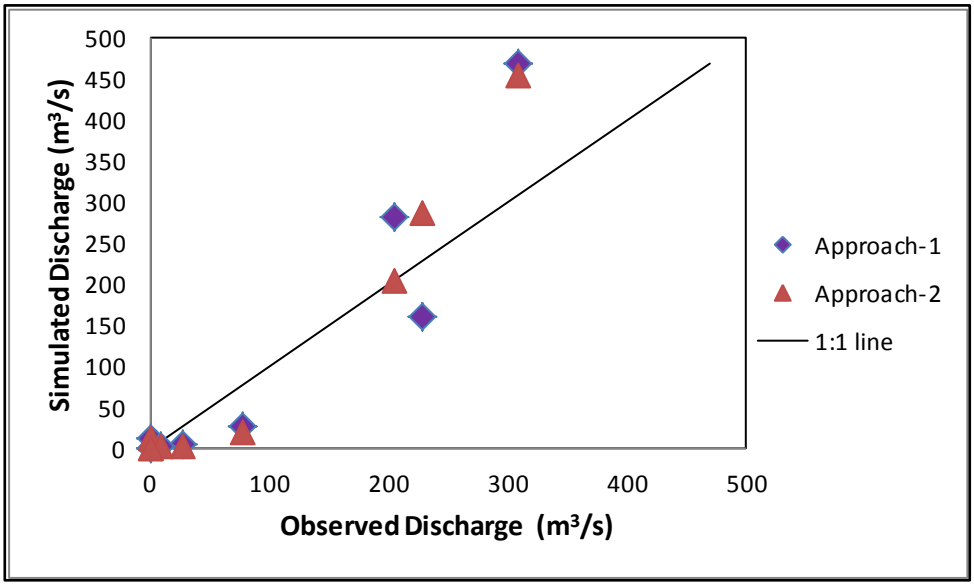

Fig. 4.33 (b): Scatter plot between observed and simulated discharge at outlet during validation using Approach-1, Approach-2 and univariate gradient method for LISS-III 2008 imagery with event-II

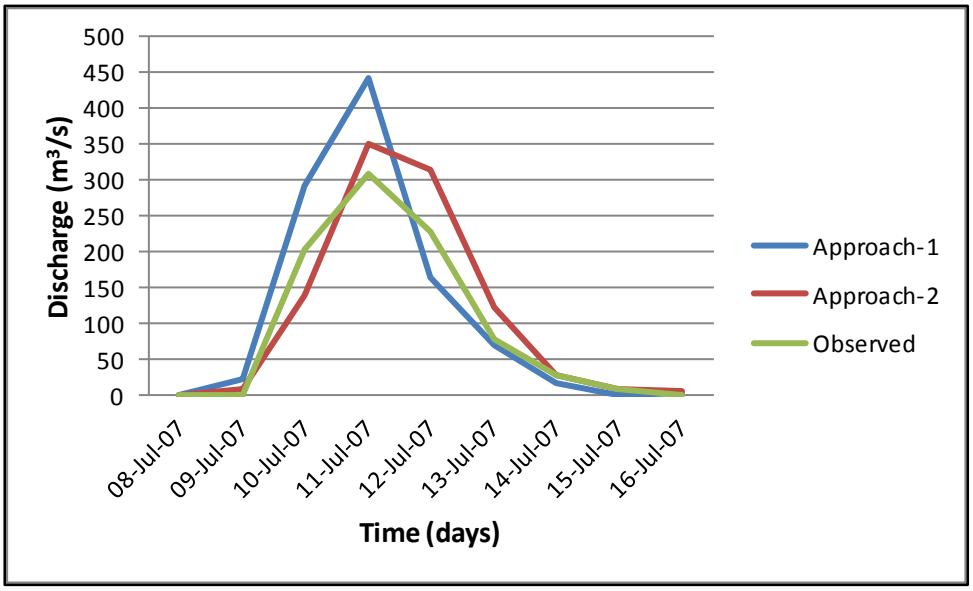

Fig. 4.34 (a): Hydrograph for observed and simulated discharge at outlet during validation using Approach-1, Approach-2 and nelder mead method for LISS-III 2008 imagery with event-II

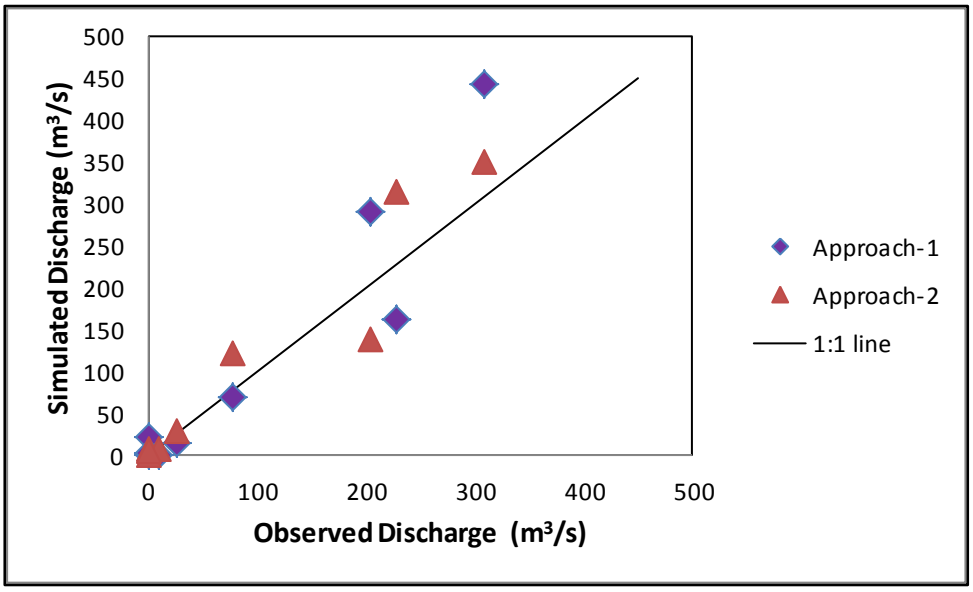

Fig. 4.34 (b): Scatter plot between observed and simulated discharge at outlet during validation using Approach-1, Approach-2 and nelder mead method for LISS-III 2008 imagery with event-II

Table 4.9: Comparison of simulated flood peak and flood volume with observed values during validation for LISS-III 2008

Method	Event : II					
	Flood Peak (m^3/s)			Flood Volume ($1000m^3$)		
	Univariate	Nelder	Observed	Univariate	Nelder	Observed
Approach-1	468.9	442.8	308.80	82598.7	86854.7	73836.58
Approach-2	455.3	351.1	308.80	84333.8	84145.7	73836.58

The better performance during the validation period clearly indicated applicability of the optimized parameters for newer or unseen events. Further it is found that the approach-2 that uses Clark transformation method performs better than the approach-1 where SCS CN transformation method is applied.

4.4.2 Calibration and validation of HEC-HMS model using LISS-III imagery of year 2012

The HEC-HMS model is calibrated using the daily dataset for the event: I and validated for the event: II. The calibration of HEC-HMS model is conducted considering different model parameters for LISS-III imagery of year 2012 as shown in Table 4.10.

Table 4.10: Simulation parameters of watershed using LISS-III imagery of year 2012 for event: I

Method	Approach-1				Approach-2			
	Method Used	Parameter	Subbasin		Method Used	Parameter	Subbasin	
			W700	W800			W700	W800
Loss method	SCS CN	Initial Abstraction (mm)	16.93	20.74	SCS CN	Initial Abstraction (mm)	16.93	20.74
		Curve Number	75	71		Curve Number	75	71
		Impervious (%)	5	5		Impervious (%)	5	5
Transform method	SCS UH	Lag Time (min)	543	229.2	Clark UH	Time of Concentration (hr)	15.08	6.36
						Storage Coefficient (hr)	22.62	9.54
Channel Routing	Muskingum	Travel time (K)	2 hrs For all the reach's					
		Weighting Coefficient (X)	0.1 For all the reach's (for natural Channel)					
Resorvoir Routing	Modified Puls	Initial elevation	280 m					

Hydrograph and scatter plot between observed and simulated discharge using Approach-1 and Approach-2 without parameters optimization has been shown in the Fig. 4.35 (a) and (b), respectively. The correlation co-efficient of approach-1 and approach-2 was found as 0.982 and 0.645, respectively.

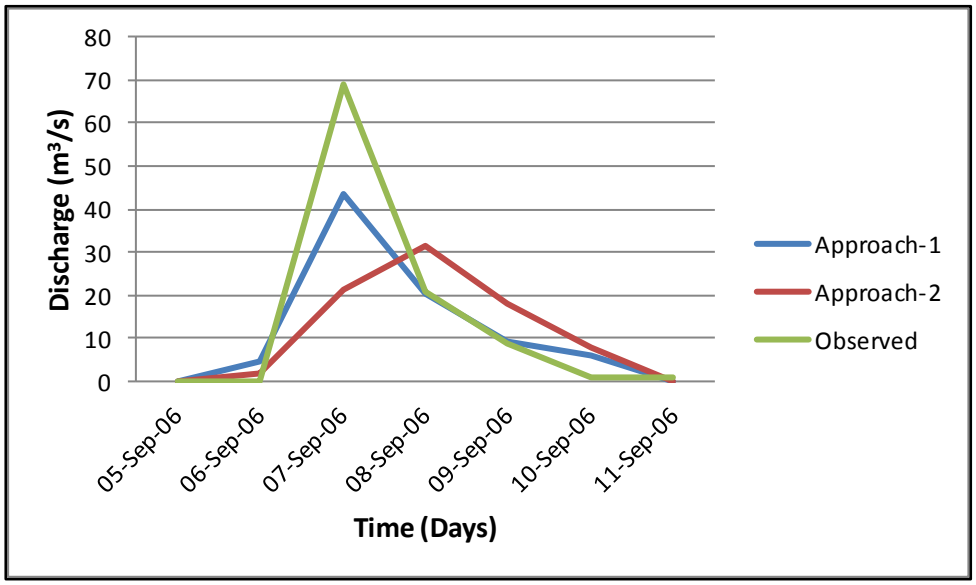

Fig. 4.35 (a): Hydrograph for observed and simulated discharge at outlet without parameter optimization using Approach-1 and Approach-2 for LISS-III 2012 imagery with event-I

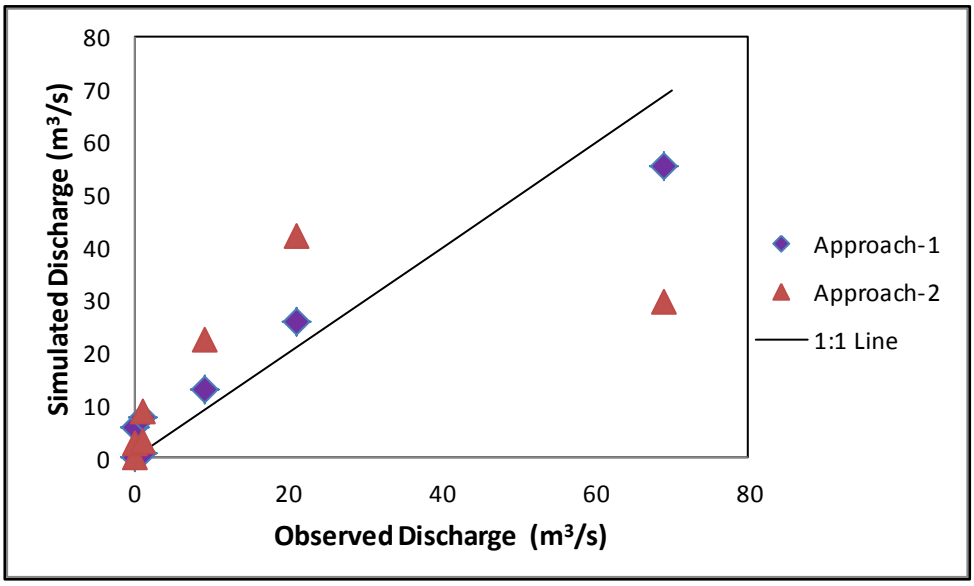

Fig. 4.35 (b): Scatter plot between observed and simulated discharge at outlet without parameter optimization using Approach-1 and Approach-2 for LISS-III 2012 imagery with event-I

The observed and modelled values of flood peak and flood volume for the event: I using approach-1 & 2 without optimization have been shown in Table 4.11.

Table 4.11: Comparison of simulated flood peak and flood volume with observed values before optimization for LISS-III 2012

Event : I				
Method	**Flood Peak (m^3/s)**		**Flood Volume ($1000m^3$)**	
	Model	**Observed**	**Model**	**Observed**
Approach-1	55.4	69.0	9356.1	8683.20
Approach-2	42.0	69.0	9260.5	8683.20

4.4.2.1 Parameters optimization for Approach-1 and Approach-2 using LISS-III 2012 imagery for Event-I

In optimization trial done with changes of initial abstraction, lag time, time of concentration, storage coefficient and muskingum K using univariate gradient method and nelder mead method with peak weighted RMS error method. The optimized initial abstraction, lag time, time of concentration, storage coefficient and muskingum K parameter values for approach-1 and approach-2 given in Table 4.12 (a) & (b)

Table 4.12: The optimized values of parameters using Approach-1 and Approach-2 for LISS-III 2012 Imagery

(a) Initial abstraction, lag time, time of concentration and storage coefficient

	Method	**Parameter**	**Sub basin W700**			**Sub basin W800**		
			Initial Value	**Optimize Value**		**Initial Value**	**Optimize Value**	
				Univariate	**Nelder**		**Univariate**	**Nelder**
Approach 1	**SCS CN**	Initial Abstraction (mm)	16.93	15.616	8.9465	20.74	20.093	23.232
	SCS UH	Lag Time (min)	543	543	542.7	229.2	229.2	230.29
Approach 2	**SCS CN**	Initial Abstraction (mm)	16.93	15.934	6.8914	20.74	21.046	20.98
	Clark UH	Time of concentration (hr)	15.08	15.08	17.133	6.36	6.36	5.5072
		Storage coefficient (hr)	22.62	10.053	18.879	9.54	9.54	4.3309

(b) Muskingum K parameter

Reach Element	Initial Value	Optimize Value			
		For Approach-1		For Approach-2	
		Univariate	Nelder	Univariate	Nelder
R220	2	0.39506	1.9101	0.59259	1.7813
R240	2	0.59259	2.3773	0.59259	5.2128
R260	2	0.87111	4.3455	0.59259	1.4127
R280	2	0.59259	4.428	0.59259	1.9633
R30	2	0.59259	0.65061	0.59259	2.7404
R350	2	0.59259	1.5426	0.59259	1.2331
R380	2	0.87111	1.9699	0.59259	1.0827
R40	2	0.59259	0.41775	0.59259	2.4498
R50	2	0.59259	2.1346	0.59259	2.7772
R70	2	0.59259	2.0852	0.59259	1.2323
R80	2	0.59259	2.2346	0.88889	2.1066

After optimizing above tabulated parameters the resultant hydrograph and scatter plot between observed and simulated discharge using Approach-1 and Approach-2 after parameters optimization with univariate gradient method has been shown in the Fig. 4.36 (a) and (b), respectively and the result obtained by using nelder mead method is shown in the Fig. 4.37 (a) and (b). The correlation co-efficient obtained after optimization for approach-1 and approach-2 with univariate gradient method are 0.981 and 0.799 respectively. The correlation co-efficient obtained after optimization for approach-1 and approach-2 with nelder mead method are 0.981 and 0.747 respectively. The observed and simulated values of flood peak and flood volume for the event: I using approach-1 & 2 after optimization have been shown in Table: 4.13. From the Table 4.11 and 4.13 it shows the improvement in the result of flood peak and flood volume using the optimized parameter.

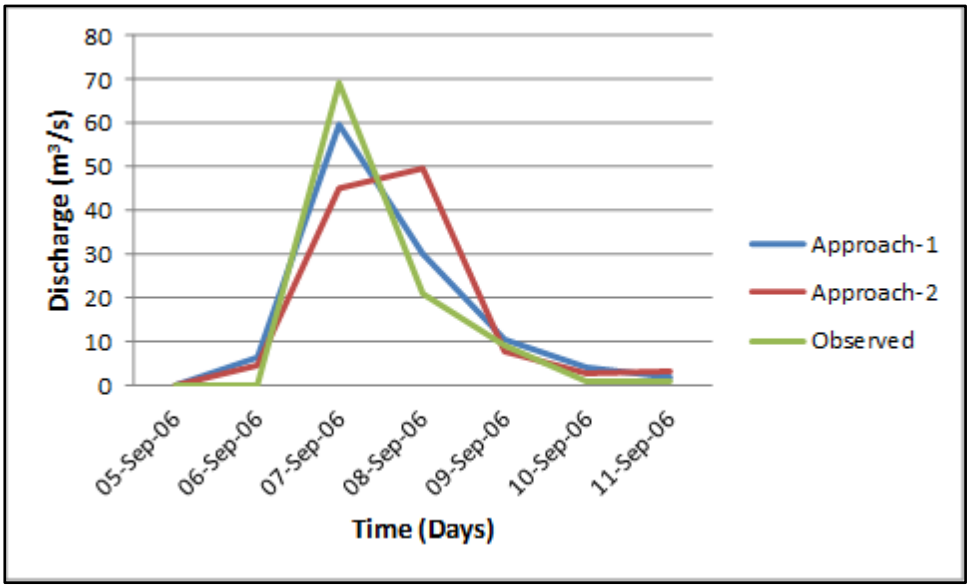

Fig. 4.36 (a): Hydrograph for observed and simulated discharge at outlet after parameter optimization using Approach-1, Approach-2 and univariate gradient method for LISS-III 2012 imagery with event-II

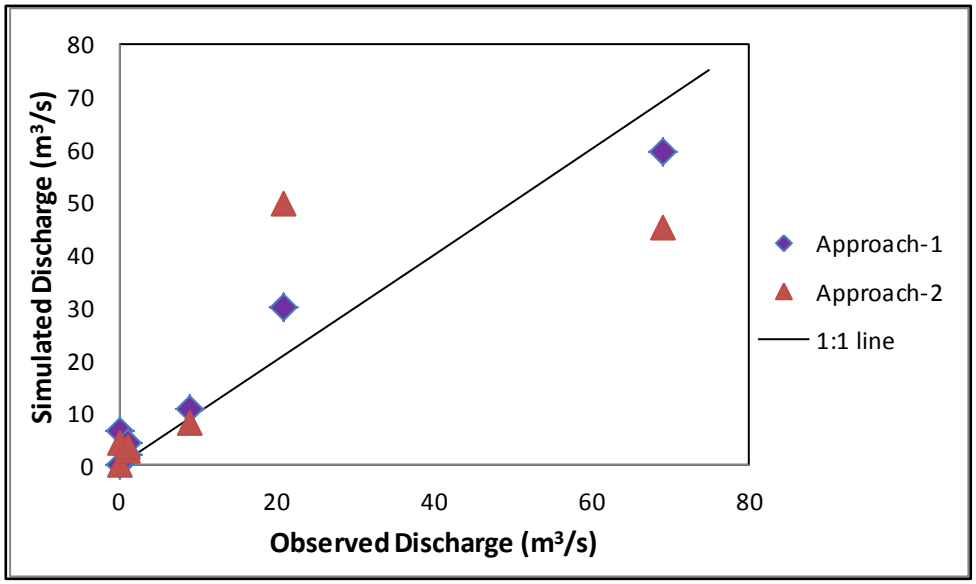

Fig. 4.36 (b): Scatter plot between observed and simulated discharge at outlet after parameter optimization using Approach-1, Approach-2 and univariate gradient method for LISS-III 2012 imagery with event-I

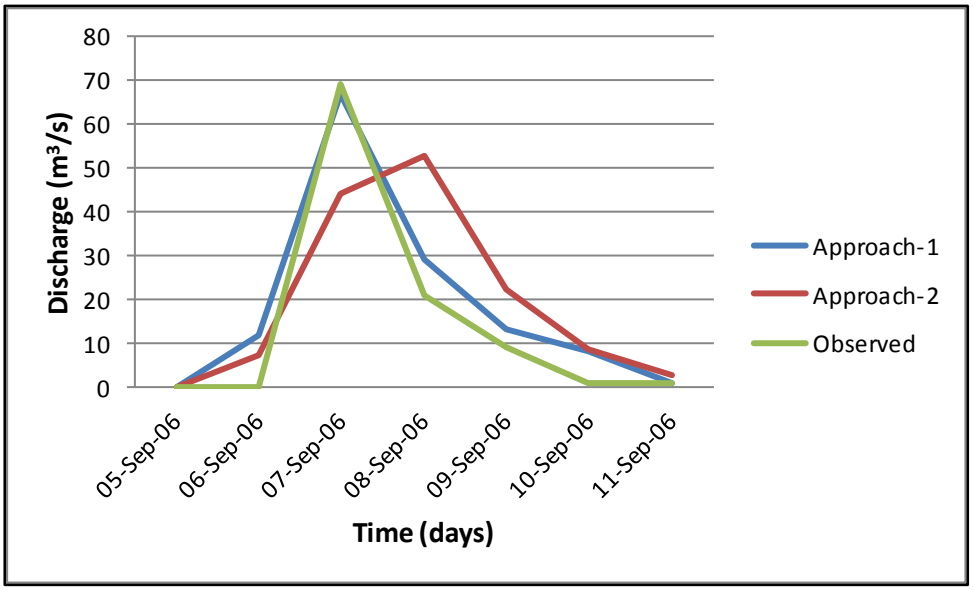

Fig. 4.37 (a): Hydrograph for observed and simulated discharge at outlet after parameter optimization using Approach-1, Approach-2 and nelder mead method for LISS-III 2012 imagery with event-I

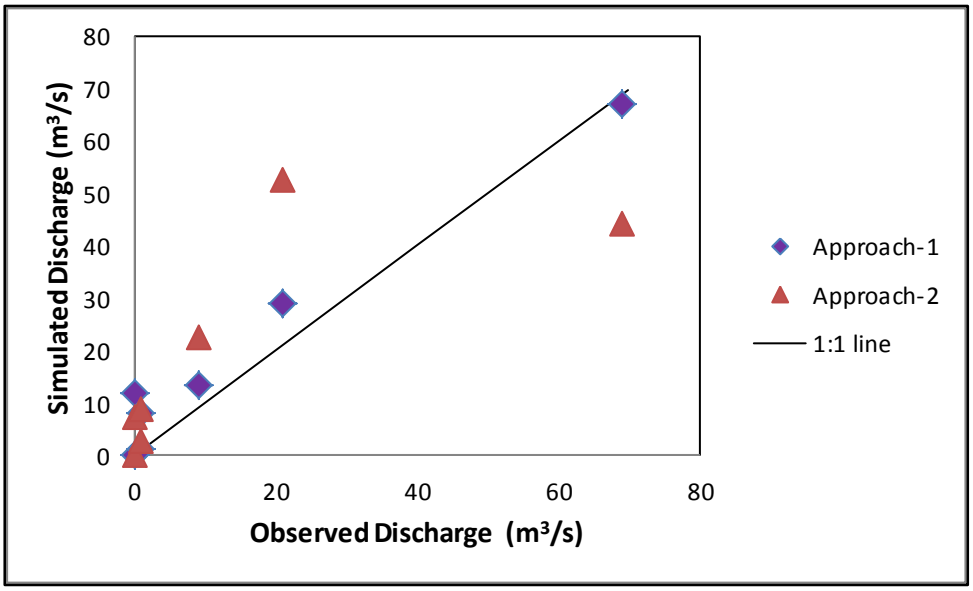

Fig. 4.37 (b): Scatter plot between observed and simulated discharge at outlet after parameter optimization using Approach-1, Approach-2 and nelder mead method for LISS-III 2012 imagery with event-I

Table 4.13: Comparison of simulated flood peak and flood volume with observed values after optimization for LISS-III 2012

Method	Event : I					
	Flood Peak (m^3/s)			Flood Volume ($1000m^3$)		
	Univariate	Nelder	Observed	Univariate	Nelder	Observed
Approach-1	59.5	67.1	69.0	9674.8	11215.9	8683.20
Approach-2	49.6	52.8	69.0	9641.9	11821.8	8683.20

4.4.2.2 Validation of HEC-HMS model using LISS-III imagery of year 2012

The above same procedure applied for validation of HEC-HMS model using LISS-III imagery of year 2012. The parameters optimized by Event: I have been applied for validation of event: II. Validation result of approach-1 and approach-2 using univariate gradient method has been graphically presented in Fig. 4.38 (a) and (b). The correlations co-efficient of approach-1 and approach-2 are obtained as 0.936 and 0.971, respectively. The resultant parameters optimized using nelder mead method has been also applied for validation of Event-II. Validation result of approach-1 and approach-2 using nelder mead method has been graphically presented in Fig. 4.39 (a) and (b).The correlations co-efficient of approach-1 and approach-2 are obtained as 0.950 and 0.977, respectively.

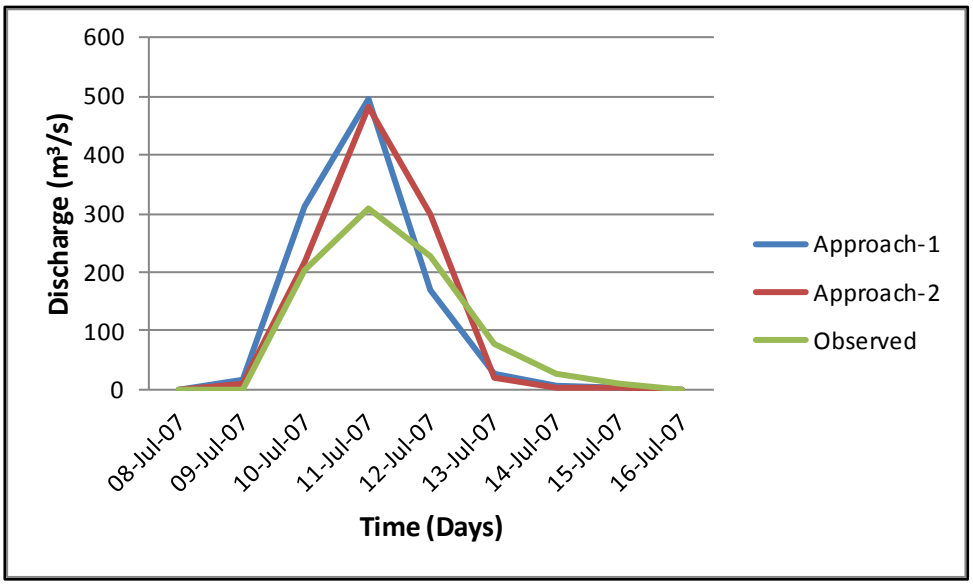

Fig. 4.38 (a): Hydrograph for observed and simulated discharge at outlet during validation using Approach-1, Approach-2 and univariate gradient method for LISS-III 2012 imagery with event-II

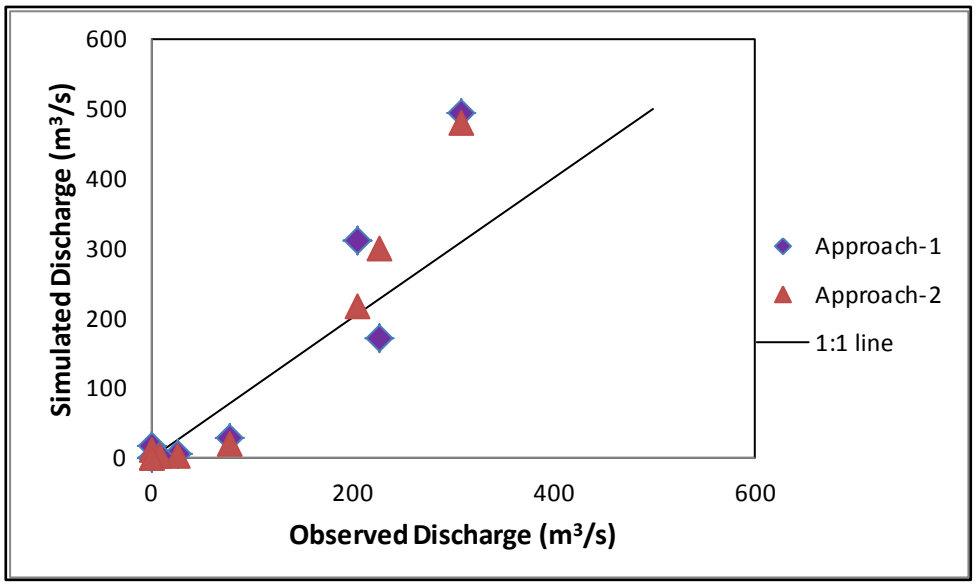

Fig. 4.38 (b): Scatter plot between observed and simulated discharge at outlet during validation using Approach-1, Approach-2 and univariate gradient method for LISS-III 2012 imagery with event-II

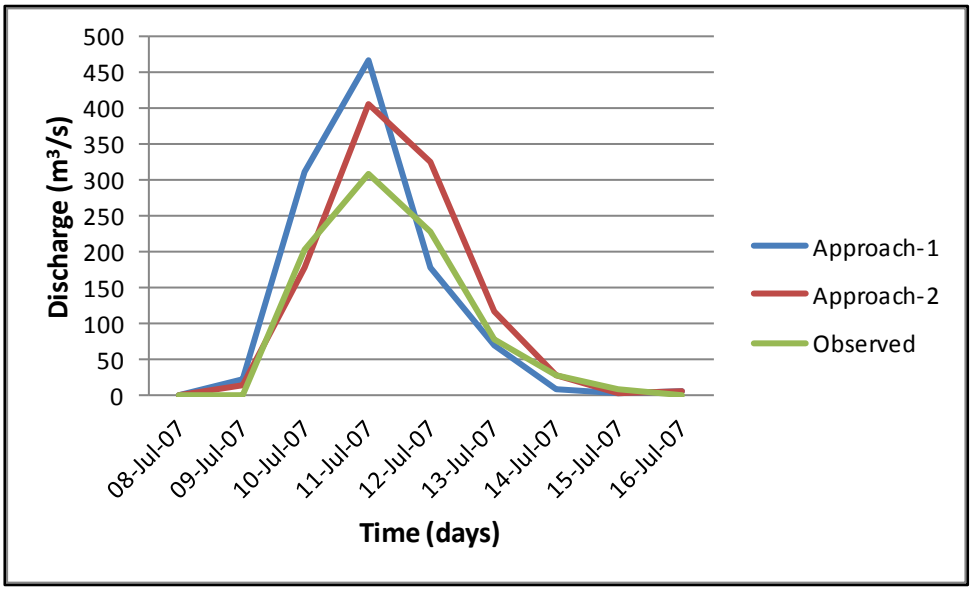

Fig. 4.39 (a): Hydrograph for observed and simulated discharge at outlet during validation using Approach-1, Approach-2 and nelder mead method for LISS-III 2012 imagery with event-II

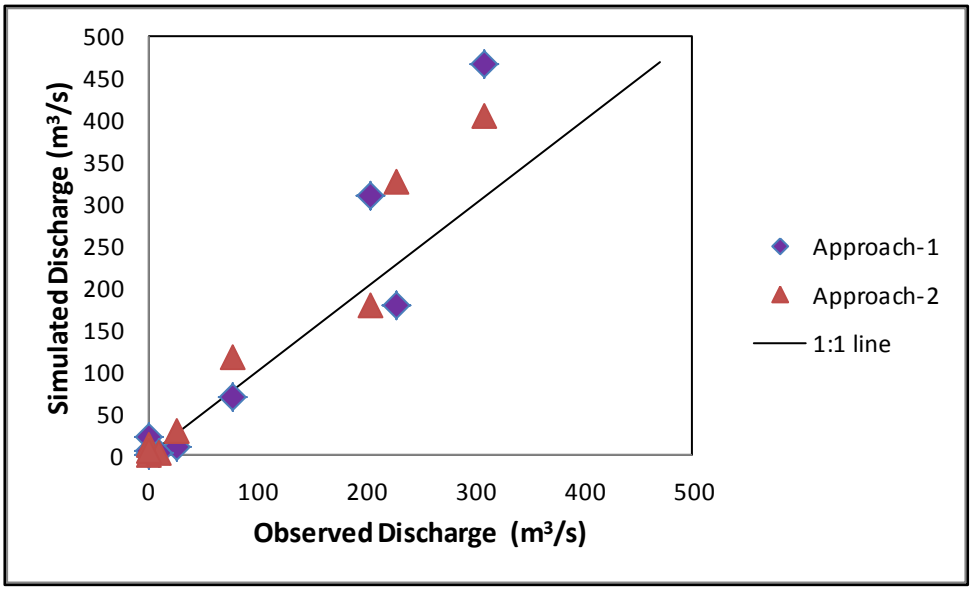

Fig. 4.39 (b): Scatter plot between observed and simulated discharge at outlet during validation using Approach-1, Approach-2 and nelder mead method for LISS-III 2012 imagery with event-II

The observed and modelled values of flood peak and flood volume for the event: II using approach-1 & 2 during validation has been shown in Table 4.14.

Table 4.14: Comparison of simulated flood peak and flood volume with observed values during validation for LISS-III 2012

Method	Event : II					
	Flood Peak (m^3/s)			Flood Volume ($1000m^3$)		
	Univariate	Nelder	Observed	Univariate	Nelder	Observed
Approach-1	494.8	466.9	308.80	88904.2	91510.1	73836.58
Approach-2	481.8	405.3	308.80	88904.6	92641.6	73836.58

4.4.3 Calibration of HEC-HMS model using LISS-IV imagery of Year 2013

The HEC-HMS model is calibrated using the daily dataset for the event: III and validated for the event: IV. The calibration of HEC-HMS model is conducted considering different model parameters for LISS-IV imagery of year 2013 as shown in Table 4.15.

Table 4.15: Simulation parameters of watershed using LISS-IV 2013 for event: III

Method	Approach-1				Approach-2			
	Method Used	Parameter	Subbasin		Method Used	Parameter	Subbasin	
			W700	W800			W700	W800
Loss method	SCS CN	Initial Abstraction (mm)	16.04	16.93	SCS CN	Initial Abstraction (mm)	16.04	16.93
		Curve Number	76	75		Curve Number	76	75
		Impervious (%)	5	5		Impervious (%)	5	5
Transform method	SCS UH	Lag Time (min)	538.2	207	Clark UH	Time of Concentration (hr)	14.95	5.75
						Storage Coefficient (hr)	22.42	8.62
Channel Routing	Muskingum	Travel time (K)	2 hrs For all the reach's					
		Weighting Coefficient (X)	0.1 For all the reach's (for natural Channel)					
Resorvoir Routing	Modified Puls	Initial elevation	279 m					

Hydrograph and scatter plot between observed and simulated discharge using Approach-1 and Approach-2 without parameters optimization has been shown in the Fig. 4.40 (a) and (b), respectively. The correlation co-efficient of approach-1 and approach-2 was found as 0.970 and 0.690, respectively.

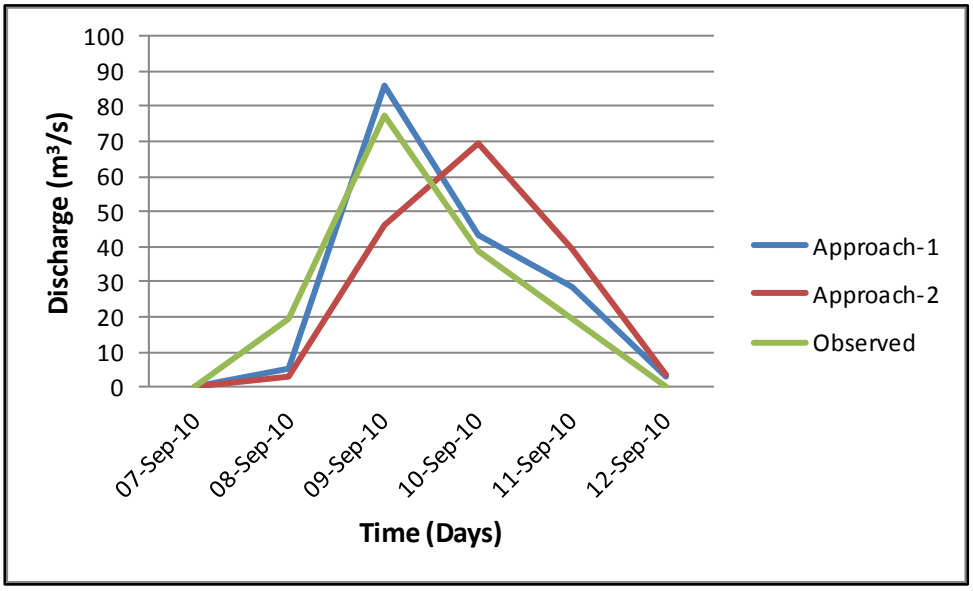

Fig. 4.40 (a): Hydrograph for observed and simulated discharge at outlet without parameter optimization using Approach-1 and Approach-2 for LISS-IV 2013 imagery with event-III

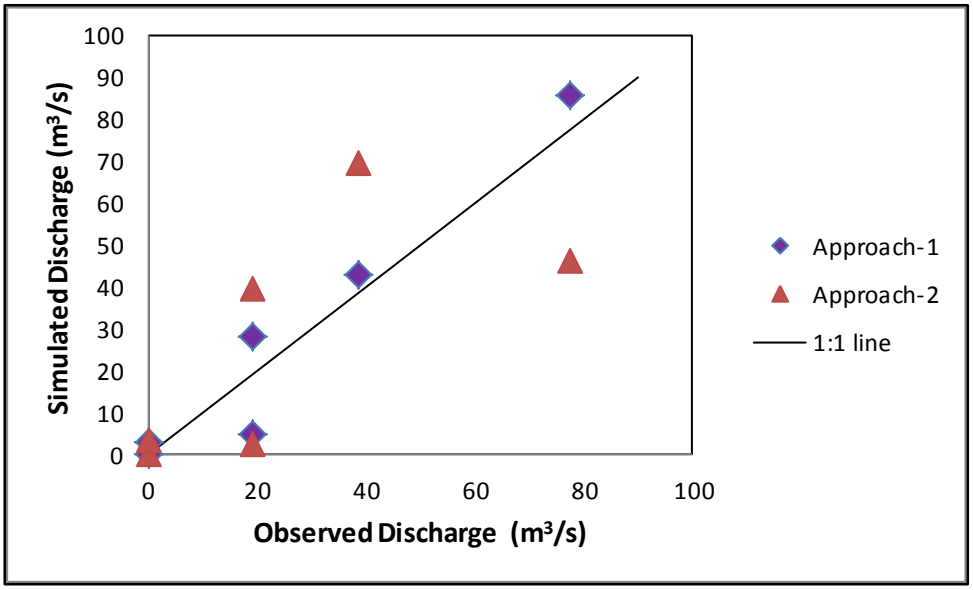

Fig. 4.40 (b): Scatter plot between observed and simulated discharge at outlet without parameter optimization using Approach-1 and Approach-2 for LISS-IV 2013 imagery with event-III

The observed and modelled values of flood peak and flood volume for the Event-III using approach-1 & 2 without optimization have been shown in Table 4.16. It can be observed that the approach-1 produces better results comparatively.

Table 4.16: Comparison of simulated flood peak and flood volume with observed values before parameter optimization for LISS-IV 2013

Event : III				
Method	**Flood Peak (m^3/s)**		**Flood Volume ($1000m^3$)**	
	Model	Observed	Model	Observed
Approach-1	85.8	77.52	14327.0	8683.20
Approach-2	69.7	77.52	14171.1	13366.08

4.4.3.1 Parameters optimization for Approach-1 and Approach-2 using LISS-IV 2013 imagery for Event-III

In optimization trial done with changes of initial abstraction, lag time, time of concentration, storage coefficient and muskingum K using univariate gradient method and nelder mead method with peak weighted RMS error method. The optimized initial abstraction, lag time, time of concentration, storage coefficient and muskingum K parameter values for approach-1 and approach-2 given in Table 4.17 (a) & (b)

Table 4.17: The optimized values of parameters using Approach-1 and Approach-2 for LISS-IV 2013 Imagery

(a) Initial abstraction, lag time, time of concentration and storage coefficient

	Method	Parameter	Sub basin W700			Sub basin W800		
			Initial Value	Optimize Value		Initial Value	Optimize Value	
				Univariate	Nelder		Univariate	Nelder
Approach 1	**SCS CN**	Initial Abstraction (mm)	16.04	16.350	20.507	16.93	17.264	18.803
	SCS UH	Lag Time (min)	538.2	538.2	538.56	207	207	206.42
Approach 2	**SCS CN**	Initial Abstraction (mm)	16.04	15.097	17.191	16.93	17.182	19.226
	Clark UH	Time of concentration (hr)	14.95	14.95	13.964	5.75	5.75	5.2110
		Storage coefficient (hr)	22.42	9.9644	11.261	8.62	8.62	7.4554

(b) Muskingum K parameter

Reach Element	Initial Value	Optimize Value			
		For Approach-1		For Approach-2	
		Univariate	Nelder	Univariate	Nelder
R220	2	2.0400	1.7896	4.5225	0.33986
R240	2	2.0299	2.3782	4.5225	6.5808
R260	2	2.0299	1.5092	4.5225	0.57631
R280	2	2.0299	0.0275567	4.5225	2.1152
R30	2	2.0298	1.7695	4.5225	2.8843
R350	2	2.0299	1.3729	6.7500	1.0228
R380	2	2.0299	4.0196	6.7500	1.3595
R40	2	2.0298	0.78145	4.5225	2.4916
R50	2	2.0298	2.4429	4.5225	2.9022
R70	2	2.0298	2.4116	4.5225	5.1285
R80	2	2.0298	3.8237	4.5225	0.77020

After optimizing above tabulated parameters the resultant hydrograph and scatter plot between observed and simulated discharge using Approach-1 and Approach-2 after parameters optimization with univariate gradient method has been shown in the Fig. 4.41 (a) and (b), respectively and the result obtained by using nelder mead method is shown in the Fig. 4.42 (a) and (b). The correlation co-efficient obtained after optimization for approach-1 and approach-2 with univariate gradient method are 0.970 and 0.874 respectively. The correlation co-efficient obtained after optimization for approach-1 and approach-2 with nelder mead method are 0.967 and 0.831 respectively. The observed and simulated values of flood peak and flood volume for the event: III using approach-1 & 2 after optimization have been shown in Table: 4.18. From the Table 4.16 and 4.18 it shows the improvement in the result of flood peak and flood volume using the optimized parameter.

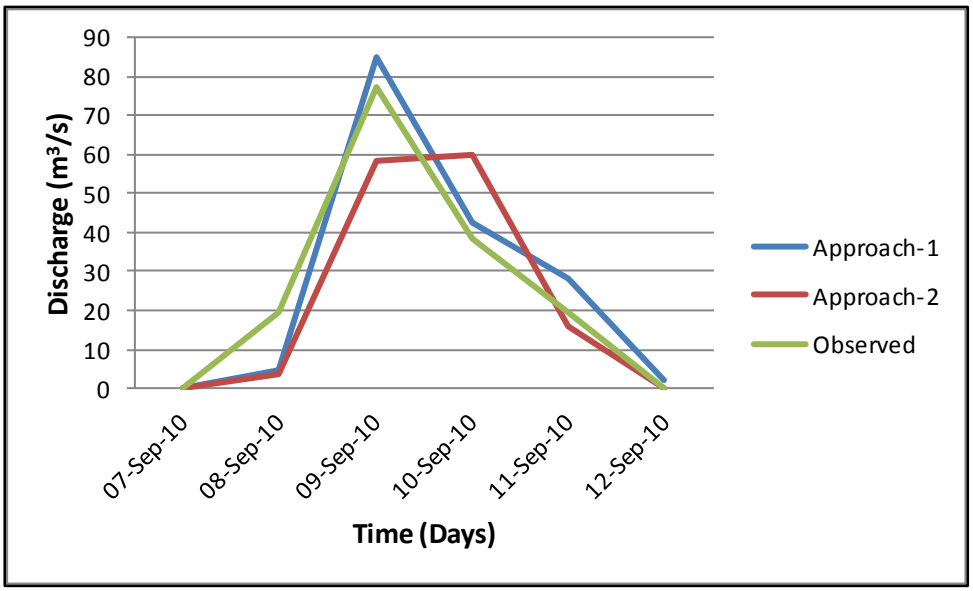

Fig. 4.41 (a): Hydrograph for observed and simulated discharge at outlet after parameter optimization using Approach-1, Approach-2 and univariate gradient method for LISS-IV 2013 imagery with event-III

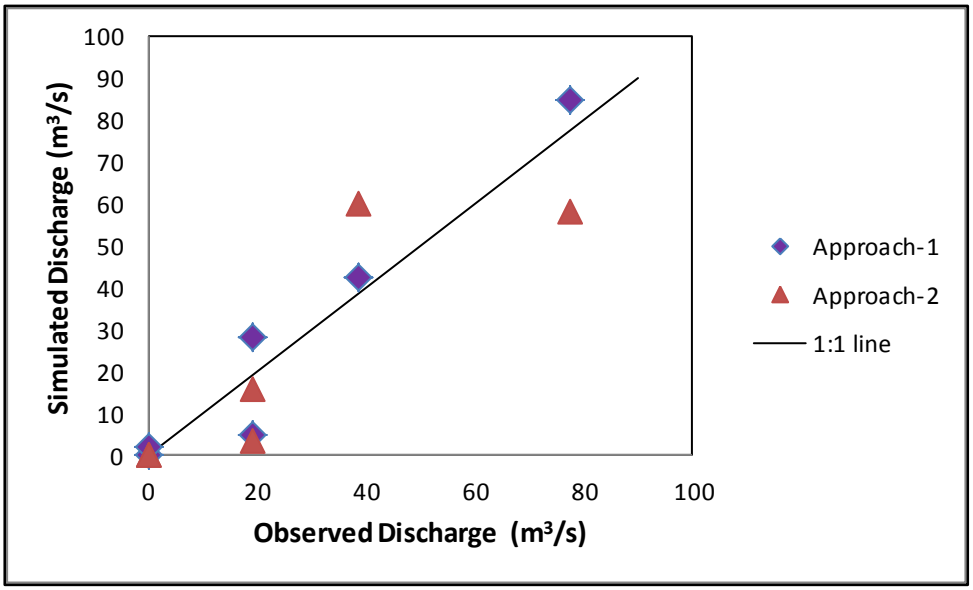

Fig. 4.41 (b): Scatter plot between observed and simulated discharge at outlet after parameter optimization using Approach-1, Approach-2 and univariate gradient method for LISS-IV 2013 imagery with event-III

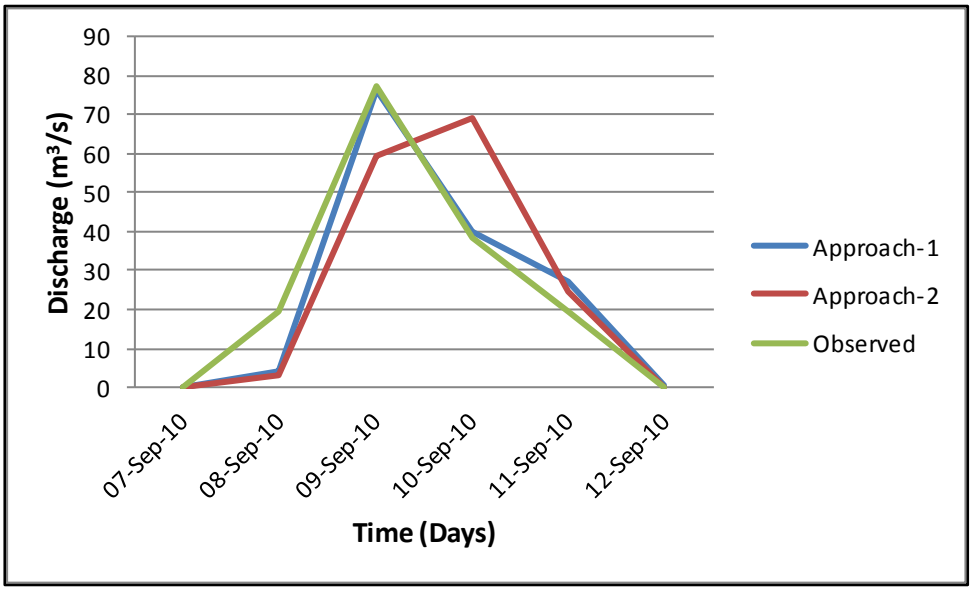

Fig. 4.42 (a): Hydrograph for observed and simulated discharge at outlet after parameter optimization using Approach-1, Approach-2 and nelder mead method for LISS-IV 2013 imagery with event-III

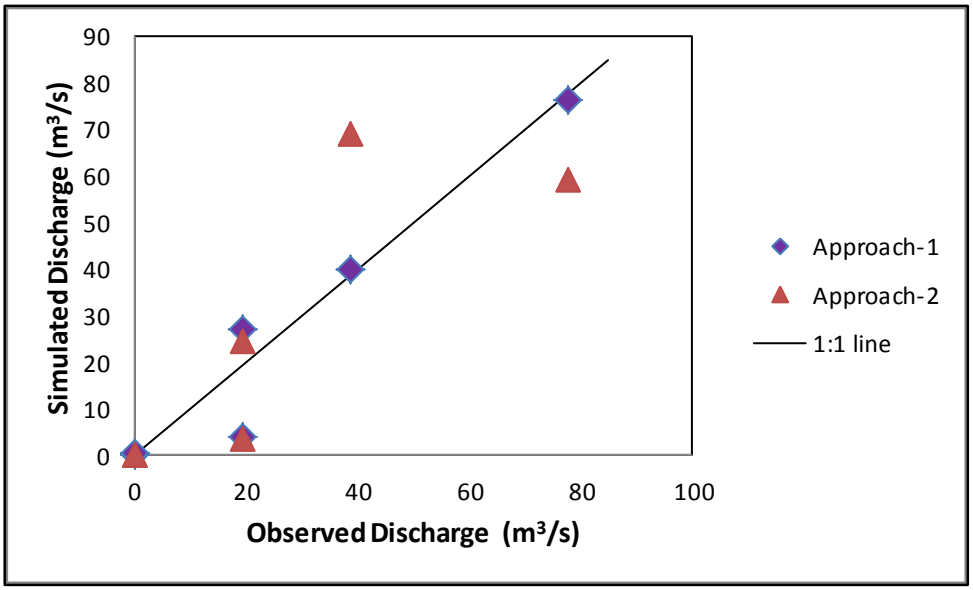

Fig. 4.42 (b): Scatter plot between observed and simulated discharge at outlet after parameter optimization using Approach-1, Approach-2 and nelder mead method for LISS-IV 2013 imagery with event-III

Table 4.18: Comparison of simulated flood peak and flood volume with observed values after parameter optimization for LISS-IV 2013

Method	Event : III					
	Flood Peak (m^3/s)			Flood Volume ($1000m^3$)		
	Univariate	Nelder	Observed	Univariate	Nelder	Observed
Approach-1	85.0	76.5	77.52	14220.1	13063.0	13366.08
Approach-2	60.2	69.3	77.52	12793.6	13943.4	13366.08

4.4.3.2 Validation of HEC-HMS model using LISS-IV Imagery of year 2013

The above same procedure applied for validation of HEC-HMS model using LISS-IV imagery of year 2013. The parameters optimized by Event: III have been applied for validation of event: IV. Validation result of approach-1 and approach-2 using univariate gradient method has been graphically presented in Fig. 4.43 (a) and (b). The correlations co-efficient of approach-1 and approach-2 are obtained as 0.836 and 0.923, respectively. The resultant parameters optimized using nelder mead method has been also applied for validation of Event-II. Validation result of approach-1 and approach-2 using nelder mead method has been graphically presented in Fig. 4.44 (a) and (b).The correlations co-efficient of approach-1 and approach-2 are obtained as 0.846 and 0.929, respectively. The observed and simulated values of flood peak and flood volume for the Event: IV using approach-1 & 2 during validation has been shown in Table 4.19.

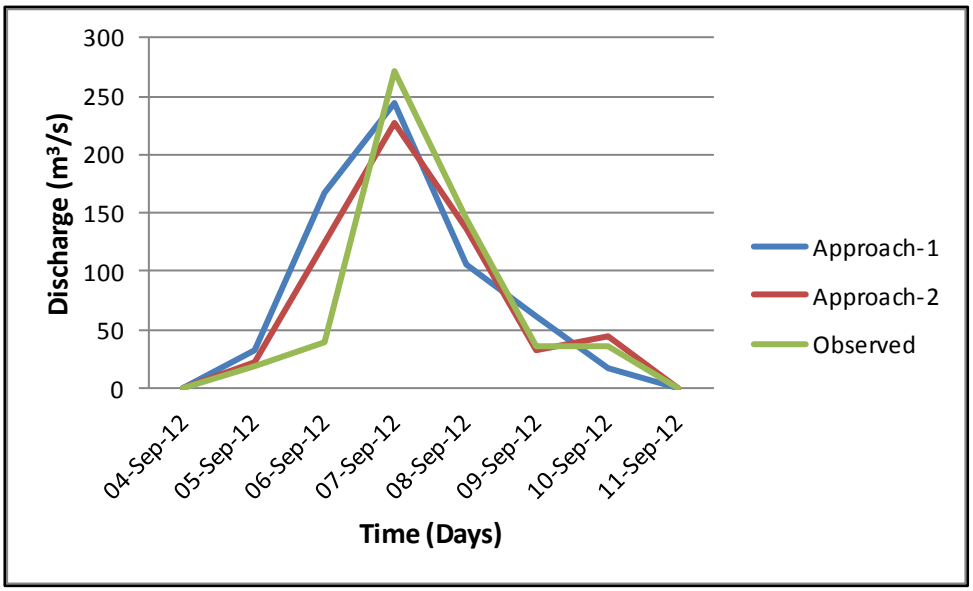

Fig. 4.43 (a): Hydrograph for observed and simulated discharge at outlet during validation using Approach-1, Approach-2 and univariate gradient method for LISS-IV 2013 imagery with event-IV

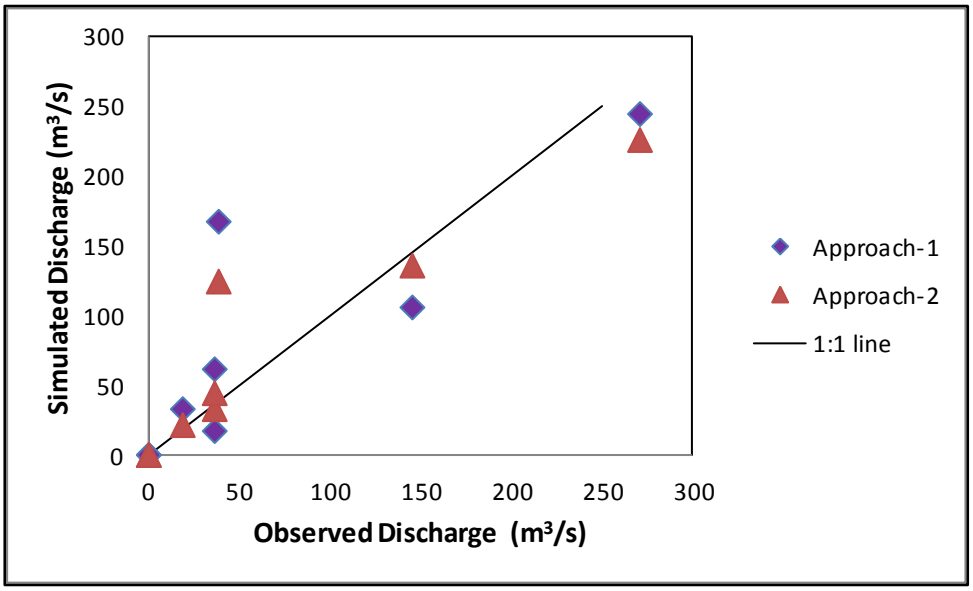

Fig. 4.43 (b): Scatter plot between observed and simulated discharge at outlet during validation using Approach-1, Approach-2 and univariate gradient method for LISS-IV 2013 imagery with event-IV

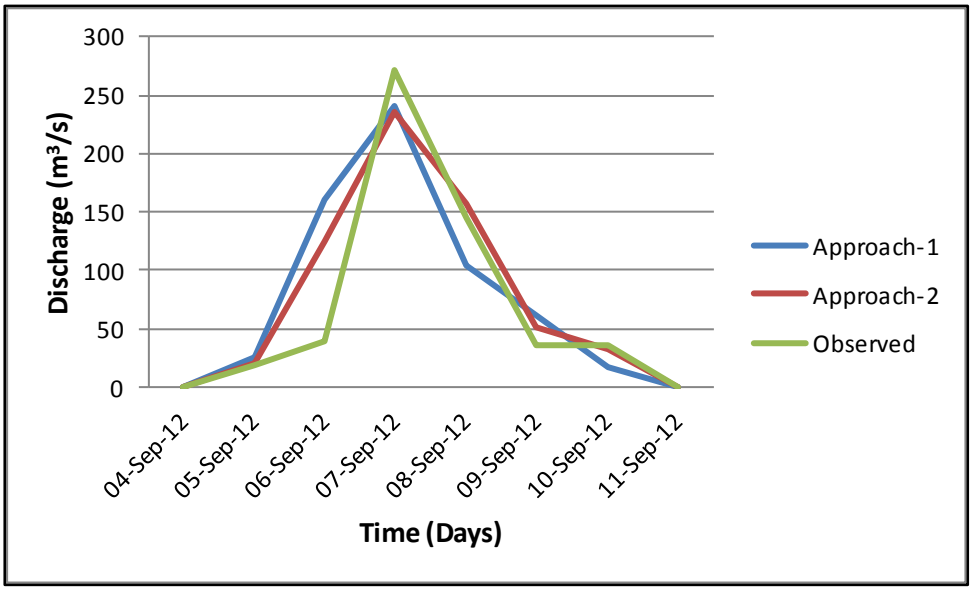

Fig. 4.44 (a): Hydrograph for observed and simulated discharge at outlet during validation using Approach-1, Approach-2 and nelder mead method for LISS-IV 2013 imagery with event-IV

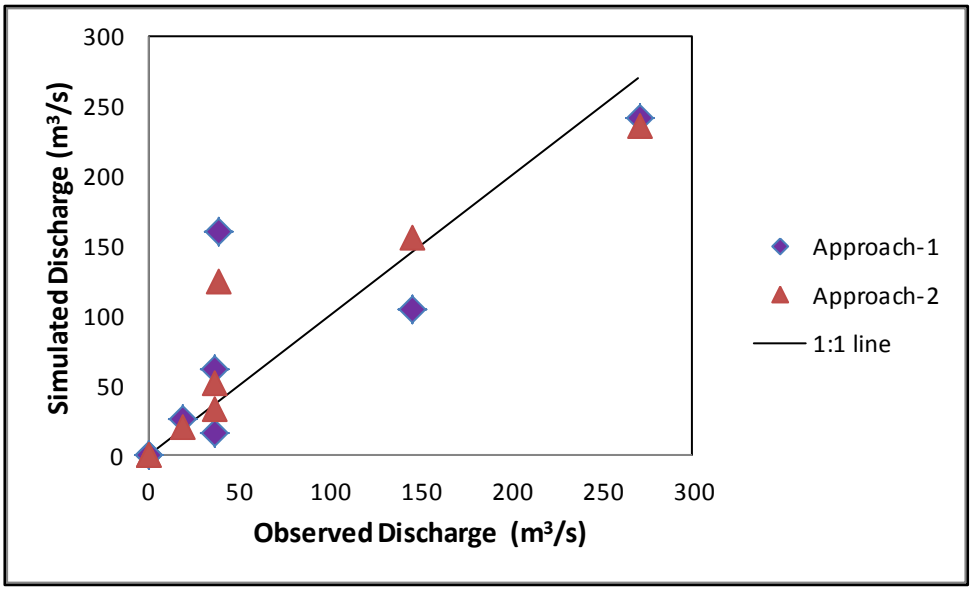

Fig. 4.44 (b): Scatter plot between observed and simulated discharge at outlet during validation using Approach-1, Approach-2 and nelder mead method for LISS-IV 2013 imagery with event-II

Table 4.19: Comparison of simulated flood peak and flood volume with observed values during validation for LISS-IV 2013

Method	Event : IV					
	Flood Peak (m^3/s)			Flood Volume ($1000m^3$)		
	Univariate	Nelder	Observed	Univariate	Nelder	Observed
Approach-1	244.5	241.3	271.0	54224.4	52672.2	47317.82
Approach-2	226.6	236.1	271.0	52320.4	53973.8	47317.82

4.4.4 Performance Comparison of HEC-HMS models

The performance evaluation of HEC-HMS models for different approaches along with univariate gradient method, nelder mead method and different remote sensing imagery for land use applied is presented in the Table 4.20 and Table 4.21, respectively. These performance are evaluated in terms of different performance indices such as: Coefficient of Determination (R^2), Nash-Sutcliffe efficiency (ENS), Percentage peak deviation (Pdv), root mean square error (RMSE), mean absolute error (MAE), Correlation coefficient (r).

Table 4.20: Performance comparison of different approaches and remote sensing imagery applied (Using Univariate gradient)

Land Use RS Imagery	Approach/Method	Performance Indices					
		R^2	E	RMSE	Pdv	MAE	r
LISS-III 2008	Approach -1 Without Opt.	0.97	81.70	10.00	37.10	5.20	0.984
	Approach -1 after Opt.	0.96	87.12	8.39	30.58	4.77	0.978
	Approach-1 Validation	0.88	65.55	66.26	-51.85	43.99	0.937
LISS-III 2012	Approach -1 Without Opt.	0.96	92.09	6.58	19.71	5.01	0.982
	Approach -1 after Opt.	0.96	94.06	5.70	13.77	4.40	0.981
	Approach-1 Validation	0.88	53.82	76.71	-60.23	49.48	0.936
LISS-IV 2013	Approach -1 Without Opt.	0.94	90.94	8.01	-10.71	6.52	0.971
	Approach -1 after Opt.	0.94	91.30	7.85	-9.68	6.20	0.971
	Approach-1 Validation	0.70	67.65	49.94	9.78	31.64	0.837
LISS-III 2008	Approach-2 without Opt.	0.38	34.67	18.90	54.35	11.13	0.615
	Approach -2 after Opt.	0.66	66.26	13.58	35.51	8.69	0.815
	Approach -2 Validation	0.94	74.41	57.11	-47.44	34.47	0.971
LISS-III 2012	Approach-2 without Opt.	0.42	41.34	17.91	39.13	12.37	0.645
	Approach -2 after Opt.	0.64	62.94	14.24	28.12	8.87	0.799
	Approach -2 Validation	0.94	65.49	66.32	-56.02	39.70	0.971
LISS-IV 2013	Approach-2 without Opt.	0.48	38.00	20.96	10.06	17.05	0.690
	Approach -2 after Opt.	0.76	74.13	13.54	22.32	10.03	0.875
	Approach -2 Validation	0.85	84.60	34.46	16.38	19.28	0.924

It can be observed that optimization of the parameters significantly improved the model performance in all the cases using LISS-III for the year 2008, LISS-III for the year 2012 and LISS-IV for the year 2013. Better performance of all these models for the new event of rainfall-runoff transformation approves the applicability of HEC-HMS model in the study area.

Table 4.21: Performance comparison of different approaches and remote sensing imagery applied (Using Nelder mead)

Land Use RS Imagery	Approach/Method	Performance Indices					
		R^2	E	RMSE	Pdv	MAE	r
LISS-III 2008	Approach -1 without Opt.	0.97	81.70	10.00	37.10	5.20	0.984
	Approach -1 after Opt.	0.96	93.10	6.14	8.99	4.59	0.979
	Approach-1 Validation	0.90	73.32	58.31	-43.39	38.00	0.947
LISS-III 2012	Approach -1 without Opt	0.96	92.09	6.58	19.71	5.01	0.982
	Approach -1 after Opt.	0.96	92.82	6.27	2.75	4.74	0.981
	Approach-1 Validation	0.90	65.36	66.44	-51.20	41.49	0.950
LISS-IV 2013	Approach -1 without Opt.	0.94	90.94	8.01	-10.71	6.52	0.971
	Approach -1 after Opt.	0.94	93.03	7.03	1.29	4.32	0.968
	Approach-1 Validation	0.72	70.22	47.91	10.96	30.49	0.847
LISS-III 2008	Approach-2 without Opt.	0.38	34.67	18.90	54.35	11.13	0.615
	Approach -2 after Opt.	0.46	45.80	17.22	42.61	11.40	0.682
	Approach -2 Validation	0.91	86.13	42.05	-13.70	28.33	0.956
LISS-III 2012	Approach-2 without Opt.	0.42	41.34	17.91	39.13	12.37	0.645
	Approach -2 after Opt.	0.56	49.88	16.55	23.48	12.40	0.747
	Approach -2 Validation	0.95	81.32	48.79	-31.25	31.76	0.977
LISS-IV 2013	Approach-2 without Opt.	0.48	38.00	20.96	10.06	17.05	0.690
	Approach -2 after Opt.	0.69	63.42	16.10	10.58	11.67	0.831
	Approach -2 Validation	0.86	85.30	33.66	12.88	19.06	0.930

CHAPTER V
SUMMARY AND CONCLUSIONS

In this study an agricultural dominated watershed upstream of the Hadaf dam is selected for rainfall runoff modeling. The area is predominant with agricultural land and falls under semi-arid zone, where water resources planning and management is necessary for irrigation scheduling, water harvesting, flood control, drought mitigation and design of various engineering structures. Considering the importance of water especially in semi-arid region, it is required to understand the rainfall-runoff relationship precisely. For this purpose HEC-HMS model is explored for precise runoff simulation in the watershed. To address the above issues, the following objectives are formulated in this study for the selected agricultural watershed in middle region of Gujarat. The objectives are (a) to study the geomorphological parameters of the study area using Remote Sensing and GIS, (b) to calibrate and validate HEC-HMS model to simulate runoff in the watershed, (c) to optimize and evaluate performance of different unit hydrograph for runoff simulation, and (d) to evaluate effect of land use change on runoff in the watershed using HEC-HMS model.

Initially, the capabilities of two different DEMs i.e. SRTM with 90 m resolution and ASTER with 30 m resolution are also evaluated to assess their effectiveness in watershed delineation and drainage network generation. After that, the geo-morphological analysis of the watershed is carried out using the capabilities of remote sensing and GIS to prioritize the watershed for soil and water conservation measures. Then, conceptual hydrological HEC-HMS model is applied in this study to transform rainfall into runoff for one of the selected event, and thereafter, the parameters related to initial loss, unit hydrographs, reservoir and channel routing, were calibrated and validated using the another event of the watershed. The effect of different land use at different years on runoff generation is also carried out in this study. Two of the important optimization methods are also evaluated to assess their effectiveness for rainfall runoff modeling in this study. In this study capabilities of HEC-HMS model using two important transformationmethods namely SCS-UH and Clark method is also applied to find out the better performing transformation method in the study area.The following conclusions are drawn from the study:

1. SRTM and ASTER DEM models are compared in this study to assess their capabilities of watershed delineation and drainage network generation, and it is found that instead of low resolution (i.e. 90 m) SRTM DEM found to be better than ASTER DEM, due to better quality of the images.
2. It is observed in this study that agricultural land is increased from 222.35 km^2 in the year 2008 to 252.47 km^2 in year 2012, whereas forest land is decreased from 198.24 km^2 in the year 2008 to 157.91 km^2 in year 2012. An increment in the waste land is also observed from 2008 to 2012 that is increased from 51.11 km^2 to 71.75 km^2.
3. The effect of finer resolution remote sensing image LISS-IV is also evaluated in this study that produced better classification and improved accuracy of HEC-HMS model in rainfall-runoff modeling.
4. It is found in this study that the Clark method (Approach-2)produces better results thanSCS-UH transformation method (Approach-1)in rainfall-runoff simulation in terms of both the runoff peak and runoff volume.
5. It has been observed that optimization of the parameters significantly improved the model performance in all the cases using LISS-III for the year 2008, LISS-III for the year 2012 and LISS-IV for the year 2012.
6. Better performance of all these models for the new event of rainfall-runoff transformation approves the applicability of HEC-HMS model in the study area.
7. Even though the performance of HEC-HMS model is better using Clark UH transformation method than the SCS-UH transformation method, it is observed that optimization techniques significantly improved the parameters in both the transformation methods.
8. Performance comparison between Univariate Gradient method and Nelder Mead method shows that the overall performance of Nelder Mead method is better compared to Univariate Gradient method for rainfall runoff modeling using HEC-HMS model.
9. It is found in this study that LISS-IV of year 2013 imagery has much better capabilities to simulate rainfall runoff transformation than LISS-III imageries of

year 2008 and 2012, as evident with the better simulation results during calibration and validation, as evident from the results.

10. Performance of HEC-HMS model for Approach-2 is better compared to Approach-1 using both Univariate gradient and Nelder mead optimization method.
11. Better performance of HEC-HMS model using LISS-III image of year 2008 than that of year 2012 for validating event-2 of year 2007, showed that land use change play an important role in the rainfall-runoff transformation.
12. The findings in the present study are very useful for water resources engineers, researchers and will play an important role in water resources planning and management.

REFERENCES

Abood, M.M.; Mohammed, T.A.; Ghazali, A.H.; Mahmud, A.R. and Sidek, L.M (2012).Impact of Infiltration Methods on the Accuracy of Rainfall-Runoff Simulation. *Research Journal of Applied Sciences Engineering and Technology*, 4(12): 1708-1713.

Ahmad, S. and Khan, N. (2013). Evaluation of morphometric parameters - a remote sensing and GIS based approach. *Open Journal of Modern Hydrology*, 3: 20-27.

Akbari, S.; Karthik, A.; Venkatesh, G.; Tobgay, R. and Penjor, K. (2012). Estimation of geomorphology parameters for small catchment using GIS. *International Journal of Earth Science and Engineering*, 5(4): 976-981.

Ali, M.; Khan, S.J.; Aslam, I. and Khan, Z. (2011). Simulation of the impacts of land-use change on surface runoff of Lai Nullah Basin in Islamabad, Pakistan). *Landscape and Urban Planning*, 102: 271– 279.

Andrzej, W. (2013). Application of HEC-HMS programme for the reconstruction of a flood event in an uncontrolled basin. *Journal of water and land development*, 18 (I–VI): 13–20.

Arnold, C.L. and Gibbons, C.J. (1996). Impervious surface coverage: the emergence of a key environmental indicator. *Journal of the American Planning Association*, 62: 243–258.

Babu, K.J.; Sreekumar S. and Aslam, A. (2014). Implication of drainage basin parameters of a tropical river basin of South India. *Applied Water Science, DOI 10.1007/s13201-014-0212-8*.

Bakir, M. and Xingnan, Z. (2008). GIS-based hydrological modeling: A comparative study of HEC-HMS and the XINANJIANG model. Twelfth International Water Technology Conference, IWTC12 Alexandria, Egypt.

Basarudin, Z.; Adnan, N.A.; Latif, A.R.A.; Tahir, W. and Syafiqah, N. (2014). Event-based rainfall-runoff modelling of the Kelantan River Basin. 8th International

Symposium of the Digital Earth (ISDE8), *Earth and Environmental Science*, 18:012084.

Beven, K.J. (1985).Chapter 13, Distributed Models. In: Anderson, M. G., and Burt, T. P. (Eds.), Hydrologic Forecasting, Wiley, New York.

Beven, K.J. (2001). Rainfall-runoff modeling – The primer, Wiley: Chichester, UK.

Biswas, S.; Sudhakar, S. and Desai, V.R. (1999). Prioritization of sub-watersheds based on Morphometric Analysis of Drainage Basin, District Midnapore, West Bengal. *Journal of the Indian Society of Remote Sensing*, 27(3): 155–166.

Chatterjee, M.; Rumpa, D.; Debasri, R.; Subhasish, D. and Asis, M. (2014). Hydrological modeling studies with HEC-HMS for Damodar Basin. India. *World Applied Sciences*, 31 (12): 2148.

Chaudhry, H.C. (1993). Open-Channel Hydraulics. Prentice Hall, NJ.

Chinh, L.V.; Iseri, H.; Hiramatsu, K.; Harada, M. and Mori, M. (2013). Simulation of rainfall runoff and pollutant load for Chikugo River basin in Japan using a GIS-based distributed parameter model. *Paddy and Water Environment*, 11:97–112.

Chopra, R.; Dhiman, R.D. and Sharma, P.K. (2005). Morphometric analysis of sub watershed in Gurudaspur district, Panjab using remote sensing and GIS techniques. *Journal of Indian Society of Remote Sensing*, 33(4): 531-539.

Choudhari, K.; Panigrahi, B. and Paul, J.C. (2014). Simulation of rainfall-runoff process using HEC-HMS model for Balijore Nala watershed, Odisha, India. *International Journal of Geomatics and Geosciences*, 5(2): 253-265.

Chow, V.T.; Maidment, D.R. and Mays, L.W. (1988). Applied Hydrology. New York: McGraw-Hill.

Clarke, R.T. (1973). A review of mathematical models used in hydrology, with some observations on their calibration and use. *Journal of Hydrology*, 19, 1–20.

Das, G. (2009). Hydrology and Soil Conservation Engineering Including Watershed Management, PHI Learning Private Limited, New Delhi. Second Edition. Chapter-5:84-85.

Das, R. (2014). Study of rainfall-runoff response of a catchment using SCS curve number combined with muskingum routing techniques. *International Journal of Strucural & Civil Enginnering Research*, 3(3).

Dastorani, M.T.; Khodaparast, R.,;Talebi, A.; Vafakhah, M. and Dashti, J. (2011). Determination of the ability of HEC-HMS model components in rainfall-run-off simulation. *Research Journal of Environmental Sciences*, 5:790-797.

Dougherty, M.; Dymond, R.L.; Grizzard,Jr, T.J.; Godrej, A.N.; Zipper, C.E. and Randolph, J.(2006). Quantifying long term hydrologic response in an urbanizing basin. *Journal of Hydrologic Engineering,*12: 33–41.

Du, J.; Qian, L.; Rui, H.; Zuo, T.; Zheng, D.; Xu, Y. and Xu, C.Y. (2012). Assessing the effects of urbanization on annual runoff and flood events using an integrated hydrological modeling system for Qinhuai River basin, China. *Journal of Hydrology*, 464–465: 127–139.

Ebrahimiyan, S. and Ghaderi, S.J. (2014). Evaluation and Calibration of the HEC-HMS/WMS model in Mahabad dam's basin. *Advances in Environmental Biology*, 8(1): 75-82.

Erol, A. (2013)Morphometric parameters of the Aksu watershed: An analysis of hydrologic processes. *Journal of Food, Agriculture & Environment*, 11(3&4): 1473-1478.

Eyad, A. and Broder, M. (2013). Modelling rainfall runoff relations using HEC-HMS and IHACRES for a single rain event in an arid region of Jordan. *Water Resources Management*, 27 (7): 2391-2409.

EzeE.B.and EfiongJ. (2010) Morphometric parameters of the Calabar River Basin: implication for hydrologic processes. *Journal of Geography and Geology*, 2(1).

Farokhsha, R.S. and Farokhsha, E.S. (2014). Rainfall and runoff process simulation model using HEC-HMS (Case study Catchment Basin Hospice). *Advances in Environmental Biology*, 8(9): 244-252.

Fasahat, V.; Honarbakhsh, A.; Samadi, H. and Sadatinejad, S.J. (2012). Determining flood routing coefficients in mountainous rivers using HEC-HMS model (A Case Study: Jooneghan-Farsan Watershed, Iran). *World of Sciences Journal*, 1(7): 124-131.

Galgale, H.M. and Shinde, M.G. (2006). Model for computation of the watershed morphologic characteristics using GIS.15th International Symposium and Exhibition on Remote Sensing and Assisting System.www.grossy.org.

Golrang, B.M.; Lai, F.S.; Sadeghi, S.H.R.; Khamurudin, M.N.; Kudus, K.A.; Mashayekhi, M. and Bagherian, R. (2013). Assessment of watershed management implemented on springal peak flood discharge and flood volume, using HEC-HMS Model (Case study: Kushk Abad sub-basin in Iran). *Science and Nature*, 2(2): 59-64.

Halwatura, D. and Najim, M.M.M. (2013). Application of the HEC-HMS model for runoff simulation in a tropical catchment. *Environmental Modelling & Software*, 46:155-162.

Hardely, R.F. and Schumm, S.A. (1961). Sediment sources and drainage basin characteristics in upper Cheyenne river basin. United States Geological survey, *Water supply paper*, 1531-B: 10-19.

Hjelmfelt, A.T. (1991). Investigation of curve number procedure. *Journal of Hydraulic Engineering*, 117(6): 725-737.

Hollis, G.E. (1975). The effect of urbanization on floods of different recurrence interval.*Water Resources*, 11: 431–435.

Horton, R.E. (1932). Drainage basin characteristics. *Transaction America Geophysical Union*. 13: 350-361.

Horton, R.E. (1945). Erosional development of streams and their drainage basins: hydrophysical approach to quantitative morphology. *Geological Society of America Bulletin*, 56: 275-370.

Iliasse, K. and Alaoui, A.H. (2014). Production of a curve number map for hydrological simulation - Case study: Kalaya Watershed located in Northern Morocco. *International Journal of Innovation and Applied Studies*, 9(4): 1691-1699.

Islam, MDR. (2004). A review on watershed delineation using GIS tools. Dept. of Civil Engineering, 415 Engineering Building, University of Manitoba, Winnipeg, Canada, R3T 5V6.

Javed, A.; Khanday. M.Y. and Ahmed, R. (2009). Prioritization of sub watersheds based on morphometric and land use analysis using remote sensing and GIS techniques. *Journal of the Indian Society of Remote Sensing*, 37(2):261–274.

Kalita, D.N. (2008). A study of basin response using HEC-HMS and subzone reports of CWC. In: Proceedings of the 13th National Symposium on Hydrology. National Institute of Hydrology, Roorkee, New Delhi.

Kathol, J.P.; Werner, H.D. and Trooien, T.P. (2003). Predicting Runoff for Frequency based Storm using a Prediction- Runoff Model, A.S.A.E. South Dakota, U.S.A.

Kaushik, S.S. (2010). Hydrological and hydraulic modelling for river Sabarmati stretch in Ahmedabad using HEe-RAS and HEe-HMS. *Water and Energy International*, 67(4).

Kumar, A.R.S.; Sudheer, K.P.; Jain, S.K. and Agarwal, P.K. (2005). Rainfall-runoff modelling using artificial neural networks: comparison of network types. *Hydrological Processes*, 19 (6): 1277-1291.

Kumar, D. and Bhattacharjya, R.K. (2011). Distributed rainfall runoff modeling. *International Journal of Earth Sciences and Engineering*, 4 (6): 270-275.

Laouacheria, F. and Mansouri, R. (2015). Comparison of WBNM and HEC-HMS for runoff hydrograph prediction in a small urban catchment. *Water Resources Management*, DOI 10.1007/s11269-015-0953-7

Linsley, R.K.; Kohler, M.A. and Paulhus, J.L.H. (1982). Hydrology for Engineers, third edition, McGraw-Hill.

Mane, M.E; Chandra, S.; Yadav, B.R.; Singh, D.K.; Sarangi, A. and Sahoo, R.N. (2013). Assessment of runoff potential in the National Capital Region of Delhi. *Journal of Soil and Water Conservation*,12(1): 23-30.

Matziaris, V. and Sakellariou, M. (2005). Modeling the effect of rainfall in unsaturated slopes, IASME Transactions. International Conference on Energy, Environment, Ecosystems, Sustainable Development, 2(3): 442-447.

McCuen, R.H. (1982). A Guide to Hydrologic Analysis Using SCS Methods Prentice Hall, Inc. Englewood Cliffs, New Jersey.

Meenu, R.; Rehana, S. and Mujumdar, P.P. (2012). Assessment of hydrologic impacts of climate change in Tunga–Bhadra river basin, India with HEC-HMS and SDSM, *Hydrological Processes,* DOI: 10.1002/hyp.

Melton, M.A. (1957). An analysis of the relations among elements of climate, surface properties and geomorphology, Project NR 389042, Technical Report 11, Columbia University.

Melton, M.A. (1957). An analysis of the relations among elements of climate, surface properties and geomorphology, Project NR 389042, Technical Report 11, Columbia University.

Mihalik, L.; Levine, N.S. and Amatya, D.M. (2008). Rainfall-runoff modeling of the chapel branch Creek watershed using GIS based rational and SCS-CN methods. Paper # 083971, St.Joseph, MI: ASABE.

Miller, V.C. (1953). A quantitative geomorphic study of drainage basin characteristics in the Clinch Mountain area, Varginia and Tennessee", Project NR 389042,

Technical Report3.,Columbia University, Department of Geology, ONR, Geography Branch, New York .

Motevalli, S.; Hosseinzadeh, M.M.; Esmaili, R.; Derafshi, K. and Gharehchahi, S. (2012). Assessing the effects of land use change on hydrologic balance of Kan watershed using SCS and HEC-HMS hydrological models – Tehran, IRAN. *Australian Journal of Basic and Applied Sciences*, 6(8): 510-519.

Mousavi, S.J; Abbaspour, K.C.; Kamali, B.; Amini, M. and Yang, H. (2012). Uncertainty-based automatic calibration of HEC-HMS model using sequential uncertainty fitting approach. *Journal of Hydroinformatics*, 14(2): 286-309.

Nag, A.; Penjor, K.; Tobgay, S. and Jamtsho, C. (2013). Hydrological modeling of watershed using HEC-HMS software and arc GIS. *International Journal of Advanced Scientific and Technical Research*, 2(3).

Nageswara, R.K.; Swarna, L.P.; Arun, K.P. and Hari, K.M. (2010). Morphometric analysis of Gostani river basin in Andhra Pradesh state, India using spatial information technology. *International Journal of Geomatics and Geosciences*, 1(2): 179-187.

Narasayya, K. (2015). A geo-informatic approach to estimate stream flow of an undeveloped catchment - A hypothetical research. *International Journal of Advancement in Remote Sensing, GIS and Geography*, 3(1): 22-31.

Nasri, M.; Sardoo, F.S. and Katani, M. (2011). Simulation of the rainfall-runoff process using of HEC-HMS hydrological model. *World Academy of Science, Engineering and Technology*, 54.

Nayak, T.R. and Jaiswal, R.K. (2003). Rainfall-runoff modeling using satellite data and GIS for Bedasriver in Madhya Pradesh, *Indian Institute of Engineers (India) Journal*, 84:47-50.

Nookaratnam, K.; Srivastava, Y.K.; Venkateshwara, R.V.; Amminedu, E. and Murthy, K.S.R. (2005). Check dam positioning by prioritization of micro-

watersheds using SYI model and morphometric analysis- Remote Sensing and GIS perspective. *Journal of the Indian Society of Remote Sensing*, 33(1): 25–38.

Ogden, F.L.; Pradhan, N.R.; Downer, C.W. and Zahner, J.A. (2011). Relative importance of impervious area, drainage density, width function, and subsurface storm drainage on flood runoff from an urbanized catchment. *Water Resources Research,* 47, W12503. http://dx.doi.org/10.1029/2011WR010550.

Pandey, A.; Chowdary, V.M. and Mal, B.C. (2004). Morphological study of watershed using GIS: Proceeding of International Conference and Emerging Technologies in agricultural and food engineering, IIT Kharagpur.

Pankaj, A. and Kumar, P. (2009). GIS based morphometric analysis of five major sub-watersheds of Song river, Dehradun district, Uttarakhand with special reference to landslide incidences. *Journal of Indian Society of Remote Sensing*, 37(1): 157-166.

Pareta, K. and Pareta, U. (2011). Hydro-morphogeological study of Karawan watershed using GIS and remote sensing techniques. *E-international scientific research journal*, 3(4): 243-268.

Patel D.P.; Srivastava P.K.; Gupta M. and NandhakumarN. (2015). Decision support system integrated with geographic information system to target restoration actions in watersheds of arid environment: A case study of Hathmati watershed, Sabarkantha district, Gujarat. *Journal of Earth System Science,* 124(1): 71–86.

Patel, D.P.; Gajjar, C.A. and Srivastava, P.K. (2013). Prioritization of Malesari mini-watersheds through morphometric analysis: a remote sensing and GIS perspective. *Environmental Earth Sciences,* 69: 2643–2656.

Patel, M.M.; Gandhi, H.M.; and Shrimali, N.J. (2014). Literature study on application of HEC-HMS for event and continuous based hydrological modeling. *International Journal for Scientific Research & Development*, 1(11): 2321-0613.

Paudel, M.; Nelson, E.J.; Downer, C.W. and Hotchkiss, R. (2011). Comparing the capability of distributed and lumped hydrologic models for analyzing the effects of land use change. *Journal of Hydroinformatics,* 13(3):461-473.

Paul, J.M. and Inayathulla, M. (2012). Morphometric analysis and prioritization of Hebbal Valley in Bangalore. *IOSR Journal of Mechanical and Civil Engineering*, 2(6): 31-37.

Pilpayeh, A. and Shahbazi, A.N. (2012). Land use effect simulation on volume of flood catchment. 14th International Conference on Computing in Civil and Building Engineering. Moscow, Rusia.

Ponce, V.M. (1981). Development of an algorithm for the linearized diffusion method of flood routing, San Diego state university Civil Engineering, Series No. 81144.

Ponce, V.M. and Hawkins, R.H. (1996). Runoff curve number, has it reached maturity?. *Journal of Hydrology*, 1(1):11–19.

Prajapati, R.N. (2015). Delineation of run of river hydropower potential of Karnali Basin-Nepal Using GIS and HEC-HMS. *European Journal of Advances in Engineering and Technology*, 2(1): 50-54.

Rajasekhar, P.; Kishore, P.V. and Malwan, F. (2013). Analysis of Rainfall-Runoff relationship in Shomali sub-basin using NRCS-CN and Remote Sensing. *American International Journal of Research in Science, Technology, Engineering & Mathematics*, 5(1): 93-100.

Refsgaard, J.C. (1996). Terminology, modeling protocol and classification of hydrological model codes. In: Abbott, M. B. and Refsgaard, J. C. (Eds.), Distributed Hydrological Modeling,Water Science and Technology Library.

Reshma, T.; Venkata, R.K. and Pratap, D. (2013). Simulation of event based runoff using HEC-HMS Model for an experimental watershed. *International Journal of Hydraulic Engineering*, 2(3):42-46.

Roy, D.; Begam, S.; Ghosh, S. and Jana, S. (2013). Calibration and validation of HEC-HMS model for a river basin in eastern India. ARPN *Journal of Engineering and Applied Sciences*, 8(1): 40-56.

Russell, S.; Kenning, B. and Sunnell, G. (1979). Estimating design flows for urban drainage, American Society of Civil Engineers. *Journal Hydraulics Division*, 105(1): 43-52.

Sabol, G. (1988). Clark unit hydrograph and R-parameter estimation. *Journal of Hydraulic Engineering*, 114 (1): 103-111.

Sanyal, J.; Densmore, A.L. and Carbonneau, P. (2014). Analysing the effect of land use/cover changes at sub-catchment levels on downstream flood peaks: a semi-distributed modelling approach with sparse data. *Catena*, 118: 28-40.

Saptarshi, P.G. and Raghavendra, R.K. (2009).GIS-based evaluation of micro-watersheds to ascertain site suitability for water conservation structures. *Journal of Indian Society of Remote Sensing*, 37: 693-704.

Sarangi, A.; Madramootoo, C.A.; Enright, P.; Prasher, S.O. and Patel, R.M. (2005). Performance evaluation of ANN and geomorphology-based models for runoff and sediment yield prediction for a Canadian watershed, *Current Science*, 8912: 2022-2033.

Sardoii, E.R.; Rostami, N.; Sigaroudi, S.K. and Taheri, S. (2012). Calibration of loss estimation methods in HEC-HMS for simulation of surface runoff (Case Study: Amirkabir Dam Watershed, Iran). *Advances in Environmental Biology*, 6(1): 343-348.

Scharffenberg, W.; Paul, E.; Steve, D.; Fleming, M. and Pak, J. (2010) Hydrologic Modeling System (HEC-HMS): Physically-based simulation components.2nd Joint Federal Interagency Conference, Las Vegas, NV.

Schulze, R.E.; Schmidt, E.J. and Smithers, J.C. (1992). SCSSA user manual PC based SCS design flood estimates for small catchments in Southern Africa, report No.

40, Department of Agricultural Engineering University of Natal, Pietermaritzburg, South Africa.

Schumm, S.A. (1956). Evolution of drainage systems and slopes in Badlands at Perth Amboy, New Jersey. *Geological Society of America Bulletin*, 67: 597-646.

Sharda, V.N. and Juyal, G.P, (2006). Conservation technologies for sustaining natural resources, Handbook of Agriculture, Directorate of information and publication of agriculture, ICAR, New Delhi: 254-299.

Sharma, S.K.; Mishra, N. and Gupta, A. (2007). Morphometric analysis of Uttalanala watershed using GIS techniques. *Sci-fronts*, 1: 178-185.

Shrestha, M.N. (2003). Spatially distributed hydrological modeling considering land-use changes using remote sensing and GIS. Map Asia Conference.

Silva, D.; Weerakoon, S.B. and Herath, S. (2014). Modeling of Event and Continuous Flow Hydrographs with HEC–HMS: Case Study in the Kelani River Basin, Sri Lanka. *Journal of Hydrologic Engineering*, 19(4):800-806.

Singh, R.K.; Bhatt, C.M. and Prasad, V.H. (2003). Morphological study of a watershed using remote sensing and GIS techniques. *Hydrology Journal Indian Asociation of Hydrologists*, 26(1-2): 55-66.

Smith, J.A.; Baeck M.L.; Meierdiercks, K.L.; Nelson, P.A.; Miller, A.J.and Holland, E.J.(2005). Field studies of the storm event hydrologic response in an urbanizing watershed. *Water Resources Research*, 41, W10413.

Soil Conservation Service (1971). National engineering handbook, Section 4: Hydrology. USDA, Springfield, VA.

Soil Conservation Service (1986). Urban hydrology for small watersheds, Technical Release 55.USDA, Springfield, VA.

Soil conservation service engineering division (1986). Urban Hydrology for Small Watersheds.U.S. Department of Agriculture (USDA), Technical Release.

Strahler, A.N. (1964). Quantitative geomorphology of drainage basins and channel networks.Handbook of Applied Hydrology (New York, Mc.Graw Hill Book Company. 411.

USACE (1998). HEC-1 flood hydrograph package user's manual. Hydrologic Engineering Center, Davis, CA.

USACE (2000). HEC-HMS Hydrologic Modeling System User's Manual. Hydrologic Engineering Center, Davis, CA.

USDA/NCRS (2007). Official Series Description- Coloma Series. Rev. AJO-GWH-MLK.

Vassova, D. (2013). Comparison of rainfall-runoff models for design discharge assessment in a small ungauged catchment. *Soil and Water Research,* 8:26–33.

Verma, A.K.; Jha, M.K. and Mahana, R.K. (2009). Evaluation of HEC-HMS and WEPP for simulating watershed runoff using remote sensing and geographical information system. *Paddy and Water Environment,* 8 (2):131-144.

Viessman, W. and Lewis, G.L. (2003). Introduction to Hydrology. Prentice Hall.

Wheater, H.S.; Jakeman, A.J. and Beven, K.J. (1993). Progress and directions in rainfall-runoff modeling. In: Jakeman, A. J., Beck, M. B., and McAleer, M. J. (Eds.), Modleing change in environmental systems. John Wiley & Sons, Chichester, UK, pp. 101–132.

Wheater, H.S.; Sorooshian, S. and Sharma, K.D. (2008). Hydrological modelling in Aridand Semi-arid Areas. Cambridge University Press, Cambridge, p. 195.

Wu, J.P.; Delleur, J.W. and Diskin, M.H. (1964). Determination of peak discharge and design hydropraphs for small watersheds in Indiana, Bulletin lndiana flood Control Resources commission at Purdue University.

Yang, X.L.; Ren, L.L.; Singh, V.P.; Liu, X.F.; Yuan, F.; Jiang, S.H. and Yong, B. (2012). Impacts of land use and land cover changes on evapotranspiration and

runoff at Shalamulun River watershed, China. *Hydrology Research,*43 (1–2): 23–37.

Yusop, Z.; Chan, C.H. and Katimon, A. (2007). Runoff characteristics and application of HEC-HMS for modelling storm flow hydrograph in oil palm catchment. *Water Science and Technology*, 56 (8):41–48.

APPENDIX-I

Sub basin	Area (km^2)	Perimeter (km)	Total Length of stream (km)	Basin length (km)	Maximum Length of stream (km)	Drainage density	Circulaory ratio	Elongation ratio	Form factor	Unity shape factor	Watershed shape factor	Compactness co efficient	Total relief (km)	Length of overland flow	Fitness ratio	Relief ratio	Relative relief	Constant of channel maintance
1	28.949	36.911	64.480	13.381	13.381	2.227	0.267	0.454	0.162	2.487	2.203	1.936	0.147	0.224	0.363	0.011	0.004	0.449
2	25.209	39.987	51.901	17.215	17.215	2.059	0.198	0.329	0.085	3.429	3.038	2.247	0.229	0.243	0.431	0.013	0.006	0.486
3	12.612	20.265	31.481	6.387	6.387	2.496	0.386	0.628	0.309	1.798	1.593	1.610	0.109	0.200	0.315	0.017	0.005	0.401
4	37.870	48.491	81.532	18.307	18.307	2.153	0.202	0.379	0.113	2.975	2.636	2.223	0.184	0.232	0.378	0.010	0.004	0.464
5	11.221	29.493	22.593	8.073	8.073	2.013	0.162	0.468	0.172	2.410	2.135	2.484	0.100	0.248	0.274	0.012	0.003	0.497
6	29.825	36.730	64.569	9.169	9.169	2.165	0.278	0.672	0.355	1.679	1.487	1.898	0.122	0.231	0.250	0.013	0.003	0.462
7	86.839	71.470	192.784	26.682	26.682	2.220	0.214	0.394	0.122	2.863	2.537	2.164	0.191	0.225	0.373	0.007	0.003	0.450
8	9.797	18.094	24.324	5.883	5.883	2.483	0.376	0.601	0.283	1.880	1.665	1.631	0.032	0.201	0.325	0.005	0.002	0.403
9	18.825	27.864	41.878	8.638	8.638	2.225	0.305	0.567	0.252	1.991	1.764	1.812	0.057	0.225	0.310	0.007	0.002	0.450
10	16.828	30.940	36.722	11.864	11.864	2.182	0.221	0.390	0.120	2.892	2.562	2.128	0.110	0.229	0.383	0.009	0.004	0.458
11	26.477	45.053	57.844	19.780	19.780	2.185	0.164	0.294	0.068	3.844	3.406	2.471	0.128	0.229	0.439	0.006	0.003	0.458
12	44.786	47.948	93.835	17.459	17.459	2.095	0.245	0.433	0.147	2.609	2.311	2.022	0.164	0.239	0.364	0.009	0.003	0.477
13	42.372	39.987	92.412	11.200	11.200	2.181	0.333	0.656	0.338	1.721	1.524	1.733	0.151	0.229	0.280	0.013	0.004	0.459
14	35.529	39.263	77.354	13.016	13.016	2.177	0.289	0.517	0.210	2.184	1.935	1.859	0.165	0.230	0.331	0.013	0.004	0.459
15	24.840	33.835	56.875	12.316	12.316	2.290	0.273	0.457	0.164	2.471	2.189	1.916	0.132	0.218	0.364	0.011	0.004	0.437
16	44.573	49.034	94.195	18.055	18.055	2.113	0.233	0.417	0.137	2.704	2.396	2.072	0.222	0.237	0.368	0.012	0.005	0.473